Generation of basal radial glia in the embryonic mouse dorsal telencephalon

DISSERTATION

zur Erlangung des akademischen Grades

Doctor of Philosphy
(Ph.D.)

vorgelegt

der Fakultät Mathematik und Naturwissenschaften
der Technischen Universität Dresden

von

Wong, Fong Kuan

geboren am 25. Juli 1982 in Kuala Lumpur, Malaysia

Gutachter: Prof. Dr. Wieland B. Huttner
Prof. Dr. Frank Buchholz

Eingereicht am: 31-March-2014
Tag der Verteidingung: 16-June-2014

老豆和老妈子

Summary

My own brain is to me the most unaccountable of machinery – always buzzing, humming, soaring, roaring, diving…

~Virginia Woolf

The human brain, as much as it is "unaccountable" in the eyes of Virginia Woolf, is a marvel. It is the evolutionary increase in brain size, especially in the cerebral cortex, that both allowed Mrs Woolf to create and us to perceive the beautiful imagery that exists in her fictional world. The evolutionary increase in brain size in part reflects the increase in the number of neurons generated during neocortical development. This in turn reflects two principal features of cortical expansion, namely, an increase in the number of neural stem and progenitor cells (from here on referred to as progenitor cells) and their neurogenic potential. Strikingly, in order to cater for this increase in progenitor cells and neurogenic potential, there is a significant expansion and diversification of basal progenitors in the subventricular zone (SVZ).

Basal progenitors can be divided into three types: basal intermediate progenitors (bIPs), basal radial glias (bRGs) and transit-amplifying progenitors (TAPs). bIPs are the most abundant progenitors in the mouse SVZ. These cells are non-polar and are Pax6 and Sox2 negative, but Tbr2 positive. They have limited proliferative capacity as they can divide only once to produce two neurons. bRGs and TAPs, on the other hand, are able to undergo multiple rounds of division and exist in higher abundance in gyrencephalic brains (for bRG, in humans up to 50% *versus* mouse 5% at mid-neurogenesis). The morphology of bRGs are reported to be dynamic (fluctuating between states of having process(es) to none), whereas TAPs are generally described to be non-polar during mitosis. bRGs are known to express Pax6 and Sox2 but not Tbr2 while TAPs are known to express both Pax6 and Tbr2. The increase in the proportion of these self-renewing basal progenitors (more specifically bRGs) might allow for cortical expansion.

Hence, the main objective of this doctoral work was to generate more bRGs in the mouse dorsal telencephalon, the region that ultimately develops to become the cerebral cortex. To achieve this objective, two approaches were used– (i) a general approach by microinjecting a pool of ferret poly-A^+ RNA and (ii) a candidate approach by conditionally expressing the transcription factor Pax6.

In the general approach, the microinjection technique was first established and validated in an organotypic slice culture of the mouse dorsal telencephalon. A pool of ferret poly-A^+ RNA extracted at P1, the developmental stage corresponding to the peak of bRG production, was then microinjected into the dorsal telencephalon. We hypothesized that at the peak of bRG production, the "instructive" messages on how to generate bRG would be at their peak. Hence, by introducing these "instructive" messages into a apical radial glia (aRG), these cells would thus "know" how to generate bRGs. At 24 h after microinjection, only aRGs, the predominant progenitor residing in the ventricular zone during mid-neurogenesis were recovered. At 48 h after microinjection, however, 75% of cells that translated the ferret poly-A^+ RNA had a morphology reminiscent of bRG. These cells were located away from the ventricular surface and had a basal but not apical process. We conclude from these experiments that we did indeed generate bRG-like cells in the mouse dorsal telencephalon via microinjection of the ferret poly-A^+ RNA.

In the candidate approach, this work aimed to conditionally express Pax6, a transcription factor that has been linked to proliferation and neurogenesis in aRG. More specifically, as there is a significant increase in the number of Pax6 positive cells (bRGs) in the SVZ of gyrencephalic animals during mid-neurogenesis, we wanted to recapitulate this phenomenon in the mouse dorsal telencephalon, where Pax6 is normally downregulated. To achieve this, the *Tis21*–$CreER^{T2}$ mouse was used. Tis21 is a pan-neurogenic marker that is switched on once aRG switches from a proliferative division (i.e. 1 aRG➔2aRG) to a neurogenic division (i.e. 1aRG➔1aRG+1bIP).

Consequently, the neurogenic aRGs and its progeny, bIPs would thus be Tis21 positive. By conditionally expressing Pax6 in Tis21 positive aRGs, the ectopic expression of Pax6 was successfully induced in the SVZ of the mouse dorsal telencephalon. Interestingly, conditional expression of Pax6 increased the percentage of proliferating cells in the SVZ. However, instead of producing more bIPs as predicted by the neurogenic division of Tis21 positive aRGs, these cells had the cell morphology, transcription factor expression profile, and division-type of bRGs and/or TAPs. Thus, using the conditional expression of Pax6 we were able to generate more bRG-like progenitors in the mouse dorsal telencephalon.

The fate of these conditionally expressing Pax6 progenitors at a later stage was then investigated. A phenotypic change in the behaviour of neurons generated was observed. Instead of migrating into the cortical plate, cells that were highly expressing Pax6 formed a heterotopia at the SVZ or intermediate zone, suggestive of Pax6 interfering with neuronal migration. Interestingly, of those lowly expressing Pax6 cells that successfully migrated to the CP, a disproportionate majority became upper layer neurons. As the fate of neurons are dependent on their date of birth (i.e early born neurons are normally found in the deep layer while late born neurons are normally found in the upper layer), the increase in the upper layer neurons is consistent with the fact that conditionally expressing Pax6 delayed the birth of these neurons by delaying neurogenesis in order to increase the number of proliferative divisions. Interestingly, this increase in upper layer neurons is consistent with the difference between small- and large-brained species.

In conclusion, through this work more bRGs was successfully generated in the mouse dorsal telencephalon through two distinct but complementary approaches.

List of abbreviation

aIP : Apical intermediate progenitor
AP : Apical progenitor
AP2 : Activating enhancer binding protein 2
APP : Amyloid precursor protein
aRG : Apical radial glia
BP : Basal progenitor
bIP : Basal intermediate progenitor
BLBP : Brain lipid binding protein
bRG : Basal radial glia
CAG : CMV early enhancer/chicken beta actin
CDK : Cyclin-dependent kinase
CNS : Central nervous system
CP : Cortical plate
CSF : Cerebral spinal fluid
Dab1 : Disabled-1
DCX : Doublecortin
DN : Dominant-negative
Dx : Dextran
E : Embryonic day
ECM : Extracellular matrix
EdU : Ethynyl deoxyuridine
FABP : Fatty acid binding protein
FGF : Fibroblast growth factor
GABA : Gamma-aminobutyric acid
GFAP : Glial fibrillary acidic protein
GFP : Green fluorescent protein
GLAST : Glutamate aspartate transporter
HD : Homeodomain
HEK : Human embryonic kidney
HES : Hairy and enhancer of split-1
Het : Heterotopia
Hind : Hindbrain
IGF : Insulin-like growth factor
IKNM : Interkinetic nuclear migration
IRES : Internal ribosmomal entry site
ISVZ : Inner subventricular zone
IUE : *In utero* electroporation
IVT : *In vitro* transcribed
IZ : Intermediate zone
LOF : Loss of function
MAP2 : Microtubule-associated protein 2
MZ : Marginal zone
N-Cam : Neural cell adhesion molecule
NDE : Nuclear distribution element
NEC : Neuroepithelial cells
Ngn2 : Neurogenin 2

NPC : Neural progenitor cells
Olig2 : Oligodendrocyte transcription factor 2
OSVZ : Outer subventricular zone
P : Post natal day
Par3 : Partitioning defective-3
Par6 : Partitioning defective-6
Pax6 : Paired box-6
PBS : Phosphate buffer saline
PCR : Polymerase chain reaction
PD : Paired domain
PH3 : Phosphohistone H3
PVim : Phosphovimentin
R-Cad : Retinal cadherin
Rac1 : Ras-related C3 botulinum toxin substrate 1
RFP : Red fluorescent protein
SATB2 : Special AT-rich sequence-binding protein
Sey : Small eyes
Shh : Sonic hedgehog
Sox : Sry box
SPAG5 : Sperm associated antigen 5
SP : Subplate
SVZ : Subventricular zone
TAP : Transit amplifying progenitors
Tbr : T-brain
tbRG : Transient basal radial glia
Tel : Telencephalon
tet : Tetracycline
TF : Transcription factor
Tuj1 : ß III tubulin
VZ : Ventricular zone

List of figures

List of Tables

Contents

Chapter 1
Introduction

If it could be demonstrated that any complex organ existed, which could not possibly have been formed by numerous, successive, slight modifications, my theory would absolutely break down. But I can find no such case.

~Charles Darwin

Literature, music and scientific theories, just to name a few, are consequences of the higher cognitive abilities that evolved together with the expanded human neocortex. This did not occur as a random event, but rather, as Darwin so aptly put, "by numerous, successive, slight modifications" during evolution. While a historical record of the soft tissue is unavailable to us, research into the evolutionary modifications to the neocortex is limited to comparative studies of the mammalian brain. Over the past century, these studies have given us a profound understanding of the cell-biological differences between mammalian species, including differences in cytoarchitecture, neuronal identity and most importantly for our understanding of evolutionary developmental of the mammalian brain, neural progenitor behaviour.

In recent years, discovery of the basal radial glia (bRG), a basal progenitor (BP) population in the developing neocortex, has led to the hypothesis that these progenitors in particular may play a role in neocortical expansion through an increase in the proliferative capacity of the subventricular zone (SVZ) (Borrell and Reillo, 2012; Fietz and Huttner, 2011; Fietz et al., 2010; Fish et al., 2008; Gertz et al., 2014; Hansen et al., 2010; Kelava and Huttner, 2013; Lewitus et al., 2013a; Lui et al., 2011; Reillo et al., 2011). Because bRG exist in different proportions across various species where it exists – at low abundance in the lissencephalic mouse brain and in high abundance in the gyrencephalic human brain (Kelava et al., 2012; Martinez-Cerdeno et al., 2012; Reillo et al., 2011; Shitamukai et al., 2011; Wang et al., 2011) -- it is hypothesised that the increased abundance of bRGs may play an important role in neocortical expansion. The main objective of this doctoral work is to

generate more bRG in the mouse dorsal-lateral telencephalon and thereupon determine their role in the evolutionary expansion of the neocortex.

1.1 Development of the mammalian brain

A journey of a thousand miles must begin with a single step.

~Lao Tzu

In early embryogenesis, there exist three germ layers, namely the ectoderm, mesoderm and endoderm. The ectoderm ultimately produces the central nervous system (CNS). The first identifiable region that dictates the formation of the brain is the neural plate, a thickened layer of the dorsal ectoderm. The induction of these cells to adopt the neural fate involves the suppression of an epidermal fate via bone morphogenetic protein antagonists such as noggin, chordin and follistatin. To form the tubular structure that is reminiscent of the neural tube, the neural plate first needs to bend to form the neural groove. The invagination of the neural plate allows for the two dorsolateral apical surfaces of the neural fold to come closer and meet at the dorsal midline. The fusion of the neural folds leads to the closure of the neural tube beginning in the middle along the craniocaudal axis and closes at both directions (towards the cephalic regions and caudal parts). The caudal region becomes the spinal cord while the rostral region becomes the brain.

The neural plate consists of neuroepithelial cells that proliferate rapidly in an unsynchronized manner. This unsynchronized proliferation allows for growth and expansion at different rates for various regions. As a consequence, at the one-somite stage, the three primary vesicles, namely, the prosencephalon (the forebrain), mesencephalon (midbrain) and the rhombencephalon (hindbrain), can be easily distinguished even before the closure of the neural tube. As the brain develops, the prosencephalon is further divided into two regions namely the telencephalon, which ultimately develops to become the cerebral cortex and the diencephalon. The rhombencephalon is also further

divided into the metacephalon and more caudally the myelencephalon (**Fig. 1**).

The patterning of the vertebrate brain along the anterior-posterior axis is achieved by various inductive factors. These inductive factors are normally signalling molecules that can either be freely diffusing and act from a distance or tethered to the cell surface (i.e. acting locally). Examples of inductive factors are FGF (Storey et al., 1998), Wnt (Kiecker and Niehrs, 2001; Nordstrom et al., 2002), Shh (Rallu et al., 2002) and retinoic acid (Maden, 1999).

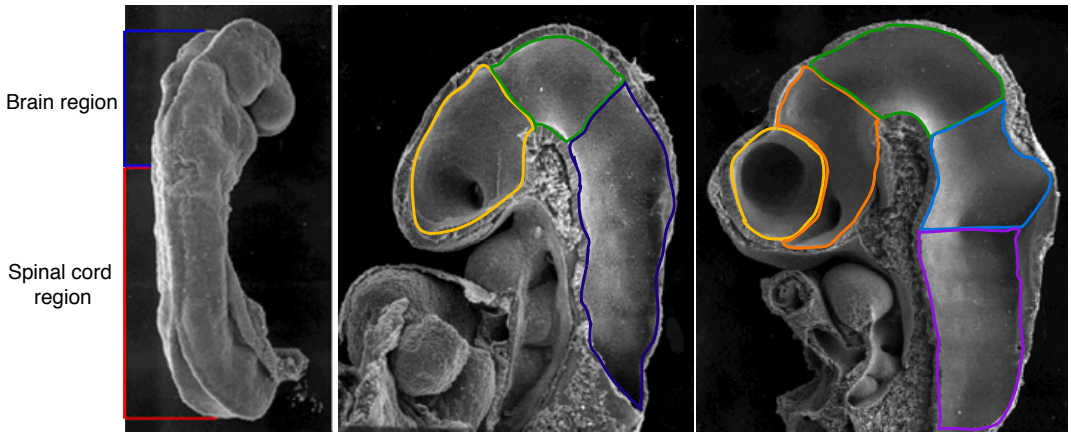

Figure 1: The primary vesicles of the developing mammalian brain. Scanning electron microscope images of the developing neocortex. *Left*: Dorsolateral view of the E8.5 mouse neural tube, prior to the completion of the neural tube closure. The neural tube can be divided into two areas, the brain region (blue) and the spinal cord region (red). *Middle*: Sagittal cut of E9.5 mouse embryo. The three primary vesicles namely the prosencephalon (yellow), mesencephalon (green) and rhombencephalon (blue) can be observed. *Right*: Sagittal cut of E10.5 mouse embryo. The secondary vesicles of the developing neocortex where the prosencephalon and rhombencephalon subdivide as development continues. The prosencephalon at this stage is divided into two parts namely the telencephalon (yellow) and diencephalon (orange). The rhombencephalon is also divided into two parts namely the metacephalon (blue) and the myelencephalon (purple). Images modified from http://www.med.unc.edu.

1.1.1. Organisation of the neocortex

The defining feature of the mammalian neocortex or telencephalon is its six-layered structure containing a mixture of neurons and glia. Cortical neurons

can be subdivided into two classes, namely interneurons and projection neurons. Interneurons are GABAergic and tend to form local connections. In rodents, these cells originate from the ventral telencephalon (namely the medial ganglionic eminence) where they migrate over long distances into the dorsal telencephalon (Anderson et al., 1997). In humans, the majority of interneurons still originate from the ventral telencephalon, however a small percentage of these interneurons are generated within the dorsal telencephalon (Hansen et al., 2013; Ma et al., 2013). Projection neurons, on the other hand, are glutamatergic and project axons to distant targets (i.e. intracortical, subcortical and subcerebral targets). These are derived from progenitors residing in germinal zones located within the dorsal telencephalon.

Projection neurons, based on the layers that they reside in, transmit information to specific regions. Broadly, layers II, III, V and VI are callosal projection neurons, layer IV consists of corticothalamic neurons and layer V contains subcerebral projection neurons (Douglas and Martin, 2004). Layer I or the marginal zone (MZ) contains Cajal-Retzius cells, the earliest born neurons originating from the cortical hem and pallial-subpallial boundary region (Bystron et al., 2006). Cajal-Retzius cells are known to play an important role in radial migration of neurons along the radial glia via Reelin secretion (Aboitiz et al., 2001).

Projection neurons, as mentioned before, originate from two main germinal zones of the dorsal telencephalon, namely the ventricular zone (VZ) and subventricular zone (SVZ). The VZ, located adjacent to the ventricles, consists mostly of apical progenitors (APs, described in detail in the next section), and is the main proliferative zone in the embryonic mouse brain (Molnar et al., 2006). The SVZ, located right above the VZ is a basal proliferative compartment that ultimately becomes the main proliferative compartment in gyrencephalic brains (**Fig. 2**). In early development, APs divide via symmetric proliferative division thus expanding the number of

progenitors in the founder pool and leading to lateral expansion. As neurogenesis begins, APs divide asymmetrically where one daughter cell differentiates to become a basal intermediate progenitor (bIP) or neuron and migrates away while the other remains as an AP (Götz and Huttner, 2005; Takahashi et al., 1996). In mouse, the SVZ begins to form around embryonic day (E) 12.5 (Smart et al., 2002). During this time, the preplate located above the SVZ splits into two, forming the MZ and subplate (SP). The newly generated neurons migrate radially into the cortical plate (CP) located between the MZ and SP (Smart et al., 2002).

Projection neurons are generated in a temporal fashion where progenitors first generate neurons from layer VI, followed by layer V, layer IV and so on. These neurons are arranged in an inside-out fashion where neurons generated earlier are found in the deep layers (typically layer V and VI) while late born neurons are found superficially (layers II to IV) (Molyneaux et al., 2007). This is in contrast with the reptilian cortex where neurons are generated in an outside-in fashion (Martinez-Cerdeno et al., 2006).

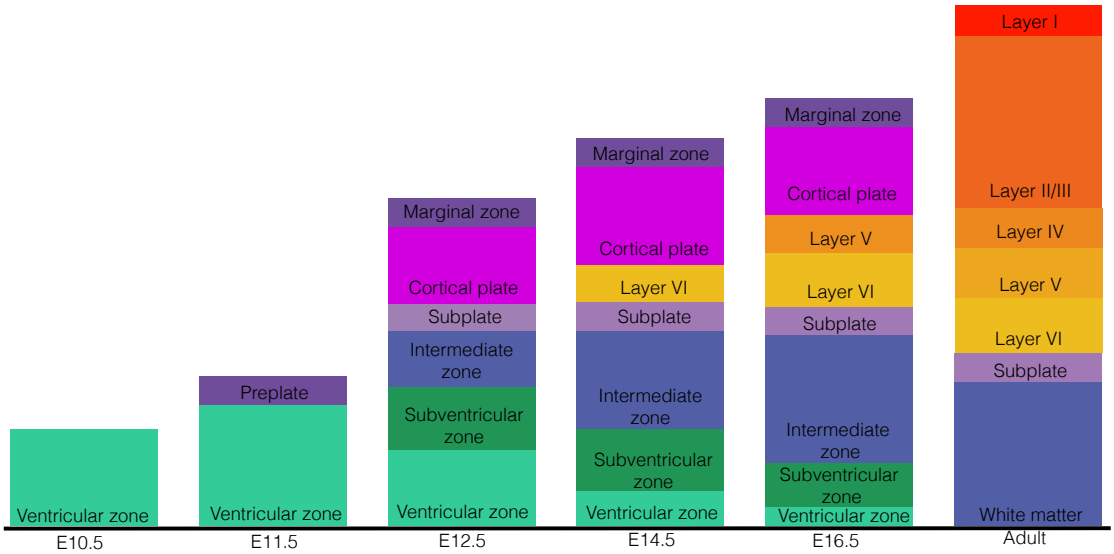

Figure 2: Formation of the various zones of the neocortex in the embryonic and adult mouse brain.

1.2. Types of progenitors

Great things are not done by impulse, but by a series of small things brought together

~Vincent Van Gogh

In this section, the various types of neural progenitor cells (NPCs) typically found in the dorsal telencephalon of the developing mammalian brain will be described below (**Fig. 3** and **Fig. 4**). As this doctoral work focuses mainly on the dorsal telencephalon, the subapical progenitors, defined by their abventricular mitosis and maintain an apical process would not be described as it has been mostly characterised in the ventral telencephalon in the mouse (Pilz et al., 2013).

1.2.1. Apical progenitors (APs)

Progenitors undergoing mitosis at the ventricular surface are categorized as APs. APs can be divided into three distinct classes namely the neuroepithelial cells, apical radial glias and apical intermediate progenitors.

1.2.1.1. Neuroepithelial cells (NECs)

The primordium of the cerebral cortex consists of a monolayer of NECs, which forms the neuroepithelium. NECs are bipolar cells with an apical process contacting the ventricular surface and a basal process contacting the basal lamina (Götz and Huttner, 2005). These cells exhibit typical epithelial cell features and apico-basal polarity. Tight junctions and adherent junctions confine apical proteins (e.g. Par3, Par6 and aPKC) to the apical domain (Aaku-Saraste et al., 1996; Kosodo et al., 2004) while restricting receptors for the basal lamina constituents, such as integrin, to the basal plasma membrane (Götz and Huttner, 2005). In addition, NECs express the intermediate filament, nestin (Götz and Huttner, 2005).

In a phenomenon known as interkinetic nuclear migration (IKNM), NECs migrate the length of the neuroepithelium, undergoing mitosis at the apical surface and S-phase at the basal surface (Bayer and Altman, 1991; Sauer, 1935; Taverna and Huttner, 2010). As a result, the neuroepithelium has a pseudostratified or layered appearance.

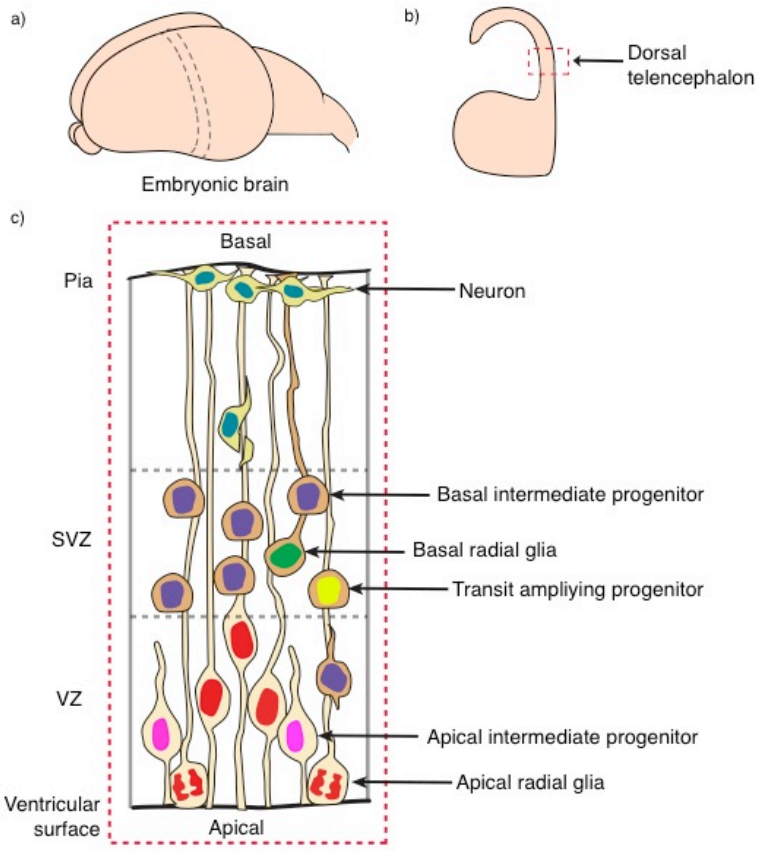

Figure 3: Types of progenitors present in the dorsal telencephalon of the developing brain. **(a,b)** Drawings depicting the location of the dorsal telencephalon in the embryonic mouse brain. The dashed line on **(a)** depicts the coronal section shown in **(b)**. The dashed box in **(b)** illustrates the position of the dorsal telencephalon. **(c)** The various progenitors can be distinguished from one another based on cell morphology, type of cell division, cell body location and transcription factors expression. The various cells can be identified by the different colour of the nucleus. Images are adapted from Kelava (2012).

As NECs are the first progenitors that exist prior to neurogenesis, they undergo symmetric proliferative division (1NEC➔2NECs). This serves to

increase the surface of the cortical primodium and at the same time expand the population of founder cells that ultimately produce all the projection neurons in the cortex.

1.2.1.2. Apical radial glias (aRGs)

aRGs, in many ways, are similar to the NECs as aRGs are a derivative of NEC. aRGs are bipolar, express Nestin and adherent junctions and exhibit apico-basal polarity (Götz and Huttner, 2005). During the transition from NEC to aRG (begins around E9.5 in mice), tight junction proteins such as Occludin are downregulated (Aaku-Saraste et al., 1996) while astroglial markers such as astrocyte-specific glutamate transporter, GLAST (Shibata et al., 1997), vimentin, Ca^{2+} binding protein, S100β (Campbell and Götz, 2002; Malatesta et al., 2000) and fatty acid binding protein (Levitt and Rakic, 1980) are acquired. This transition allows for the presence of a distinct class of progenitors that contains both neuroepithelial as well as astroglial cell properties (Götz and Huttner 2005). In addition, aRGs are known to be positive for certain sets of transcription factors (TFs) such as Pax6, Sox2 and Hes1 but negative for Tbr2 (Lui et al., 2011). Similar to NECs, aRGs are known to undergo IKNM (Taverna and Huttner, 2010). However, the cell bodies of aRGs do not translocate the entire span of the tissue. Instead, they are restricted only to the VZ where the aRGs still undergo mitosis at the ventricular surface but stop at the boundary between VZ and SVZ at S-phase, rather than traversing up to the pia.

Initially, the aRG, with its long basal process, was thought to serve only as a scaffold for neurons to migrate to the CP (Rakic, 1995). However, this has been proven to be untrue. In early stages of neocortical development (E10.5 to E12.5), aRGs divide symmetrically producing two aRGs. However, as development continues, instead of self-amplification, aRGs divide asymmetrically producing a self-renewing daughter and a differentiated daughter, which can be either a neurogenic bIP or less often a neuron

(Huttner and Kosodo, 2005). The switch from symmetric to asymmetric division coincides with the expression of the anti-proliferative marker, Tis21 (Haubensak et al., 2004). At the end of neocortical development, aRGs switch from being neurogenic to gliogenic where they produce astrocytes and oligodendrocytes instead (Tan and Shi 2013).

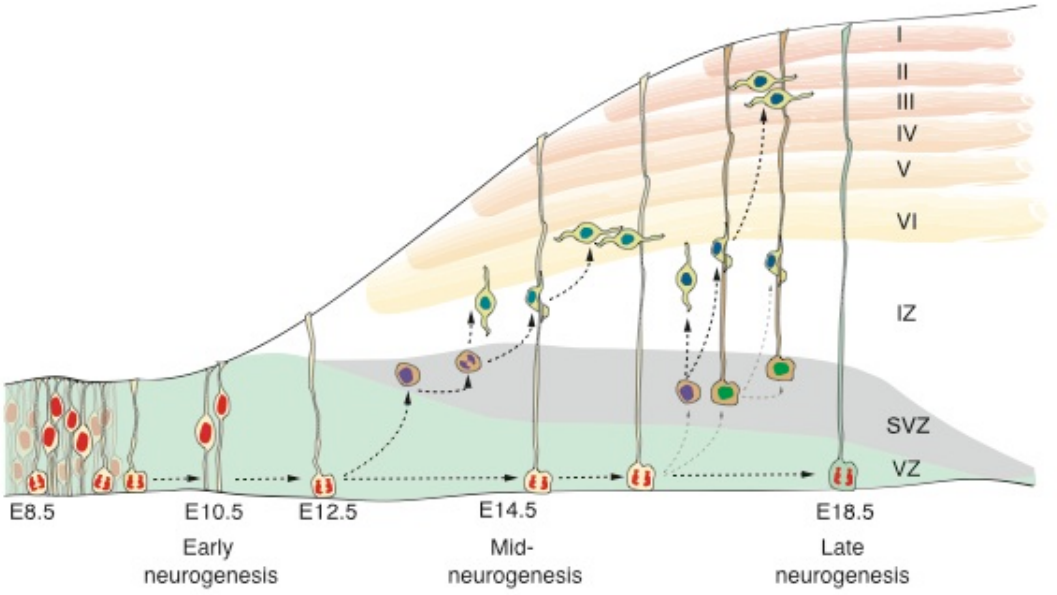

Figure 4: Neural progenitor cells divisions. The cartoon depicts the various modes of progenitor division and changes in the germinal zone size (shaded) during mouse neurodevelopment with the bottom axis representing time. Adapted from Kelava (2012).

1.2.1.3. Apical intermediate progenitors (aIPs)

aIPs (or previously known as short neural precursors), are morphologically different from the previously described APs, where they have either a short basal process or none and exist in low abundance in the mouse (~10%) (Gal et al., 2006; Stancik et al., 2010; Tyler and Haydar, 2013). They can be distinguished from other APs as they express the Tα1 promoter (Gal et al., 2006). aIP undergoes symmetric consumptive division where one aIP directly produces two neurons (Stancik et al., 2010; Tyler and Haydar, 2013). The

characteristic of these cells and its role in cortical development remains poorly described.

1.2.2. Basal progenitors (BPs)

Progenitors dividing basally are known as BPs. These cells are found in the SVZ and can be divided into three types: the bIPs, bRGs and transit-amplifying progenitors (TAPs).

1.2.2.1. Basal intermediate progenitors (bIPs)

In the mouse dorsal telencephalon, a large proportion of bIPs is derived from the asymmetric division of aRGs (1aRG ➔1bIP+1aRG) (Haubensak et al., 2004; Miyata et al., 2004; Noctor et al., 2004). bIPs are nonpolar non-epithelial cells and in the mouse SVZ are the most abundant BPs. Like aIPs, bIPs normally undergo symmetric consumptive division, where they generate two neurons after each division (Haubensak et al., 2004; Miyata et al., 2004; Noctor et al., 2004). Hence, it is not surprising that the evolutionary expansion of the neocortex was initially linked to these cells ((Kriegstein et al., 2006) see next section). These cells are molecularly distinguishable from aRGs as they are Tbr2 positive while negative for Pax6, Sox2 and Hes1 (Englund et al., 2005; Lui et al., 2011).

1.2.2.2. Basal radial glias (bRGs)

More recently, a new type of BP has been described in the developing mammalian neocortex (Fietz et al., 2010; Hansen et al., 2010; Reillo et al., 2011). Initially, bRGs were described as a basal process-bearing monopolar cells, located in the SVZ (Fietz et al., 2010; Hansen et al., 2010; Reillo et al., 2011). Recently, however, bRGs are reported to be more dynamic in terms of cell morphology where it can be divided into four distinct groups in the macaque neocortex. These cells are classified based on cell morphology,

namely a) apical process-bearing bRGs, b) apical and basal process-bearing bRGs, c) basal process-bearing bRGs and finally d) bRGs that alternate between stages showing either an apical and/or basal process and stages with no processes (transient bRG/tbRG) (Betizeau et al., 2013). Like aRGs, these cell maintain certain sets of epithelial and astroglia properties such as vimentin, BLBP and GFAP. bRGs are molecularly more similar to aRGs in terms of TFs expression as bRGs are known to be positive for Pax6, Sox2 and Hes1 but not Tbr2 (Fietz et al., 2010; Hansen et al., 2010; Reillo et al., 2011).

As these cells lack an apical process anchoring them to the apical junction, bRGs do not undergo IKNM. However, the cell body of bRG has been described to move rapidly basally or apically (depending on the processes present) prior to cytokinesis (Betizeau et al., 2013, LaMonica et al., 2013) and this phenomenon has been coined as mitotic somal translocation (Hansen et al., 2010).

The generation of bRG in the developing brain has been described in mouse (Shitamukai et al., 2011), ferret (Gertz et al., 2014; Reillo and Borrell, 2012) and human (LaMonica et al., 2013). bRGs are first generated by aRGs that have undergone a non-vertical cleavage (with respect to the ventricular surface) where the daughter inheriting the basal process becomes a bRG while the daughter inheriting the apical process becomes a bIP. In this respect, both daughters leave the VZ and move to the SVZ. In the mouse SVZ, bRGs undergo asymmetric division, giving rise to a self-renewing bRG and a neuron (Gertz et al., 2014; Wang et al., 2011) while in monkeys and most likely human, bRGs undergo symmetric proliferative division (i.e. both daughter becomes progenitors) giving rise to virtually any BPs (Betizeau et al., 2013; Hansen et al., 2010; LaMonica et al., 2013)

1.2.2.3. Transit amplifying progenitors (TAPs)

The final class of BPs is TAPs. The exact morphology and molecular characteristic of these cells have not been fully revealed. The recent discovery of the tbRG by Betizeau et al. (2013) may now blur the distinction between a tbRG and a TAP as both of these cells have the capacity to self-renew and lack any process (Betizeau et al., 2013). Thus a bRG can easily be classified as a TAP and vice versa. Traditionally, as the name suggests, TAPs have self-renewing capability where they have been shown to self-amplify where one TAP has been shown to generate two TAPs. The extent of this self-renewing capacity, however, has yet to be elucidated (Hansen et al., 2010). These cells have been shown to be Pax6 and Tbr2 positive (Fietz et al., 2010; Betizeau et al., 2013). TAPs occur at low abundance in the embryonic mouse brain (~10%, (Arai et al., 2011)) while much higher in humans.

	NE	aRG	SNP	IP	bRG	TAP
Morphology at mitosis	Bipolar	Bipolar	Monopolar	Nonpolar	Monopolar/ Bipolar	Nonpolar
Location	VZ	VZ	VZ	SVZ	SVZ	SVZ
Transcription factor/regulator	Pax6 Sox2 Hes1	Pax6 Sox2 Hes1	Pax6	Tbr2	Pax6 Sox2 Hes1	Pax6 Tbr2
Self-renewal capacity	High	High	Low	Low	High	High

Table 1: Summary of the various progenitors found in the developing dorsal telencephalon.

1.3. Cell fate determinants

Why so much grief for me? No man will hurl me down to Death, against my fate. And fate? No one alive has escaped it, neither brave man nor coward, I tell you – it's born with us the day that we are born

~Homer

A progenitor is defined not only by morphology and TF expression but also by the type of division it makes. A progenitor dividing symmetrically (regardless of terminal or proliferative) would have to devise a mechanism in which factors involved in cell fate are distributed equally while one that divides asymmetrically would have to induce a bias in inheritance of those factors. So, how do progenitors determine the fate of their progeny at the end of cytokinesis? In the following part, the different intrinsic and extrinsic factors governing cell fate will be described (**Fig. 5**).

1.3.1. Intrinsic factors

It is a mistake to regard age as a downhill grade toward dissolution. The reverse is true. As one grows older, one climbs with surprising strides.

~George Sands

The model proposed by Chenn and McDonell (1995) hypothesized that the asymmetric distribution of cell fate constituents during cytokinesis is the main reason leading to the asymmetric cell fates in daughter cells. Progenitors undergoing symmetric division will divide with a vertical cleavage (with respect to the ventricular surface). In this manner, cell fate constituents can be distributed equally to the individual daughter cells. In contrast, progenitors undergoing asymmetric division divide with a horizontal cleavage where based on their compartments, cell fate constituents are distributed unequally. However, this model was overturned when it was shown that majority of progenitors in the mouse neuroepithelium divide with a vertical cleavage even when asymmetric division is at its' peak (Kosodo et al., 2004). The inheritance of the apical domain, which constitutes around 1-2% of the plasma

membrane, was then suggested to be vital in determining the fate of the progeny (Kosodo et al., 2004). Symmetric division of the apical domain will thus lead to both progeny acquiring the same cell fate, while a cleavage orientation that bypass the apical domain, will lead to asymmetric inheritance of the apical domain and progeny with different cell fates.

The apical domain located at the cell surface contacting the ventricle, is separated from the basolateral membrane by apical junctions. It is the presence of the junctional belt that prevents apical proteins such as Par3, Par6, and beta-catenin from traversing into the basolateral membrane (Aaku-Saraste et al., 1996; Kosodo et al., 2004). In recent years, several papers have demonstrated that apical proteins such as Par3 can be differentially inherited by daughter cells leading to asymmetry in fate. The differential inheritance is mediated by variation in cell signalling between daughters (i.e. Notch) (Bultje et al., 2009).

With the development of *en face* imaging, it was demonstrated that at E12.5, 90% of aRGs divide vertically and the apical domain is inherited by both daughter cells regardless of the fate of the progeny (Konno et al., 2008; Shitamukai et al., 2011). The size of the inherited apical domain was also shown not to have an effect on the fate of the progeny (Shitamukai et al., 2011). Furthermore, in cells with non-vertical division, the progeny inheriting the apical domain differentiates to become a bIP while the progeny inheriting the basal process will re-establish the apical domain and become an aRG. These findings, obtained first in zebrafish (Alexandre et al., 2010; Dong et al., 2012) and later in mouse (Shitamukai et al., 2011), challenge the importance of apical domain in determining cell fate.

Beside the apical domain, the basal process is also suggested to be an important factor in determining cell fate. In early stages of development, the basal process has been shown to split into two during cytokinesis with the cleavage furrow originating from the basal side moving towards the apical end

(Kosodo et al., 2008). In this instance, both daughter cells will inherit the basal process and will be symmetrical in terms of cell fate. However, as development progresses and with the advent of asymmetric division of the aRG, this cleavage is seldom (or never) observed during mid-neurogenesis. Instead, the basal process is inherited only by the basally located daughter cell, thus distributing basal-specific cell fate constituents preferentially to the basal daughter cell (Konno et al., 2008; Shitamukai and Matsuzaki, 2012). Although basal-specific cell fate constituents are still relatively unknown, both integrin beta-3 receptor (Fietz et al., 2010) and cyclin D2 mRNA (Tsunekawa et al., 2012) have been shown to mediate this effect. Disruption of either compound's expression leads to a reduction in the self-renewal capacity of basal process-bearing cells.

Furthermore, inheritance of specific structures such as centrosomes and primary cilium, have been shown to determine the fate of the progeny (Wang et al., 2009). Prior to cell division, centrioles undergo duplication in a semi-conservative manner, resulting in the presence of an older (i.e. the one that inherits the older/mother centriole) and a younger centrosome (i.e. the one that inherits the younger/daughter centriole). The mother centriole hypothesis posits that the inherent difference in the age of the centrioles, allows for the asymmetric segregation of cell fate determinant. The pericentriolar materials surrounding the centrioles are believed to contain cell fate determinants. The mother centriole, as it is more mature, inherits and accumulates pericentriolar materials more rapidly and is inherited by the daughter cell that is destined to be an aRG, while the younger centriole is inherited by the other differentiating daughter cell.

The primary cilium, which protrudes out into the ventricles, acts as an interface between the cell and the cerebral spinal fluid (CSF) (Louvi and Grove, 2011). The CSF contains signalling molecules that promote cell proliferation (Lehtinen et al., 2011) (for more detailed explanation, see below). It is via the primary cilium that the aRG detect some of these self-renewal

signals. Consistently, for progeny that are fated to become bIP, the primary cilium is located at the basolateral side, instead of the apical surface facing the ventricles (Wilsch-Bräuninger et al., 2012). This reduces the exposure of the primary cilium to self-renewing factors in the CSF and hence drives the progenitor to differentiate to become bIP. Up until recently, the primary cilium was believed to be completely disassembled during mitosis and reassembled in the next cell cycle. Paridaen et al. (2013) has recently demonstrated that this is not the case. Instead, part of the ciliary remnant located in a vesicle tethered to the mother centriole is asymmetrically inherited by the daughter cell fated to become the aRG (Paridaen et al., 2013). The presence of the ciliary remnant allows for a faster reestablishment and hence, function of the primary cilium.

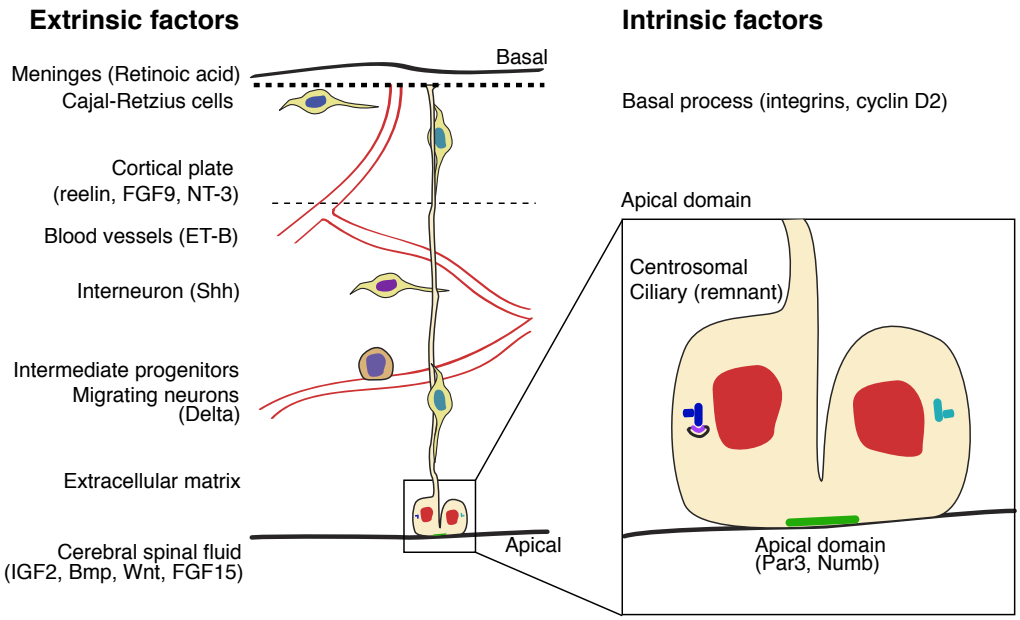

Figure 5: Cell fate determinants associated with intrinsic and extrinsic factors. Adapted from Shitamukai and Matsuzaki (2012).

1.3.2. Extrinsic factors

When we try to pick out anything by itself, we find it hitched to everything else in the universe

~John Muir

As progenitors do not exist as a separate entity, but are part of a tissue, the environment and thus the external factors have been shown to play a role in cell fate. This can be from exposing progenitors to CSF, interaction between neighbouring cells and extracellular matrix (ECM) and finally detecting secreted factors from non-neuroepithelial tissue at the basal end.

The CSF is produced mostly by the choroid plexus. In a pulsating manner, the CSF circulates around the subarachnoid space, the ventricles and the spinal cord (Dziegielewska et al., 1981; Lehtinen and Walsh, 2011). The CSF has been traditionally known to function as a fluid cushion to absorb any impact on the CNS and for maintaining the extracellular ionic balance (Lehtinen and Walsh, 2011). Not limited to that, recent studies have shown that the CSF contains a complex mixtures of secreted proteins (Dziegielewska et al., 1981; Parada et al., 2005; Zappaterra et al., 2007) that ranges from components of the ECM, growth factors (i.e. FGF (Zappaterra et al., 2007), IGF (Lehtinen et al., 2011), signalling molecules (i.e. sonic hedgehog (Huang et al., 2010), Wnt (Zappaterra et al., 2007)) and also membrane particles (i.e. prominin (Marzesco et al., 2005)). More interestingly, the content of the CSF has been shown to be dynamic, where components could change drastically during development, both in time and space (Lehtinen and Walsh, 2011). Hence, by controlling and changing the molecules these progenitors are exposed to at different developmental stages, the CSF may play an important role in influencing the behaviour of the neuroepithelium during development.

The aRG with its bipolar morphology has a large membrane surface. As such, it has a large surface area in contact with neighbouring cells that can

influence the behaviour of the progenitor. One of the best examples is lateral inhibition via Notch signalling. Lateral inhibition allows for the generation of two distinct cell types, where the delta signalling to Notch induces the Notch expressing cells to remain as a progenitor, while the delta-expressing cell (as it has reduced Notch signalling) will differentiate (Campos et al., 2001; Yoon et al., 2008). aRG expresses Notch receptors throughout the cell membrane (Gaiano et al., 2000) and could thus receive delta signalling from neighbouring differentiated cells such as bIP or migrating neurons. The induction of Notch induces the transcription of the basic helix-loop-helix genes such as Hes1 and Hes5, TFs known to be important in self-renewal.

Interneurons have been shown to have an effect on the proliferative capacity of progenitors in the dorsal telencephalon. GABA regulates neurogenesis by affecting the rate of DNA synthesis via the activity of voltage-gated calcium channels (LoTurco et al., 1995; Owens and Kriegstein, 1998). In addition, GABA affects the progression of cell cycle where the tonic release of GABA in tissue induces an increase in the ambient GABA levels (Wang and Kriegstein, 2009). In turn, this activates the calcium channels and elevates the intracellular Ca^{2+}. The hyperpolarization of the progenitor cells activates S/G2 DNA damage checkpoint, essentially preventing the cell from progressing through the cell cycle and consequently, reducing the number of proliferating cells in the dorsal telencephalon (Liu et. al. 2005).

In addition to intrinsic factors associated with the inheritance of the basal process, basal process-bearing cells are also exposed to signals secreted by non-neuroepithelial tissue such as meninges and basal lamina (Barakat et al., 1981; Wojcik-Stanaszek et al., 2011). An example of such is retinoic acid secreted by the meninges. By using the mutant Foxc1 mice that displayed a defect in the forebrain meningeal formation, Siegenthaler et al. (2009) has shown a significant reduction in retinoic acid production. Interestingly, this reduction in turn has an effect on the productions of BPs and neurons (Siegenthaler et al., 2009). While not limited to the meninges, components of

the basal lamina, such as integrins, have also been shown to affect progenitor behaviour (Stenzel et al., 2014; Wojcik-Stanaszek et al., 2011). Integrins are heterodimers consisting of different alpha and beta subunits. In the CNS, a variety of subunits have been described. More recently, it has been demonstrated that inhibition of integrin αvβ3 by echistatin reduced the number of cycling cells with basal process such as aRGs and bRGs in the ferret neocortex (Fietz et al., 2010). This data highlights the interesting capacity of the basal process in receiving signals that may influence the proliferative capacity only in basal process-bearing cells.

Recent work from our lab has highlighted the importance of ECM in determining cell fate (Fietz et al., 2010; Arai et al., 2011; Fietz et al., 2012; Stenzel et al., 2014). However, little has been done to demonstrate how the expression, production and composition of ECM components contribute to determining NPC fate. Nonetheless, recent work in adult neural stem cells has demonstrated that stiffness and topography of the tissue have a role in determining the fate of progenitors (Watt and Huck, 2013). While little has been done on the effect of biophysical properties of ECM in determining the fate of NPCs, recent studies conducted on integrin-mediated signal transduction have demonstrated the importance of ECM on cell fate. Integrins are the major receptors for the ECM constituents. Thus it is likely that the extracellular signals affecting stem cell maintenance, proliferation and differentiation by the ECM is mediated via integrins. In a recent study, activation of the residual integrin αvβ3 on mouse bIPs was shown to induce a switch in the fate of the daughter cells produced. Instead of producing neurons, these daughter cells have a capacity to re-enter the cell cycle, suggestive of a TAP-like behaviour (Stenzel et al., 2014). It would thus be interesting to determine the role ECM may play in determining cell fate, especially in the developing brain.

1.4. **Evolution of the mammalian neocortex**

"It is a question of cubic capacity," said he; "a man with so large a brain must have something in it."

~Arthur Conan Doyle

Rockel et al. (1980) reported a striking observation where underneath a millimetre of neocortical surface, the number of neurons that is present is the same across cortical areas and species, with one striking exception in the primate visual cortex (Carlo and Stevens, 2013; Rockel et al., 1980). What this necessitates is that an expansion in brain size during evolution would require these species to maintain the number of neurons within a millimetre of neocortical surface, while increasing the total number of neurons. Thus, by logic, the expansion of the neocortex would require an enlargement of the surface area without increasing the number of neurons within a cortical area. The mechanism leading to this increase in neuronal number thus became one of the main questions in the field of neurodevelopment. Since then, several hypotheses have arisen and are discussed in detail in the following section. There is however an overall theme to the following hypotheses where the evolutionary increase in neuronal productions is tightly linked to the change in the number and types of progenitor present in the germinal zone and the type of divisions these progenitors makes.

1.4.1. Radial unit hypothesis

The basis of this hypothesis that was first expounded by Pasko Rakic is the dichotomy that lies between the enormously expanded cortical surface during evolution and the lack of change in cortical thickness (Rakic, 1988, 2009). To explain this dichotomy, Rakic proposed the ontogenetic column where neuronal clones are generated by the same precursor and migrate radially in the form of cell stack according to the cell cycle that they are produced ((Rakic, 1995), **Fig. 6**). As the cortical layer is made up of these ontogenetic columns, an expansion of the neocortex is synonymous to an increase in the

number of these ontogenetic columns. This in turn can be done by increasing the number of founder cells via symmetric proliferative division of APs (**Fig. 6a**). The switch from symmetric to asymmetric division during development reflects a change from lateral to radial expansion. Asymmetric division of APs lead to the production of neurons that migrate to the CP, thus contributing to the thickness of the CP (**Fig. 6b**). The idea of expansion of the neocortex hence is tightly embedded in the switch of the mode of division of these cells. A delay in the switch together with a concurrent increase in the neurogenic period will thus lead to an increase not only in the number of ontogenetic columns but also neuronal output and expansion of the neocortex, without substantially increasing the number of neurons within each column. As described below, the radial unit hypothesis is contradicted by observations in larger-brained species and, therefore, must be considered, at best, incomplete.

1.4.2. Transit amplification by intermediate progenitor

The discovery of the bIP (Haubensak et al., 2004; Miyata et al., 2004; Noctor et al., 2004) brought about an amendment to the radial unit hypothesis. One of the limitations of the original radial unit hypothesis suggested by Rakic was that the rate of neuronal production via direct neurogenesis by aRG is relatively low and is insufficient to account for all the neurons produced that are present in the CP. With the discovery that bIPs undergo terminal symmetric division producing 2 neurons, bIPs were heralded as the major producer of neurons in the mouse (Haubensak et al., 2004; Miyata et al., 2004; Noctor et al., 2004). This became the basis of the intermediate progenitor hypothesis (Kriegstein et al., 2006; Fish et al., 2008), which states that because bIPs reside in the SVZ, it follows that a larger SVZ would lead to an increase in bIPs without a concomitant depletion of aRGs and, ultimately, an increase in neuronal output. The expanded SVZ in humans and other large-brained primates (Smart et al., 2002) provides considerable support for this hypothesis. To expand the two-step pattern of neurogenesis (first in the

VZ, followed by the SVZ) even further, the neuronal output can be increased further should these bIPs expand exponentially. This can be achieved if bIPs were to undergo symmetric proliferative division (1bIP➔2bIPs), or so-called TAP-like divisions (Lui et al., 2011) (**Fig. 6c**). As neurons produced at the end of each TAP division will have the same birth date, this will lead to lateral expansion rather than a radial expansion, thus maintaining the overall number of neurons within a column. One caveat that remains with this hypothesis is that the exponential increase in neuron without a corresponding increase in the radial glia scaffold may induce congestions in the glia-mediated neuronal migration.

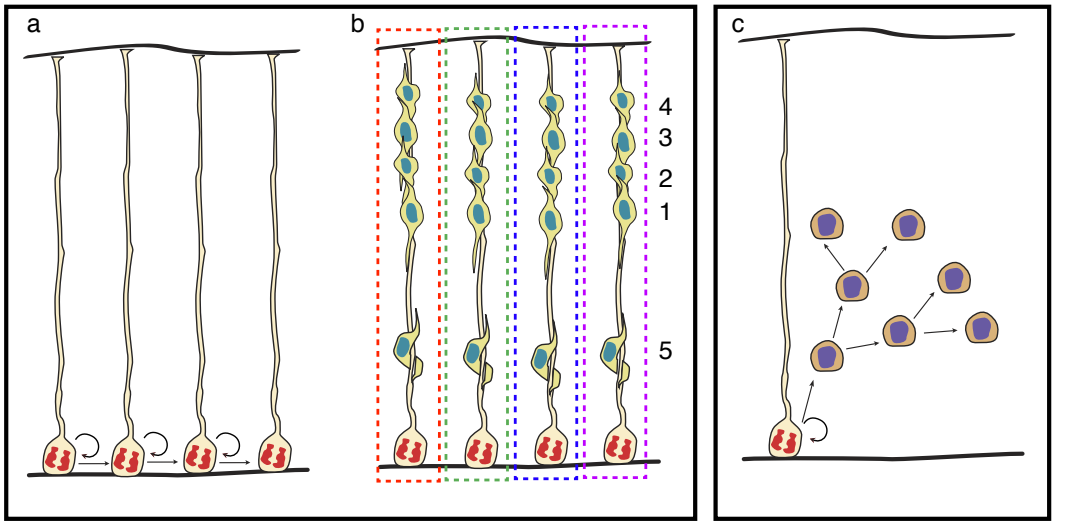

Figure 6: Hypotheses regarding the expansion of the neocortex via the radial unit hypothesis and the transit amplifying intermediate progenitor. **(a)** In the radial unit hypothesis, the aRG would first undergo symmetric proliferative division to increase the number of ontogenetic column. **(b)** The switch from the lateral expansion to radial expansion. aRG would divide asymmetrically to produce neurons directly. The neurons produced would migrate to the cortical plate in an inside out fashion. **(c)** The transit amplifying intermediate progenitor hypothesis involves a two-part progenitor production where there exist an intermediary step of bIP producing neurons.

1.4.3. The role of SVZ in the expanding the neocortex

The two-step pattern of neurogenesis as described above illustrates the importance of SVZ in the expansion of the neocortex. Although direct

neurogenesis from aRG allows for the development of ontogenetic columns, it is a highly limited mechanism for neuronal production. This is best exemplified by comparing the mammalian cortex to the reptilian cortex (Martinez-Cerdeno et al., 2006; Molnar et al., 2006; Nomura et al., 2013) (**Fig. 7**). The mammalian cortex is composed of a 6-layered cortex in comparison to the reptilian 3-layered cortex. The aRG in reptilian cortex undergoes direct neurogenesis as it lacks or has a rudimentary SVZ (Nomura et al., 2013). In addition, most mitoses occur apically, suggesting a lack of basal mitotic BPs. In the absence of the SVZ, there is a significant reduction in the neuronal output and this is reflected by the lack of upper layer neurons (layer II to IV) in the reptilian cortex (Martinez-Cerdeno et al., 2006). Based on cell morphology, connectivity and neurotransmitters, the deep layer neurons from the mammalian neocortex is more akin to the 3-layered cortex of the reptilian cortex (Aboitiz et al., 2001). This suggests that the presence of the SVZ is a prerequisite in the formation of the 6-layered cortex found in the mammalian cortex.

If the presence of the SVZ is a prerequisite to the production of the upper layer neuron, it therefore holds that the thickness of the SVZ would influence the thickness of the overall CP (**Fig. 7**). This is clearly illustrated by the comparison between the mouse and monkey cortex. While both species have a SVZ that allows for a 6-layered cortex, the SVZ of the monkey is greatly expanded (Smart et al., 2002). In species with an expanded SVZ, this germinal zone is further specialized and divided into inner and outer SVZ. Thus allowing for more BPs to reside and produce projection neurons. The expanded SVZ of monkey is also reflected by a substantial increase in upper layer neurons. In gyrencephalic animals, the generation of gyri and sulci are also marked by the difference in the proliferative capacity of the SVZ. In regions that are designated to be the prospective gyrus, the number of BPs is significantly increased (Borrell and Reillo, 2012; Lewitus et al., 2013a). For instance, in ferrets the density of outer SVZ mitoses is three-fold higher in the prospective splenial gyrus than lateral sulcus (Lewitus et al., 2013a).

While the expanded SVZ allows for more BPs, the composition of BPs also contributes to the proliferative capacity of the SVZ (i.e. the type of BPs present) (Kelava and Huttner, 2013; Lewitus et al., 2013b). While the number of neurons generated by bIP is sufficient to produce a 6-layered cortex as seen in mice cortex, the neuronal production is still limited by the fact that these cells undergo symmetric consumptive division (1bIP➔2 neurons). However, TAPs and bRGs have the capability to undergo self renewal (and even self amplification), where its neurogenic capacity can be extended to multiple rounds of cell cycles as they do not self-consume (Betizeau et al., 2013; Dehay and Kennedy, 2007; Gertz et al., 2014; Hansen et al., 2010; Lukaszewicz et al., 2005). Thus an increase in the proportion of BPs that can self-renew would increase the overall neuronal production of this germinal zone. Hence, the expansion of the SVZ is also linked to the divergence of the composition of BPs (Lewitus et al., 2013b, Fietz and Huttner, 2011). In the mouse SVZ, the majority of BPs present is bIPs (90%) while the rest is a sprinkling of bRG and TAP (Arai et al., 2011; Noctor et al., 2004; Shitamukai et al., 2011; Wang et al., 2011). Recent studies show that not only do bRGs constitute a majority percentage of the SVZ population in large-brained species (Fietz et al., 2010; Hansen et al., 2010; Lui et al., 2011) but those bRGs are remarkably diverse in their behaviour and morphology (Betizeau et al., 2013). Therefore, it seems that both an expanded SVZ and, perhaps more importantly, an increase in a diversity of bRG-types occupying that SVZ are essential for the evolutionary expansion of the neocortex.

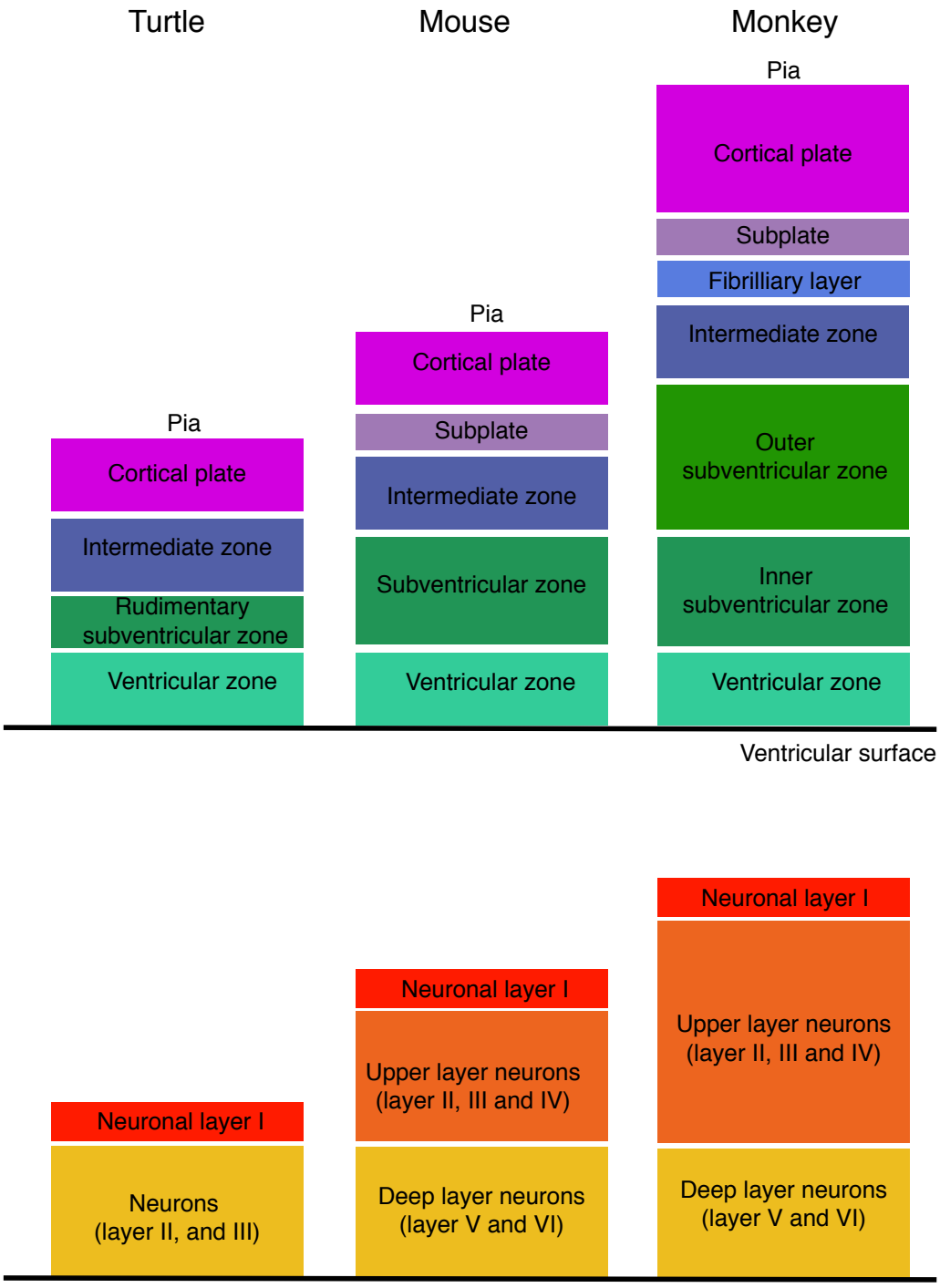

Figure 7: Comparison of the cortical layers between reptiles (such as turtle) and mammalian (mouse and human) brain for the **(top)** developing brains and **(bottom)** adult stage.

1.5. Gyrencephalic brains

In the expansion of the neocortex, the increase in the neuronal output only plays one part, albeit an important part. The problem that arises with an increase number of neurons is where to place these cells without enlarging the overall width and size of the brain in an exponential manner. Nature has solved this conundrum by creating the gyrencephalic brain, a brain that has a convoluted surface as oppose to the lissencephalic brain, which has a smooth surface (Owens, 1857) (**Fig. 8**). The convoluted surface allows for a large cortical area with its increase in neuronal numbers compacted inside a cranium by folding the surface into many gyri and sulci.

Currently, the exact mechanism leading to the folding of the brain is unknown. It is hypothesised however that bRGs may play an important role in assisting this process. The presence of these bRGs, provide additional scaffolding for these neurons to migrate to the cortical surface especially by allowing for tangential dispersion of migrating neurons due to the fanning out of the fibres (Borrell and Reillo, 2012; Kelava and Huttner, 2013; Lewitus et al., 2013a; Lui et al., 2011; Stahl et al., 2013, Fietz and Huttner, 2011). The tangential dispersion of these migrating neurons, thus provide a mechanism to allow for an increase in neuronal production and dispersion of these neurons while maintaining the total number of neurons within a millimetre of cortical area. Because Pax6 positive bRGs are abundant in gyrencephalic but not lissencephalic species (Fietz et al., 2010; Martinez-Cerdeno et al., 2012; Shitamukai et al., 2011; Wang et al., 2011, Hansen et al., 2010, Reillo et al., 2011), and the presence of these progenitor-types putatively drives cortical folding during development, we may assume that an evolutionary increase in Pax6 positive bRGs has led to neocortical expansion and gyrification in certain species. It will be interesting, therefore, to reconstitute this progenitor in the mouse – and thereby simulate its evolution in large-brained mammals – by taking messages or “instructions” from gyrencephalic animals at the peak of bRG production and introduce them into the mouse neocortex.

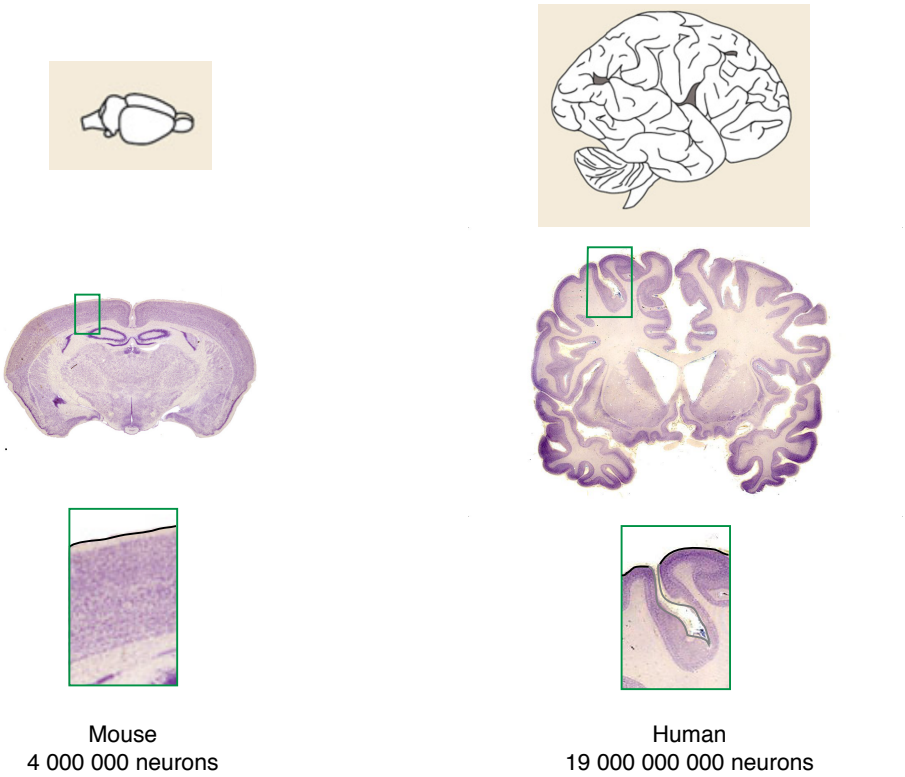

Figure 8 : Lissencephalic vs. gyrencephalic brains. (Left) Mouse brain (right) Human brain. Both drawings (Kelava and Huttner, 2013) are followed by coronal sections from the respective adult brains with a green boxed area to highlight the cortical surface difference between the mouse and human brain (images adapted from www.brainmuseum.org, permission requested). Data on the number of neurons in the cerebral cortex are obtained from Herculano-Houzel (2008).

1.6. Pax6

I am the master of my fate:
I am the captain of my soul.

~William Ernest Henley

1.6.1. Background

The paired-box family of TFs was first discovered in Drosophila gene *paired* (Bopp et al., 1986). Members of this family are distinguished by their characteristic bipartite DNA-binding regions, namely the paired-domain (PD) and homeodomain (HD). Subsequent studies have revealed that the paired-box family consists of 9 members that are conserved from the invertebrates.

Pax6, a member of this paired-box family, has been coined as the master regulator for eye development. Its discovery and functional importance that helped build this reputation arose from the genetic mutation seen in the human disease, anridia and also in the *small eye* (Sey) mouse and *eyeless* (ey) in Drosophila. Homozygous mutation of Pax6 in human is lethal and the foetus displays complete failure in eye formation and severe brain damage. The heterozygous human suffering from anridia is characterized by hypoplasia of the iris, cataract formation and glaucoma and progressive vision impairment (Ton et al., 1991). Not limited to the eye, structural brain abnormalities are also observed (Georgala et al., 2011a).

Pax6, like the rest of the paired-box family, contains two DNA binding domains linked via a glycine rich domain. Both PD and HD bind to specific DNA sequences that ultimately affect the binding affinity of one another when occupied. The ability of these domains to recognize different DNA consensus sequence allows for regulation of distinct functions by controlling particular targets either individually or collectively (Haubst et al., 2004; Holm et al., 2007; Ninkovic et al., 2010; Walcher et al., 2013). For instance, the HD, but

not PD, has been shown to play an important role in regulating the survival of mature dopaminergic neurons in the adult olfactory bulb and also in regulating lens formation and retinal specification (Haubst et al., 2004; Ninkovic et al., 2010). The PD is structured in a manner that is similar to *Pax6*. Within the PD, it contains two DNA binding regions, namely the PAI subdomain and the RED subdomain, of which the molecular function of each subdomain again supports distinct functions (Walcher et al., 2013). The Pax6 protein can be alternatively spliced to three major isoforms (**Fig. 9**), namely a canonical Pax6, a truncated form that lacks the PD ("paired-less"), and one with an insertion of 14 amino acids into the PAI subdomain of the PD, which renders the PAI subdomain null (Haubst et al., 2004; Osumi et al., 2008).

The presence of the multiple DNA-binding domains renders the Pax6 capability to be involved in several developmental processes by the same protein. The expression of Pax6 has been observed as early as E8.5 or as soon as the neural tube closes (Georgala et al., 2011a). Pax6 has been shown to be involved in the dorsal-ventral specification, NPC proliferation and neurogenesis, and axonal connection formation. However, for this set of work, the role of Pax6 in proliferation, neurogenesis and migration will be examined.

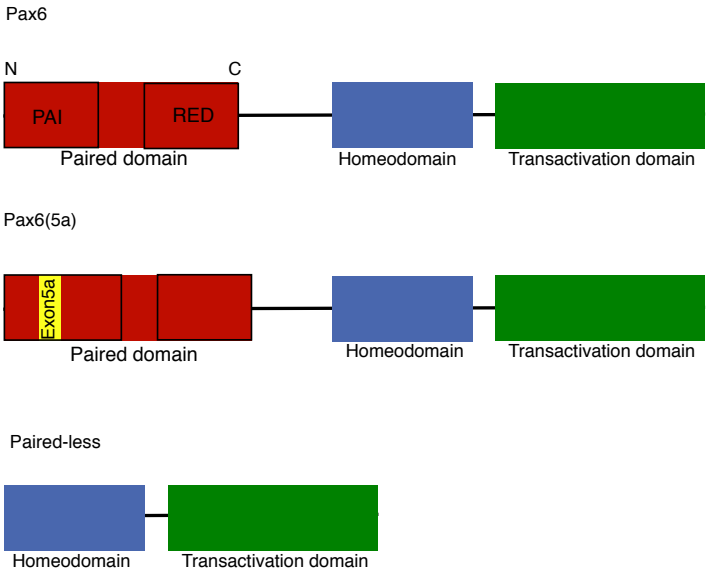

Figure 9: Various isoforms of Pax6 in the central nervous system.

1.6.2. Role of Pax6 in proliferation and neurogenesis.

Since its discovery, work done on the brain has focused mostly on dissecting the role of Pax6 in cortical development. All of the work done so far, involve genetically manipulating Pax6 expression (i.e. knockdown or overexpression) in APs. Using this approach, the role of Pax6 in cell cycle progression, neurogenesis, proliferation and migration was first discovered.

1.6.3. Pax6 and cell cycle progression

Based on the transcriptome data obtained from the cortex and hindbrain of Pax6-overexpressed and -knockout animals (Numayama-Tsuruta et al., 2010; Sansom et al., 2009), Pax6 binding sites have been found in genes that are known to regulate cell cycle progression and are thus capable of regulating cell cycle length (Mi et al., 2013; Sansom et al., 2009). Loss of function (LOF) of Pax6 in the dorsal telencephalon of the *Sey* mouse has been linked to a shorter cell cycle (Estivill-Torrus et al., 2002). These data however, can be misleading. In the *Sey* mice, the chronic loss of Pax6 has affected its role in other developmental processes such as the specification of the dorsal ventral region (Georgala et al., 2011a). Furthermore, the dorsal telencephalon is most often ventralised (Asami et al., 2011). Hence, these cells, instead of producing glutamatergic neurons, have been known to produce GABAergic interneurons. Progenitors from the ventral telencephalon have a shorter cell cycle and therefore, ventralisation of the dorsal telencephalon does not necessarily reflect the true function of Pax6 in cell cycle progression. Some of the results obtained from LOF models during early neurogenesis are contradictory (Estivill-Torrus et al., 2002; Quinn et al., 2007). From mid to late neurogenesis, however, the LOF of Pax6 has been shown to increase cell cycle length and in turn, increase the number of cells exiting the cell cycle (Estivill-Torrus et al., 2002). Similarly, in the overexpression models, the elevated Pax6 expression has been shown to lengthen cell cycle and promote cell cycle exit at late stages of corticogenesis. This reduction of progenitor pool size at the late stage of neurogenesis is reflected by the reduction in

upper layer neurons (Georgala et al., 2011b). As both LOF and gain of function demonstrated a reduction in the proliferative capacity, these findings also highlight the importance of the concentration of Pax6 protein present in the progenitor. A small shift in the equilibrium may affect the cell cycle dynamics and proliferative capacity.

The function of Pax6 is not limited to its neurogenic capability. Pax6 has also been shown to regulate proliferation and self-renewing capability of the aRG via the Wnt/β-catenin pathway (Gan et al., 2014) and Fabp7 (Arai et al., 2005). Hence, the function of Pax6 in this instance seems to be context dependent.

1.6.4. Pax6 and cell specification

As neurogenesis progresses, the progeny of the dividing NPC follows a sequence of TF expression where it first expresses Pax6, followed by Tbr2 and finally Tbr1 (Englund et al., 2005). Tbr2, like Pax6 exhibits a rostro-lateral^{high} to caudo-medial^{low} gradient (Bulfone et al., 1999). Interestingly, in the Pax6-/- mutants, APs that divide abventricularly do not express Tbr2 (Quinn et al., 2007), suggesting that Pax6 expression is required for the specification of bIP and glutamatergic projection neurons. More recently, Pax6 has been shown to directly promote bIP production by acting upstream of several TFs that play a role in specifying bIP such as Ngn2 (Britz et al., 2006; Kikkawa et al., 2013; Miyata et al., 2004; Scardigli et al., 2003), AP2γ (Holm et al., 2007; Pinto et al., 2009) and Tbr2 (Englund et al., 2005; Sansom et al., 2009).

1.6.5. Pax6 and neuronal migration

One of the most prominent features of the Pax6-/- mutant is the presence of cell clustering at the border of SVZ and IZ towards the end of neurogenesis (Schmahl et al., 1993; Stoykova et al., 1996). These mislocalised cells are neuronal in nature as they express markers such as MAP2, Sox11 and III β-

tubulin (Tuj1)(Caric et al., 1997; Fukuda et al., 2000; Lee et al., 1990). However, they seem to be unable to mature properly as they failed to express mature neuronal marker such as NeuN (Caric et al., 1997; Quinn et al., 2007). This mislocalisation of cells indicates Pax6 may play a role in neuronal migration as the abnormal maturation of cortical neuron may play a role in the inability of these cells to migrate up to the CP. In addition, Pax6 has been shown to affect the expression of certain cell adhesion molecules such as N-CAM and R-Cadherin (Asami et al., 2011; Berger et al., 2007; Stoykova et al., 1997). This altered expression may prevent these cells from migrating properly into the CP as they may form preferential attachment to one another.

1.7. Objectives

It is essential to understand our brains in some detail if we are to assess correctly our place in this vast and complicated universe we see all around us.

~Francis Crick

The expanded SVZ in the primate neocortex suggests that the increase proliferative capacity of this germinal zone has played a vital role in the expansion of the cortex (Borrell and Reillo, 2012; Fietz and Huttner, 2011; Fish et al., 2008; Kelava and Huttner, 2013; Lewitus et al., 2013a; Lui et al., 2011). The expanded SVZ has been linked to an increased number of bRG in the basal compartment as can be seen in gyrencephalic animals (e.g., ferret, macaque and human) where regions of the prospective gyrus contain more bRGs as compared to the prospective sulcus (Borrell and Reillo, 2012; Lewitus et al., 2013a). Although the presence of bRG may not be sufficient to induce gyrencephaly, the increase in self-renewing capacity in bRG may still be important in increasing neuronal production (Kelava et al., 2012). The aim of this thesis is to generate more bRGs in the embryonic mouse telencephalon. To this end, two methods were chosen: a general and a candidate approach.

1.7.1. General approach

As bRG-specific markers are still unknown, bRGs are currently identified based on their morphology, location and a combination of several cell-markers. While the exact mechanisms involved in specifying bRG generation are unknown, it is not unlikely that RNA messages involved in generating these bRGs are highest at the peak of bRG production in gyrencephalic animals. Using this logic, the general approach aims to induce the production of bRG by microinjecting pools of poly-A^+ RNA messages obtained from gyrencephalic animals such as the ferret in developmental stages coinciding with the height of bRG generation into the aRG of the mouse dorsal telencephalon and track the fate of these cells.

1.7.2. Candidate approach

As there is a significant increase in Pax6 positive cells in the SVZ of gyrencephalic animals, this work aims to recapitulate their increase by conditionally expressing Pax6 in neurogenic APs (i.e. Tis21 positive progenitors, (Haubensak et al., 2004)). As neurogenic APs are the main producers of BPs in the mouse SVZ, progeny of these cells would thus inherit the Pax6 expression. With that, one would be able to ectopically express Pax6 in the SVZ and study the effect of Pax6 in BP diversity and proliferation using the mouse model.

By using the general approach, basal process-bearing cells located at the SVZ that is characteristic of the bRG at 48 h after microinjection, were recovered. The data suggest that ferret poly-A^+ RNA preferentially generated bRG and could override the mouse neurodevelopmental programme. By using the candidate approach, we succeeded in increasing the proliferative capacity of the SVZ by increasing the percentage of self-renewing BPs (including bRGs) at the expanse of bIPs. Thus, the data from both approaches have demonstrated we have succeeded in the main objective of this doctoral work, which was to generate more bRGs in the mouse dorsal telencephalon.

Chapter 2
Results

2.1. General approach

The microinjection technique was first shown to be an effective tool to manipulate and track the fate of the single NPCs mostly in the mouse hindbrain (Taverna et al., 2012). One of the main advantages of using this technique is that it allows the expression of multiple genes simultaneously as compared to other gene delivery methods that allow for the expression of one to three genes at most (i.e. *in utero* electroporation (IUE)). The genes required for the specification and generation of bRGs are currently unknown and it is possible that the interplay of multiple genes is necessary to generate these cells. This technique thus allows one to use a shotgun or a general approach by allowing in an unbiased manner, the expression of multiple genes simultaneously without having the need to select for a specific few genes. This is done by microinjecting pool of poly-A^+ RNA messages into single cells (Taverna et al., 2012). We hypothesise that at the peak of bRG generation in the ferret brain (post natal (P) 1 or 2), the "instructions" to generate these cells is at its peak and thus able to induce the generation of bRG-like cells when delivered to the recipient cells of the mouse dorsal telencephalon.

2.1.1. Establishment of the microinjection technique in mouse dorsal telencephalon

In order to generate bRG-like cells via microinjection, we first adapted the microinjection technique to the mouse dorsal telencephalon (Wong et al., 2014). We microinjected dextran-tagged with Alexa Fluor dyes (Dx-488) into AP by targeting the apical domain of these cells via the ventricular surface of E14.5 embryos (corresponding to mid-neurogenesis, **Fig. 4**). After microinjection, the organotypic slices were either fixed immediately or cultured for 24 h before fixation. We chose to culture for 24 h as it is previously shown that the average cell cycle length of a progenitor at E14.5 is ≈24 h (Arai et al., 2011). This would thus allow the microinjected progenitors to undergo one round of cell division, following which the identity of the progeny can be examined. At 0 h, all targeted cells had a bipolar morphology and most were located close to the ventricular surface (on average, <50 μm from the surface,

Fig. 10a,d). This suggests that at t= 0 h, all microinjected cells were aRGs. At 24 h, some of the progeny still maintained the bipolar morphology of aRGs (**Fig. 10b**). Others, however, had adopted a different morphology where they appeared to be multipolar (**Fig. 10c**). Furthermore, the progeny were located further away from the ventricular surface, consistent with the lineage progression moving towards the SVZ (**Fig. 10d**). The data suggest that like previously published data on the hindbrain (Taverna et al., 2012) the microinjection technique could be used to track the fate of the microinjected cells and their progeny.

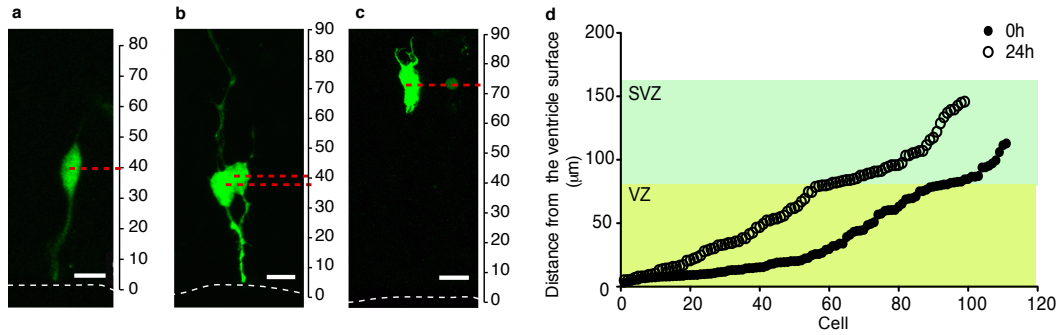

Figure 10: (a-d) Fate of microinjected cells and their progeny with dextran-3-A488 (Dx-488, green) at **(a,d)** 0 h and **(b-d)** 24 h. Dashed white lines, ventricular surface; Dashed red lines, distance from the ventricular surface; Scale bar, 20 μm. **(d)** Distance of microinjected cells and their progeny from the ventricle surface at 0 h (filled circle) and 24 h (open circle). For 0 h, n= 71 cells, 24 h, n= 97 cells. Taken from Wong et al. (2014).

2.1.2. Characterisation of microinjected cells and their progeny in mouse organotypic slice tissue

Progenitor identities are classically defined based on several criteria, namely by cell morphology, cell marker expression and location (**Table 1**). By using these criteria, we wanted to evaluate the identity of microinjected cells and their progeny by using the *Tis21*–GFP knock-in mice (Haubensak et al., 2004). Tis21 is a pan-neurogenic gene that begins expression when aRGs undergo neurogenic division (i.e. 1aRG ➔1aRG +1bIP). Additionally, we examined the expression of the bIP marker Tbr2 to determine the proportion of microinjected cells and subsequently their progeny that had committed to

become bIP. Slices were microinjected with Dextran 10 000 Alexa fluor 594 (Dx-594) and fixed at 0 and 24 h after microinjection. As described earlier, cells targeted at t=0 were bipolar and located within the VZ, indicative of aRG. However, upon closer examination, we observed around 32% and 17% of microinjected cells were positive for Tis21 and Tbr2, respectively (**Fig. 11a,c,d**). The data suggest that in addition to aRG, we have also targeted nascent bIPs that still maintain an apical contact and have yet to delaminate from the ventricular surface. After undergoing one round of cell cycle, at t=24 h, we observed an increase in proportion of basally located cells that do not have an apical contact, multipolar and were Tis21 and Tbr2 positive (55% and 47% respectively, **Fig. 11b-d**) that are likely to be bIPs. Taken together, these data demonstrate that this technique is suitable in tracking the fate of microinjected cells and their progeny at a single cell resolution.

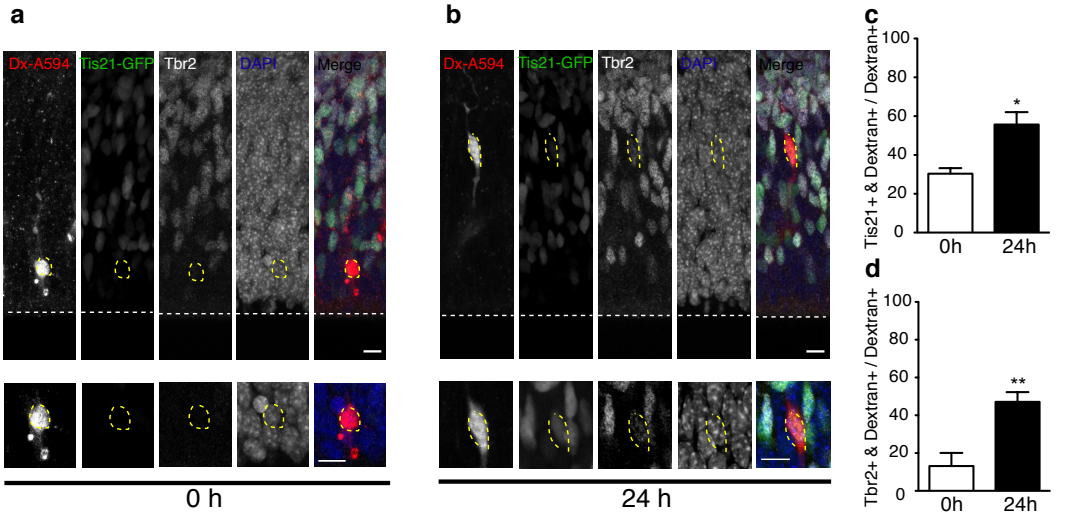

Figure 11: Evaluation of cell population of microinjected cells in organotypic slices at **(a)** 0 and **(b)** 24 h after microinjection on E14.5 dorsal telencephalon of the *Tis21*–GFP (green) knock-in mouse using dextran 10 000 A594 (Dx–A594, red). Slices were stained with DAPI (blue) and Tbr2 (white). White dashed lines, ventricular surface; yellow dashed lines, dextran positive cells; Scale bar, 20 µm. Percentage of cells that were **(c)** Tis21+ and **(d)** Tbr2+ at 0 (white bars) and 24 h (black bars) after microinjection. Bars represent the mean percentage of 3 independent experiments ± SEM; 0 h, n= 67 cells, 24h, n= 97 cells. * p<0.05. ** p<0.01. Taken from Wong et al. (2014)

2.1.3. Acute manipulation of aRGs with Rac1 dominant-negative protein in mouse dorsal telencephalon

As we had successfully tracked the fate of the microinjected cells and their progeny, we wanted then to investigate if the same technique could be used to manipulate APs. As a proof of principal, we microinjected dominant-negative Rac1 protein (Rac1 DN, 0.5 μg protein μl^{-1} final concentration) together with Dx-A488 and studied the behaviour of microinjected aRG acutely (6 h in culture). We chose to study the effect of Rac1 DN acutely as previous work has demonstrated that 6 h was sufficient time for a recombinant protein to elicit an effect (Taverna et al., 2012). Rac1 is a small GTPase involved in progenitor proliferation and survival in the developing dorsal telencephalon (Leone et al., 2010). In aRG microinjected with Rac1 DN protein (**Fig. 12**), a significant increase in the proportion of Tbr2 positive cells was observed (**Fig. 12b**). Although no significant difference in the distance of the microinjected cells from the ventricle surface was observed, Rac1 DN microinjected cells tend to be located closer to the surface. This is consistent with the previously published data that Rac1 disruption may have an effect on IKNM (Minobe et al., 2009). Together, this suggests that an acute disruption of Rac1 activity was sufficient to induce a change in cell fate and plausibly disrupted certain cell behaviour such as IKNM. We therefore conclude that by using microinjection we could manipulate and track the fate of the single APs in the dorsal telencephalon.

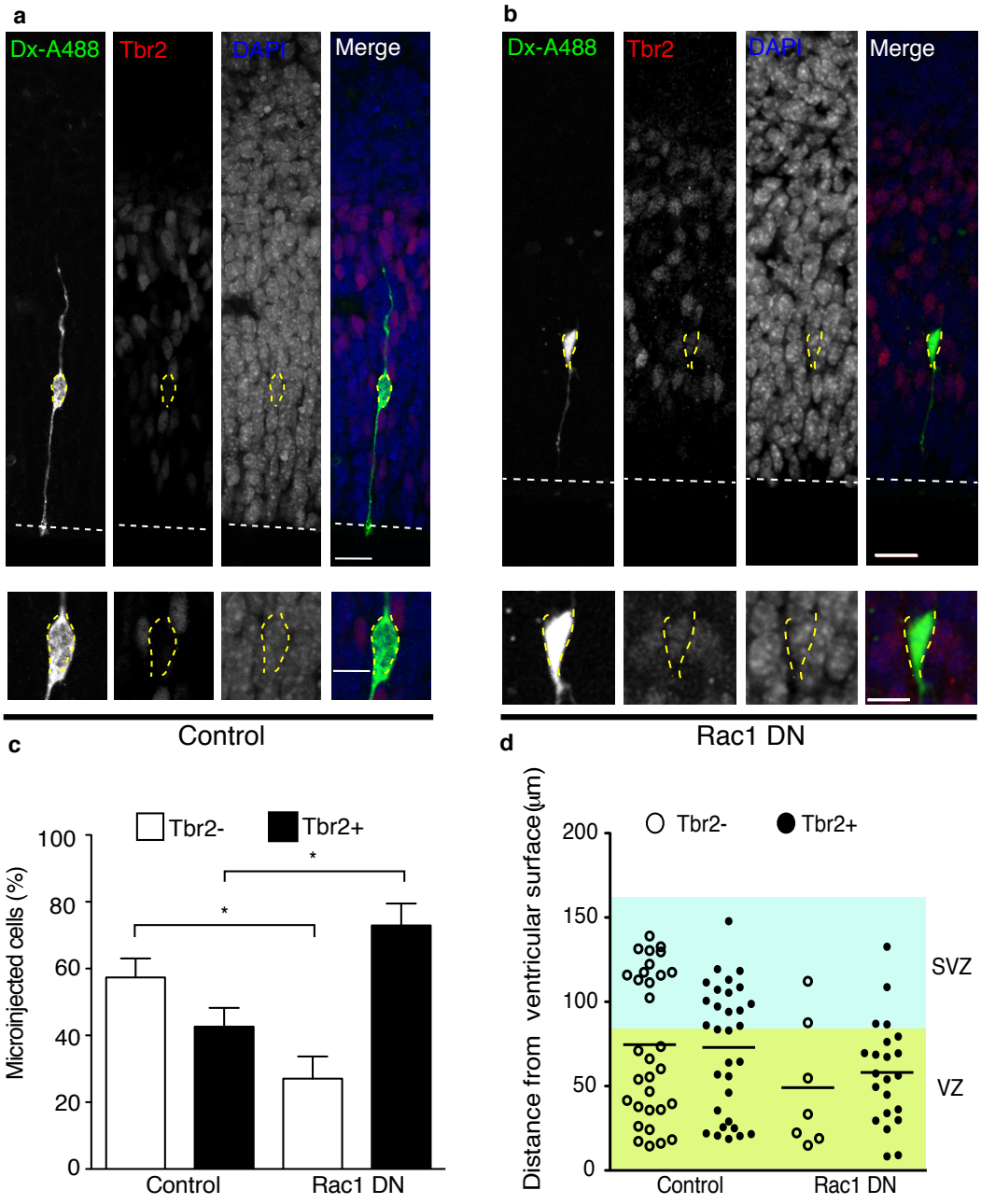

Figure 12: Acute manipulation of Rac1 induces cell fate change. Microinjection of **(a)** control (Dextran-3-A488, Dx-A488) and **(b)** Rac1 dominant-negative (DN) protein together with Dx-A488 at 6 h after microinjection. Sections were stained for DAPI (blue) and Tbr2 (red). White dashed lines, ventricular surface; scale bar, 20 μm **(c)** Percentage of cells that are Tbr2–(white) and Tbr2+(black) at 6 h after microinjection in control (left two bars) and Rac1 DN (right two bars). Mean ± SEM from 3 independent experiments; control = 62 cells; Rac1 DN = 29 cells. * $p<0.05$. **(d)** Distance of microinjected cells from the ventricular surface with Tbr2–(open circles) and Tbr2+(filled circles) in control (2 left scatter plots) and Rac1 DN (2 right scatter plots). Sum from 3 independent experiments; control = 62 cells, Rac1 DN = 29 cells. Taken from Wong et al. (2014).

2.1.4. Characterisation of the microinjected cell and their progeny in ferret slice tissue

To demonstrate the versatility of this technique, we adapted the microinjection technique to a non-conventional species, dorsal telencephalon of developing ferret pups (in collaboration with Dr Elena Taverna). Organotypic slice tissues obtained from P1 ferret pups were microinjected with Dx-A488 and were kept in culture for up to 48 h. At 0 and 24 h, all dextran positive cells recovered were bipolar cells, most likely aRGs. At 48 h, however, in addition to the recovery of bipolar cells, we also recovered delaminated, basally located, monopolar cells that had a basal process (likely bRG) (**Fig. 13**). The recovery of a different progenitor type only at 48 h is consistent with the longer cell cycle of the ferret (≈40 h) (Reillo et al., 2011; Turrero García, 2013), thus suggesting that the bRG-like cells recovered were plausibly generated after the microinjected cells had undergone cell division. The data suggest that the microinjection technique could be adapted to track the fate of microinjected cells even in non-conventional species such as the ferret. Of note, in order to do so, one would have to adapt the slice culture according to the developmental differences (i.e. cell cycle length) between species.

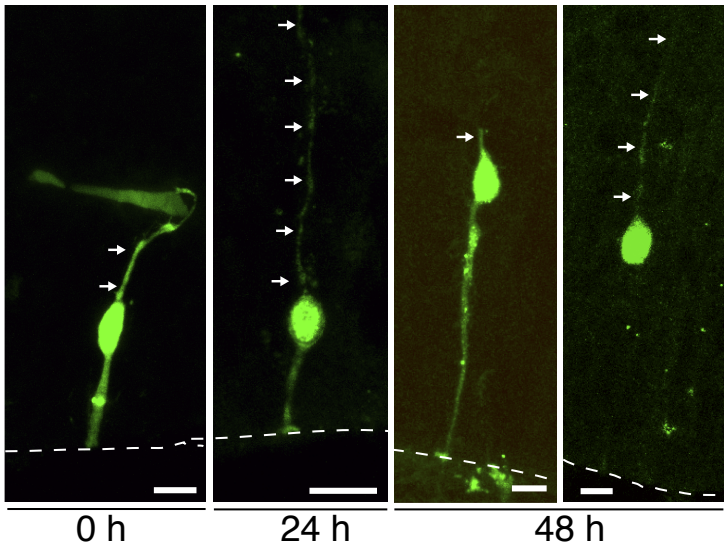

Figure 13: Evaluating the fate of microinjected cells in ferret slice tissue. P1 ferret slice tissues were microinjected with Dextran-3-A488 (green) and kept in culture for 0, 24 and 48 h after microinjection. The fate of microinjected cells and their progeny was established based on cell morphology. White arrows, basal process; dashed white lines, ventricular surface; scale bar, 10 µm. Taken from Wong et al. (2014).

2.1.5. Microinjection of in vitro transcribed RFP poly-A$^+$ mRNA

We next wanted to determine the translational efficiency of microinjected poly-A$^+$ RNA message using an *in vitro* and *in vivo* system. Microinjection of RNA messages is typically conducted with a co-injection of a trace amount (1%) of *in vitro* transcribed RFP (IVT-RFP) poly-A$^+$ mRNA that acts as a reporter message, together with the Dextran-tagged Alexa fluor dyes (Taverna et al., 2012). As it is unlikely that the pool of microinjected mRNA are selectively translated, all co-injected cells that translate the reporter IVT-RFP poly-A$^+$ mRNA are likely to translate the rest of the microinjected poly-A$^+$ RNA messages. We first tested the translation efficiency by microinjecting only the IVT-RFP poly-A$^+$ mRNA (0.5 μg μl^{-1} final concentration) *in vitro* using HEK293T cells. Cells were fixed 24 h later. At 24 h, 79% of the dextran positive cells were RFP positive while the remaining cells were dextran positive but RFP negative (i.e. cells were microinjected but did not translate the mRNA) (**Fig. 14**) suggesting that the efficiency of translating the poly-A$^+$ mRNA *in vitro* was relatively high in cells.

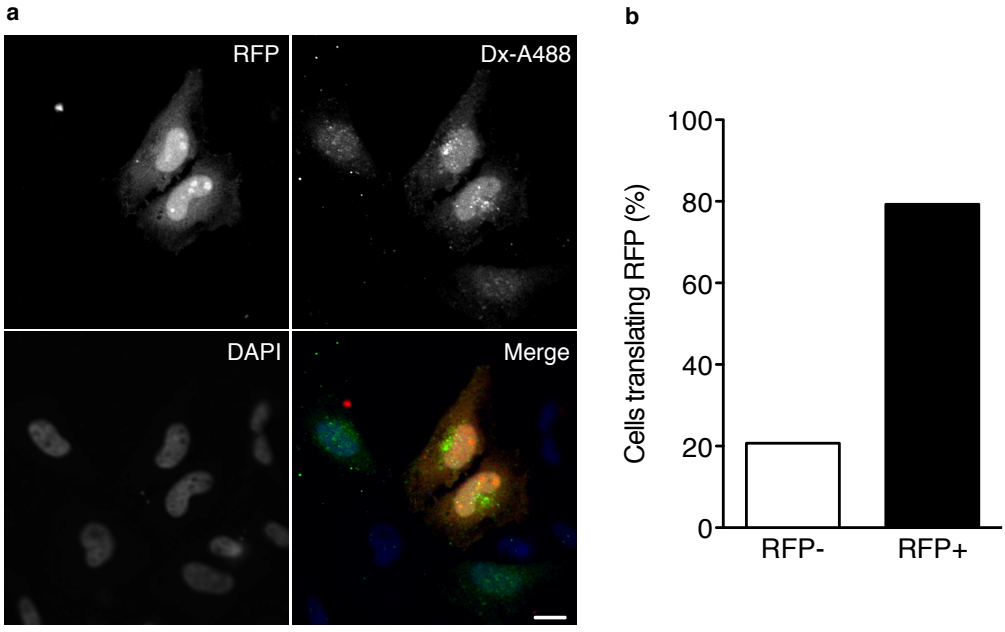

Figure 14: Microinjection of the *in vitro* transcribed RFP (IVT-RFP) message in HEK293T. **(a)** Cells were microinjected with Dextran-3-A488 (Dx-A488, green) and were kept in culture for 24 h after microinjection. Cells were then stained for RFP (red) and DAPI (blue). Scale bar, 20 µm **(b)** Percentage of microinjected cells that are RFP– (white) and RFP+(black), n=96 cells.

We next sought to determine the translational efficiency *in vivo.* We first microinjected the IVT-RFP poly-A$^+$ mRNA in the hindbrain and the dorsal telencephalon, in order to determine whether there is a regional difference in translation. In both regions, around 20% (**Fig. 15**, 17% and 19% respectively) of dextran positive cells were RFP positive, suggesting that there is no difference in the translational efficiency between regions. In the hindbrain, it was previously reported that around one third of dextran positive cells translate the IVT-RFP poly-A$^+$ mRNA (Taverna et al., 2012). The cause for this low translational efficiency observed in both instances is currently unknown, but the presence of both microinjected cells that translate and do not translate the poly-A$^+$ mRNA provide a valuable internal control in future experiments.

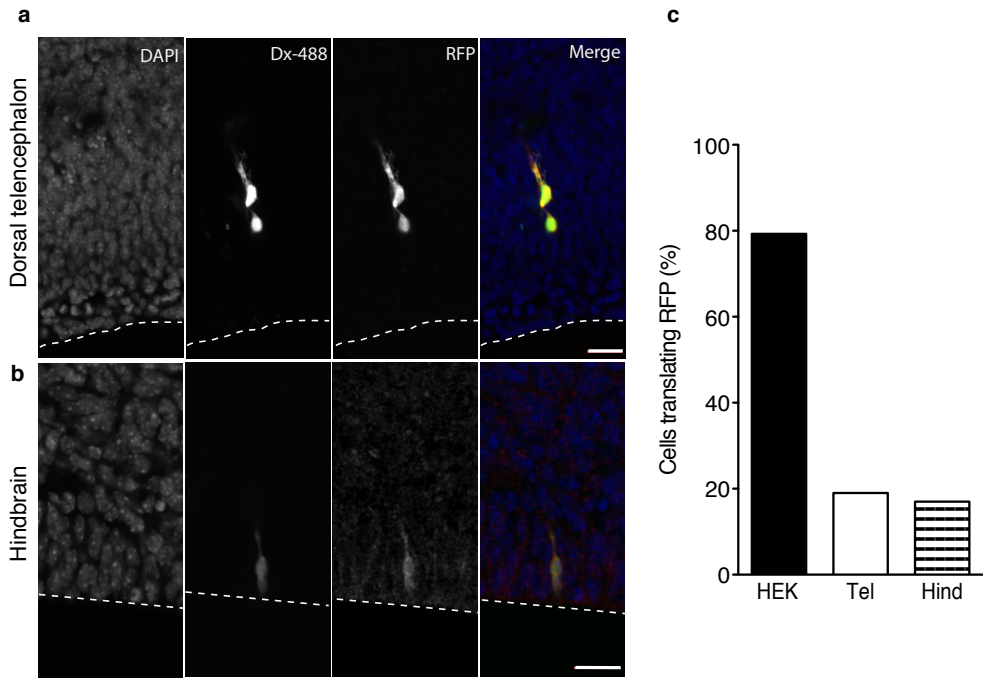

Figure 15: Microinjection of the *in vitro* transcribed RFP (IVT-RFP) poly-A$^+$ mRNA together with Dextran-3-A488 (Dx-A488, green) in **(a)** dorsal telencephalon and **(b)** hindbrain. Slices were kept in culture for 24 h and were stained for RFP (red) and DAPI (blue). White dashed lines, ventricular surface; scale bar, 20 µm. **(c)** Percentage of microinjected cells that expressed RFP in HEK293T cells (HEK, black), dorsal telencephalon (Tel, white) and in the hindbrain (Hind, striped). For HEK, n= 96 cells, for Tel, n=37 cells, for Hind, n= 7 cells.

2.1.6. Microinjection of ferret poly-A$^+$ RNA message in the mouse dorsal telencephalon

As the previous sets of experiments demonstrated that we had successfully established the microinjection technique in the dorsal telencephalon of mouse and ferret neocortices, we went on to the main aim of our experiments which was to manipulate and track the fate of cells microinjected with poly-A$^+$ RNA messages obtained from a gyrencephalic animals such as ferret in a lissencephalic animal. A pool of ferret poly-A$^+$ RNA message (0.5 μg μl^{-1} final concentration), a trace of IVT-RFP (0.02 μg μl^{-1} final concentration) and Dx-A488 were microinjected into aRGs of the mouse dorsal telencephalon and were kept in culture for 24 h. In total, 49 dextran positive cells were recovered and out of these cells, only 3 were RFP positive. All 3 RFP positive cells were bipolar and located in the VZ, thus, most likely were aRG (**Fig. 16**).

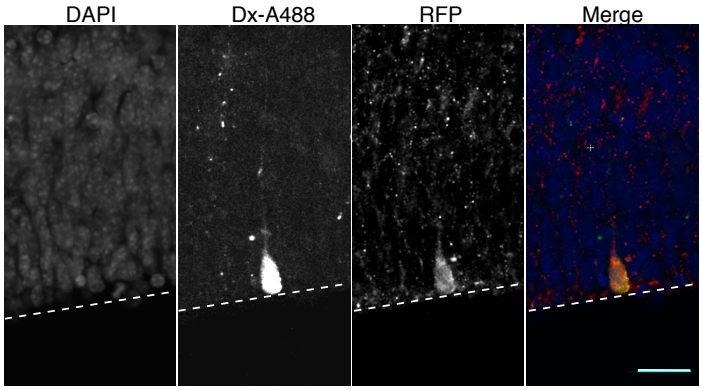

Figure 16: Evaluation of the effect of ferret poly-A$^+$ RNA message in inducing cell fate change at 24 h after microinjection. Microinjection of ferret poly-A$^+$ RNA, *in vitro* transcribed RFP (IVT-RFP, red) mRNA and Dextran-4-A488 (Dx-A488, green) in the dorsal telencephalon. Nuclei were stained with DAPI (blue). White dashed lines, ventricular surface; scale bar, 20 µm.

We then examined the fate of the cells microinjected with ferret poly-A$^+$ RNA at 48 h. Using our current protocol, high levels of pyknotic nuclei in the SVZ was observed (**Fig. 17**, left), making it difficult to detect or ensure the survival of the basally located, delaminated bRG. We attributed this increase in pyknotic nuclei to the prolonged tissue-handling prior and during microinjection. Hence, we modified the current microinjection protocol (Taverna et al., 2012; Wong et al., 2014) to cater for longer organotypic slice

culture. Instead of sectioning the slice tissues using the vibratome, we opted to slice the mouse brain manually using a microknife as this would reduce the amount of time required for tissue handling prior to microinjection. Consequently, we observed a reduction in the number of pyknotic nuclei in the SVZ and an overall improvement in tissue condition (**Fig. 17**, right).

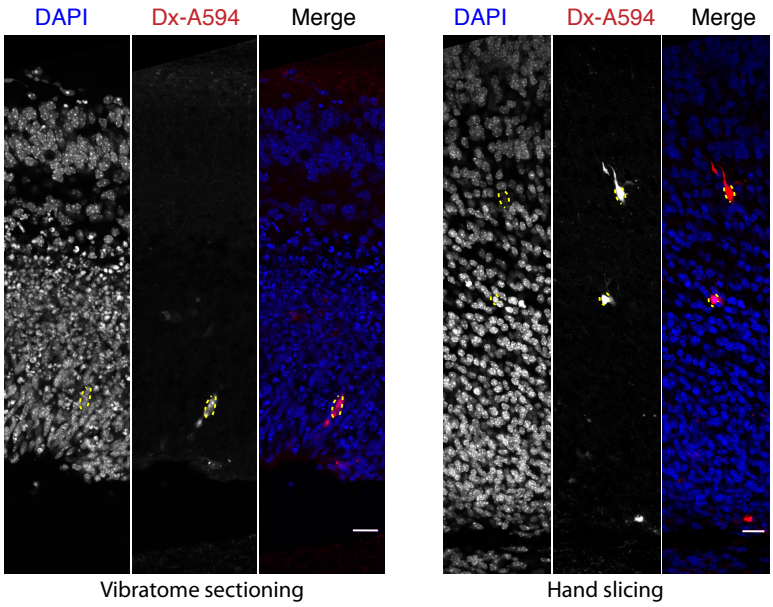

Figure 17: Optimisation of microinjection protocol for long-term slice culture. E14.5 slices obtained from vibratome sectioning (left) or by hand slicing (right) to ≈250 μm were microinjected with dextran-594 (Dx-A594, red) and were kept in culture for 48 h after microinjection. Nuclei were stained with DAPI (blue). Scale bar, 10 μm.

We then repeated the experiment described previously but kept slices in culture for 48 h instead of 24 h. We recovered 15 dextran positive cells, of which 4 expressed RFP, thus making the translational efficiency ≈27%. In all of the dextran positive but RFP negative cells, these cells were basally located and were multipolar, similar to a neuron (**Fig. 18**). Interestingly, in 3 out of 4 of the cells that were RFP positive, these cells were basally located, delaminated monopolar cells that had a basal process, reminiscent of a bRG. The data suggest that the pool of ferret poly-A^+ RNA was sufficient to override the inherent differentiative mouse program and the inherently low bRG production in the mouse SVZ, thus altering the fate of these cells as judged by cell morphology. Furthermore, the high recovery of bRG-like cells in the RFP positive population suggests that the pool of ferret poly-A^+ RNA contained

sufficient information and preferentially generated bRG-like cells in a model organism in which bRG is physiologically present in low abundance (Martinez-Cerdeno et al., 2012; Reillo et al., 2011; Shitamukai et al., 2011; Wang et al., 2011, Fietz et al., 2010).

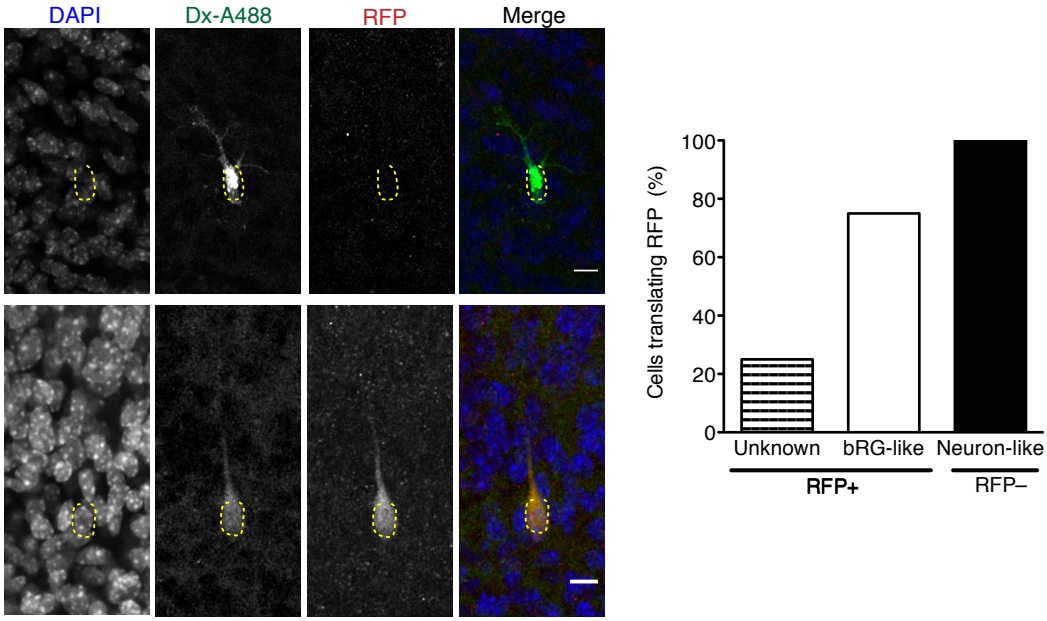

Figure 18: Evaluation of the effect of ferret poly-A$^+$ RNA message in inducing cell fate change at 48 h after microinjection. Microinjection of ferret poly-A$^+$ RNA, *in vitro* transcribed RFP (IVT-RFP, red) mRNA and Dextran-4-A488 (Dx-A488, green) in the dorsal telencephalon. Nuclei were stained with DAPI (blue). Scale bar, 10 µm. Graph on the right depicts the percentage of recovered dextran positive cells that are RFP+ and RFP– and grouped according to the cell type based on their cell morphology. n=15 cells.

2.2 Candidate approach

Although we have successfully generated bRG-like cells by microinjection of P1 ferret poly-A^+ RNA messages, the recovery of cells translating the poly-A^+ RNA messages is relative low. We thus opted to generate more bRGs in the embryonic mouse brain using a candidate gene approach via IUE. As IUE targets significantly more cells at a given time, it would increase the throughput of bRG production. We chose the TF Pax6 as it has been shown to play a major role in proliferation and neurogenesis, albeit only in aRG. However, we believed that the evolutionary significance of this TF has not been fully explored as there is a significant increase in the number of Pax6 positive cells in the SVZ of gyrencephalic neocortex corresponding to an increase in bRGs when compared to the mouse SVZ (Borrell and Reillo, 2012; Kelava and Huttner, 2013; Lui et al., 2011, Fietz and Huttner, 2011). We thus hypothesised that Pax6 may play a role in the generation of bRGs and ultimately a vital role in the evolutionary expansion of the neocortex.

2.2.1. Characterisation of the Tis21–CreER^{T2} mouse

As the majority of the mouse BPs is generated by neurogenic, Tis21 positive aRGs, we used an approach that allows conditional expression of Pax6 in Tis21 positive progenitors. To target this particular progenitor population, the *Tis21*–CreER^{T2} mouse was used. This would thus allow the progeny of the Tis21 positive aRG to inherit Pax6 expression and ultimately induce the ectopic expression of Pax6 in the SVZ.

The *Tis21*–CreER^{T2} mouse line was previously established in the lab by Dr Jifeng Fei where the entire coding sequence of the *Tis21* exon 1 was replaced with CreER^{T2} (Fei, 2008). As characterization of the mouse line was previously done at an earlier developmental stage (E10.5) (Fei, 2008), we characterized the mouse at mid-neurogenesis (E13.5), the time point in which BP-genesis is at its peak and the time point in which we would like to conditionally express Pax6. We first checked for the localization of the Cre protein (identified by HSV immunostaining as the Cre protein contains a HSV-

tag) by crossing the mice with the homozygous *Tis21*–GFP knock-in mice (Haubensak et al., 2004). The Cre expression co-localized with the *Tis21*–GFP expression where Cre is expressed only in the cytoplasm of Tis21 positive cells in the absence of tamoxifen (**Fig. 19**).

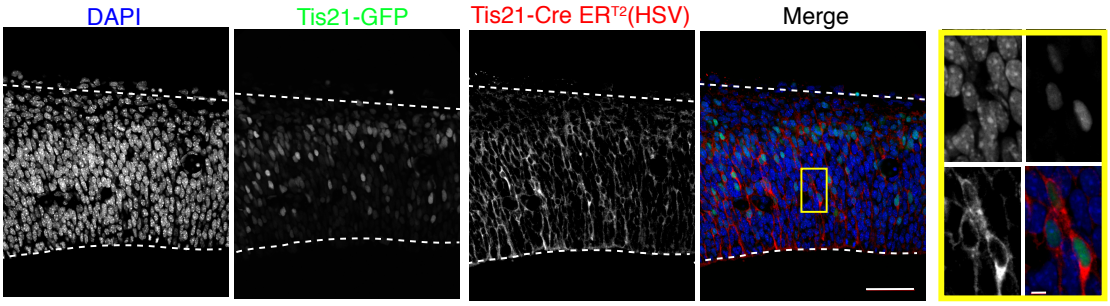

Figure 19: Localisation of Cre in *Tis21*–GFP positive cells. Immunofluorescence staining of Cre (identified by HSV tag, red) on E13.5 *Tis21*–GFP+/+ crossed with *Tis21*–CreER^{T2}+/+ embryos (cryosections). Nuclei were stained with DAPI (blue). Dashed white lines, outline of the tissue; scale bar, 20 µm. Yellow box inset show magnification of *Tis21*–GFP (green) and Cre positive cells. Scale bar, 5 µm.

We then determined the efficiency and fidelity of the inducible system by crossing either the heterozygous and homozygous *Tis21*–CreER^{T2} mutants, with a reporter line, the RCE:loxP (Jackson). The RCE:loxP is a mouse line that harbours a Rosa26 promoter driving the expression of a STOP cassette flanked by two loxP sites followed by GFP. Upon Cre recombination, the LoxP sites containing the STOP signal are excised, allowing for the expression of GFP. To induce Cre recombination, we treated the mouse with tamoxifen orally at E13.5 and examined the telencephalon 24 h later. In the absence of tamoxifen, no GFP positive cells were observed in the *Tis21*–CreER^{T2} homozygous mutant (**Fig. 20a,b**). When treated with tamoxifen, no GFP positive cells were observed in *Tis21*–CreER^{T2}–/– telencephala, whereas GFP positive cells were observed only in the *Tis21*–CreER^{T2} heterozygous telencephala (**Fig. 20a,c,d**). Based on these findings, we conclude that the *Tis21*–CreER^{T2} is suitable for subsequent experiments as the inducible system was efficient and specific to cells in the embryonic dorsal telencephalon.

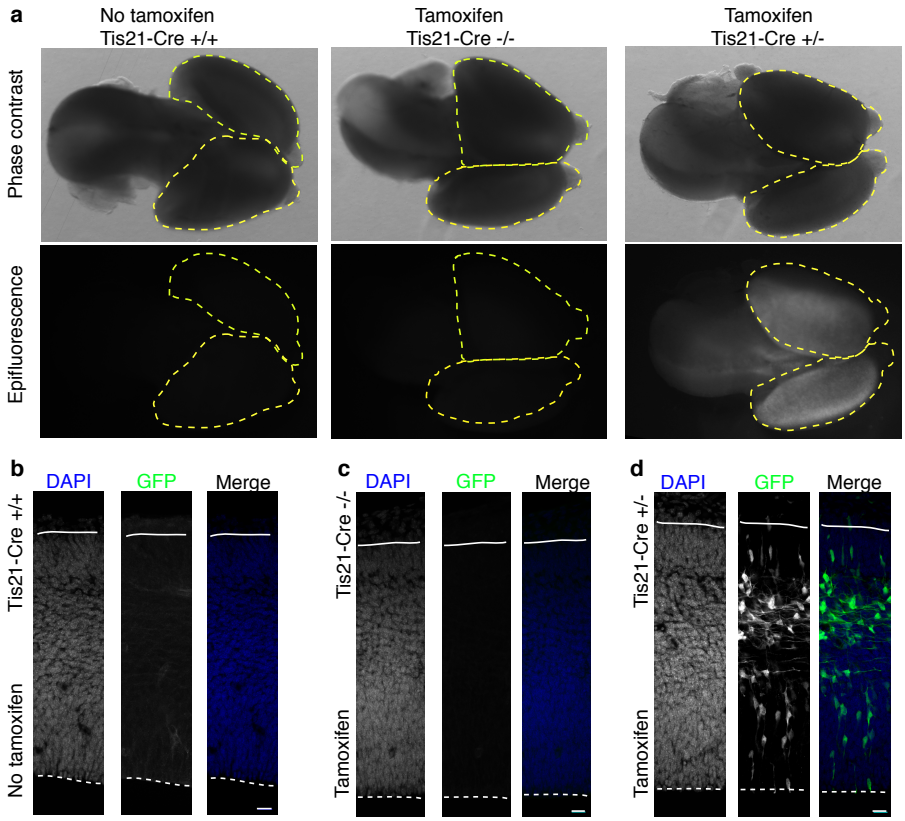

Figure 20: Cre recombination can only occur in the presence of estrogen analog, tamoxifen. **(a-d)** E13.5 embryos crossed with RCE:loxP with either heterozygous or homozygous *Tis21*–CreER^{T2}, with and without tamoxifen treatment. **(a)** Whole brain phase contrast (top) and epifluorescence (bottom) for the different crossings and tamoxifen treatment. Dashed yellow lines, outline of brain hemispheres. **(b-d)** GFP immunofluorescence of the dorsal telencephala of the various crossing and tamoxifen treatment. Presence of GFP (green) positive cells demonstrated successful Cre recombination. Nuclei were stained with DAPI (blue). Dashed white lines, ventricular surface; solid white line, pia surface; scale bar, 20 µm.

2.2.2. Conditional expression of Pax6 in neurogenic progenitors

To conditionally express Pax6 in the neurogenic aRG, we constructed a plasmid containing a Gap43–GFP cassette flanked by two loxP sites under the CAG promoter followed by nuclear RFP (nRFP) and/or Pax6 (**Fig. 21**). In the absence of Cre, the constitutively active CAG promoter will only drive the expression of the membrane-localised GFP. In the presence of Cre however, the Gap43–GFP cassette is excised, leading to simultaneous expression of Pax6 and nRFP. In the control, a similar plasmid was used but without the coding sequence for Pax6 in the region following the Gap43–GFP cassette.

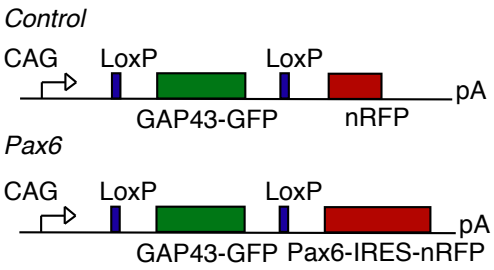

Figure 21: Constructs used for conditional activation of Pax6.

The efficiency and fidelity of the plasmid was first tested *in vitro* using a cell line devoid of endogenous Pax6 expression such as HEK293T (**Fig. 22**). Lipofectamine transfected cells with either control (not shown) or Pax6 only construct were GFP positive in the absence of Cre. Cells transfected with both control and a Cre-recombinase expressing construct were stained positive for RFP but not Pax6. However, in cells transfected with Pax6 and a Cre-recombinase expressing construct, almost 100% of these transfected cells were both RFP and Pax6 positive, demonstrating that Cre was able to excise the GFP containing cassette, thus allowing the expression of Pax6 and RFP simultaneously.

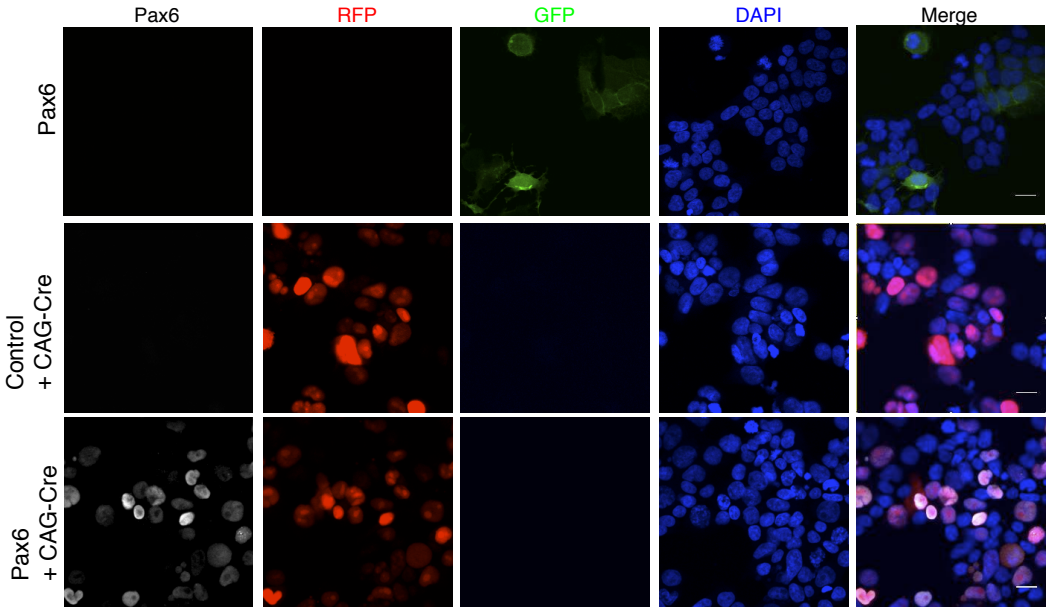

Figure 22: Lipofectamine transfection of constructs in HEK293T cells. Immunofluorescence of Pax6 (white) on lipofectamine transfected cells after 48 h. In the absence of Cre (first row), only Gap43–GFP (green) was expressed. In the presence of Cre, the control-transfected cells expressed RFP (red) but not Pax6 (middle row) while for Pax6, in the double transfection of Pax6 and Cre recombinase constructs (last row), transfected cells expressed Pax6 and RFP. Scale bar, 20 µm.

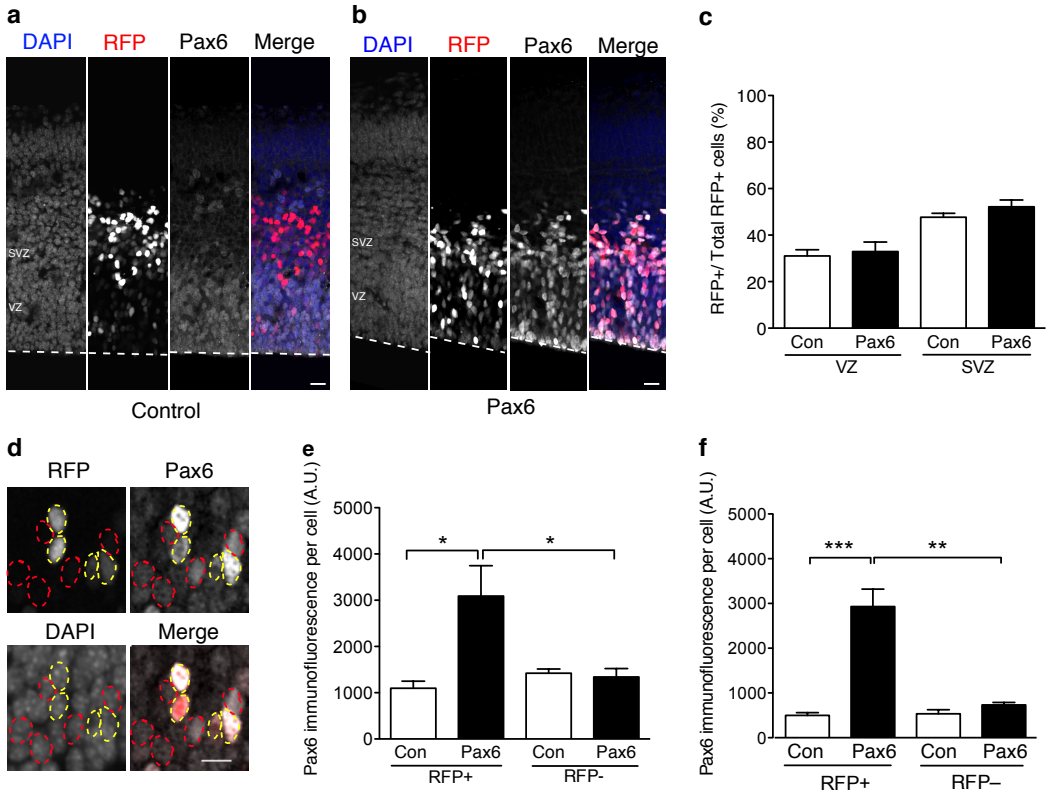

Figure 23: Conditional expression of Pax6 in E14.5 heterozygous *Tis21*–CreER^{T2} embryos at 24 h after IUE. **(a,b)** Immunofluorescence of Pax6 (white) in **(a)** control and **(b)** Pax6 electroporated cells to determine the colocalisation of Pax6 and RFP (red) positive cells. Nuclei were counterstained with DAPI (blue). Dashed white lines, ventricular surface; scale bar, 20 µm. **(c)** Distribution of RFP positive cells in the different germinal zone in control (white bars) and Pax6 (black bars) electroporated cells. Mean of 3 independent experiments ± SEM. Each experiment = 2-4 embryos **(d-f)** Quantification of the immunofluorescence intensity of Pax6 protein. **(d)** The immunofluorescence intensity of Pax6 was measured in RFP+ (dashed yellow outlines) and RFP– cells (dashed red outlines) in control and Pax6 in **(e)** VZ and **(f)** SVZ. Values are mean corrected total cell fluorescence (against background) ± SEM of 4 embryos. * $p<0.05$, ** $p<0.01$, *** $p<0.001$.

We then tested the constructs in the *Tis21*–CreER^{T2} mouse line by IUE and examined the effects 24 h later. Throughout this entire setup, we first induced the translocation of Cre by administrating tamoxifen prior to (E12.5) and on the day of IUE (E13.5). We observed a significant increase in the number of Pax6 positive cells in the SVZ when electroporated with the Pax6 construct and these cells had almost 100% co-localisation with RFP positive cells (**Fig. 23a,b**). We then examined the distribution of electroporated cells in the germinal layers of E14.5 dorsal telencephalon (**Fig. 23c**). We observed no significant difference between control and Pax6 groups in the VZ and SVZ

suggesting that Pax6 expression at 24 h did not alter the distribution of the electroporated cells (RFP positive).

We then examined the relative amount of Pax6 that were expressed by the electroporated cells via immunofluorescence intensity. In the VZ, cells electroporated with the control plasmid were positive for Pax6 as they were mostly aRGs that inherently expressed Pax6. Hence, no significant difference was observed in the immunofluorescence intensity between RFP positive and negative cells in the VZ (**Fig. 23a,e**). In the SVZ of control embryos, the RFP positive cells were stained negative for Pax6, consistent with the fact that these cells were bIPs produced by asymmetric division of Tis21 positive aRGs (**Fig. 23a,f**). For brains that were electroporated with the Pax6 constructs, however, there was a significant increase in the Pax6 immunofluorescence signal intensity in the electroporated population in both VZ and SVZ (3-fold and 6-fold difference respectively, **Fig. 23b,e,f**) where even bIPs in the SVZ were stained positive for Pax6, demonstrating that the plasmid was sufficient in inducing the ectopic expression of Pax6 in the SVZ of mouse dorsal telencephalon.

2.2.3. Conditional expression of Pax6 does not induce apoptosis

The function of Pax6 has been described to be concentration dependent where a slight alteration in the balance may elicit different responses (Sansom et al., 2009). It was previously reported that conditional expression of Pax6 using Emx2-Cre and hGFAP-Cre mouse lines have shown a significant increase in apoptosis (Berger et al., 2007) due to high levels of Pax6 expression. As Emx2 and hGFAP are both expressed by APs, albeit at different time points, we wanted to investigate whether conditional expression of Pax6 in the neurogenic aRG would similarly induce apoptosis. To detect apoptotic cells, sections were stained for caspase-3. Quantification of the number of caspase-3 positive cells (**Fig. 24**) and pyknotic cells (data not shown) showed no significant difference between groups, suggesting that conditional expression of Pax6 in neurogenic APs, unlike previously reported

(Berger et al., 2007), does not induce cell death in the electroporated neurogenic AP.

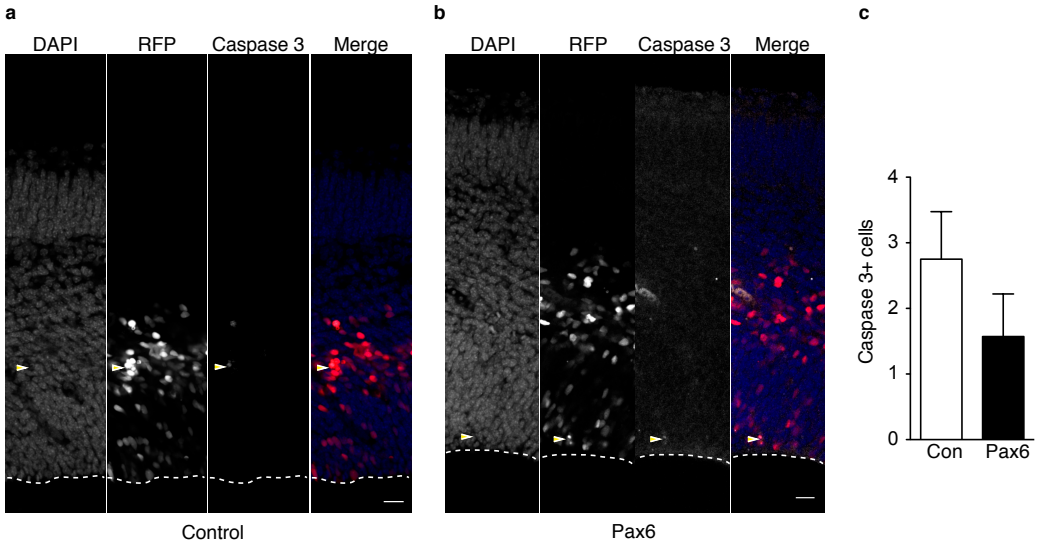

Figure 24: Conditional expression of Pax6 in E14.5 heterozygous *Tis21*–CreER^{T2} embryos at 24 h after IUE does not induce cell death. **(a,b)** Immunofluorescence for caspase-3 (white) in embryos electroporated with **(a)** control or **(b)** Pax6 plasmids. Nuclei were stained with DAPI (blue). Dashed white lines, ventricular surface; arrowheads, caspase-3 positive cells; scale bar, 20 µm. **(c)** Quantification of number of caspase-3 positive cells among electroporated cells (RFP+) within a 200 µm wide electroporated area of the dorsal telencephalon in control (white bar) and Pax6 (black bar). Mean ± SEM from 3 independent experiments; each experiment = 2 embryos.

2.2.4. Conditional expression of Pax6 increases number of cycling cells

As conditional expression of Pax6 increased the number of Pax6 positive cells in the SVZ of the mouse dorsal telencephalon, we wanted to determine whether these cells were progenitors or cells that have differentiated (i.e. direct neurogenesis). Hence, the marker for cycling cell, Ki67, was used to determine whether these cells were in fact progenitors (**Fig. 25**). Surprisingly, a significant increase in the number of Ki67 positive cells among the RFP positive population was observed when conditionally expressing Pax6 (**Fig. 25c**). To determine whether this effect was specific to a particular germinal zone, the percentage of Ki67 and RFP double positive cells in the VZ and SVZ respectively was quantified. While no difference was observed in the VZ, what was surprising was that there was a significant increase in the

percentage of Ki67 positive cells in the SVZ when Pax6 was conditionally expressed. The data suggest that conditional expression of Pax6 increases the percentage of cycling cells, specifically in the SVZ.

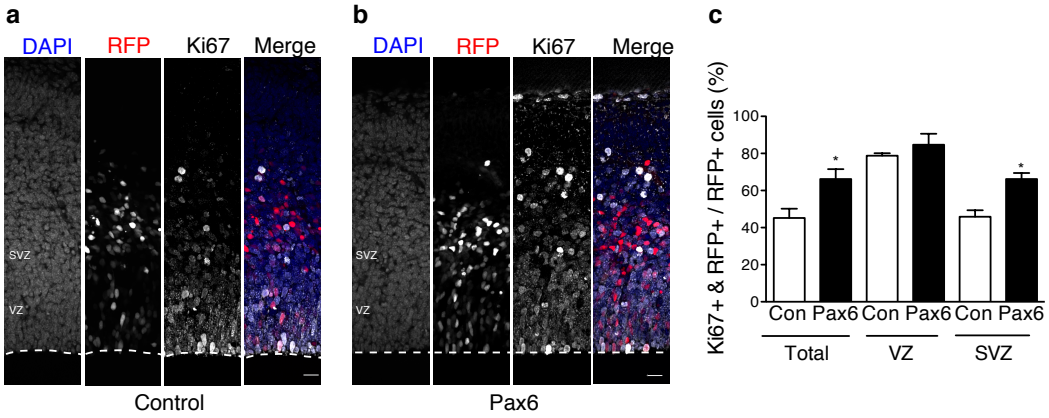

Figure 25: Conditional expression of Pax6 in E14.5 heterozygous *Tis21*–CreER^{T2} embryos at 24 h after IUE increases percentage of Ki67 positive cells specifically in the SVZ. **(a,b)** Immunofluorescence for Ki67 (white) in embryos electroporated with **(a)** control or **(b)** Pax6 plasmids. Nuclei were stained with DAPI (blue). Dashed white lines, ventricular surface; scale bar, 20 µm. **(c)** Quantification of the percentage of Ki67+ and RFP+ cells in electroporated cells (RFP+) within a 200 µm wide electroporated area in the dorsal telencephalon in control (white bars) and Pax6 (black bars). Mean ± SEM from 3 independent experiments; each experiment = 3-4 embryos. * $p<0.05$.

2.2.5. Conditional expression of Pax6 alters cell cycle

The increase in percentage of cycling cells shown previously could be explained by two scenarios, namely, the expression of Pax6 (i) lengthened the cell cycle or (ii) increased the number of cycling progenitors. In order to investigate which of the two possibilities was more likely, the effect of Pax6 expression on cell cycle progression was investigated.

To study the effect of Pax6 on S-phase, 1 mg ml^{-1} EdU was administered one hour prior to animal sacrifice. A significant increase in the percentage of EdU and RFP double positive cells was observed when conditionally expressing Pax6 (**Fig. 26**). This is consistent with previously shown data where more

progenitors were found to be cycling; and this increase was also reflected by an increase in progenitors undergoing S-phase.

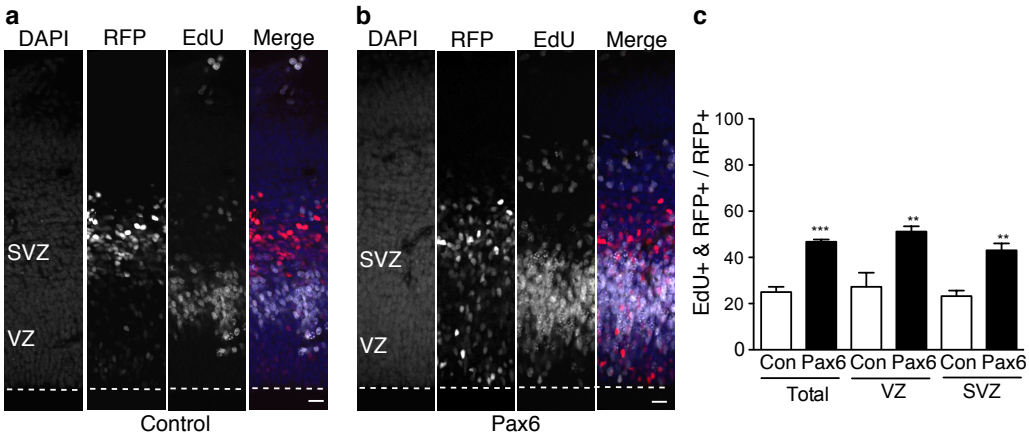

Figure 26: Conditional expression of Pax6 in E14.5 heterozygous *Tis21*–CreER^{T2} embryos at 24 h after IUE increases percentage of EdU positive cells. **(a,b)** Immunofluorescence for EdU (white) in embryos electroporated with **(a)** control or **(b)** Pax6 plasmids. Nuclei were stained with DAPI (blue). Dashed white lines, ventricular surface; scale bar, 20 µm. **(c)** Quantification of the percentage of EdU+ and RFP+ cells in electroporated cells (RFP+) within a 200 µm wide electroporated area in the dorsal telencephalon in control (white bars) and Pax6 (black bars). Mean ± SEM from 3 independent experiments, each experiment = 2-4 embryos. ** $p<0.01$, *** $p<0.005$.

In order to determine whether the increase in the percentage of EdU positive cells was a reflection of a longer S-phase or more progenitors undergoing S-phase, the late G2 to M-phase was examined using phospho-histone H3 (PH3). We reasoned that if Pax6 expression prolonged S-phase, the proportion of cells moving forward to G2 and/or M-phase would be reduced as more of these cells would remain in S-phase. However, if the S-phase duration were unaltered, the proportion of cells moving forward to G2 and/or M-phase would increase, thus we should observe an increase in PH3 positive cells. When conditionally expressing Pax6, a significant increase in PH3 positive cells was observed, apically and basally (**Fig. 27**). Based on EdU and PH3 data, an increase in proportion of progenitors progressing through the cell cycle was observed. These data suggest that the conditional expression of Pax6 leads to the generation of more progenitors rather than the prolongation of the cell cycle length.

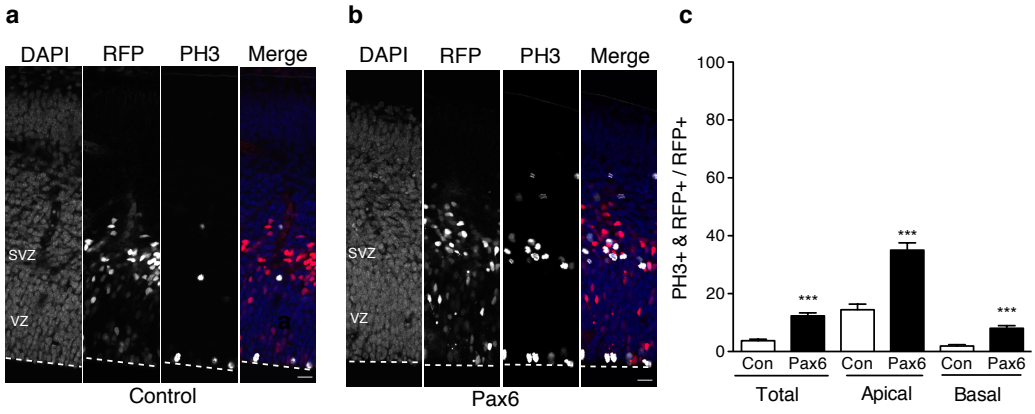

Figure 27: Conditional expression of Pax6 in E14.5 heterozygous *Tis21*–CreER^{T2} embryos at 24 h after IUE increases percentage of PH3 positive cells. **(a,b)** Immunofluorescence for PH3 (white) in embryos electroporated with **(a)** control or **(b)** Pax6 plasmids. Nuclei were stained with DAPI (blue). Dashed white lines, ventricular surface; scale bar, 20 µm. **(c)** Quantification of the percentage of PH3+ and RFP+ cells in electroporated cells (RFP+) within a 200 µm wide electroporated area in the dorsal telencephalon in control (white bars) and Pax6 (black bars). Mean ± SEM from 3 independent experiments, each experiment = 2-4 embryos. *** $p<0.005$.

The length of the G1 phase has been shown to have an effect on the proliferative capacity of progenitors (Arai et al., 2011; Dehay and Kennedy, 2007; Lange et al., 2009; Nonaka-Kinoshita et al., 2013) where a shorter G1 phase delays neurogenesis and promotes proliferative divisions while a longer G1 phase has the reverse effect. To determine whether conditional expression of Pax6 has an effect on the G1 phase, cyclin D1 was stained in order to identify cells undergoing mid- to late- G1 phase. Although no significant difference was observed when conditionally expressing Pax6, there was a reduced tendency for conditionally expressing Pax6 cells to be cyclin D1 positive (**Fig. 28**). When the individual germinal zones were examined, a significant reduction of cyclin D1 positive cells in the VZ was observed, suggesting that these cells might have a shorter G1 phase. As the expression of cyclin D1 has been previously reported to be found mostly in the VZ (Glickstein et al., 2007), the lack of significance in the SVZ could be a reflection of the downregulation of cyclin D1 in BPs. Based on the data on the various cell cycle phases, we conclude that the conditional expression of Pax6 generates more cycling progenitors and these progenitors may have an altered cell cycle, indicative of an increased proliferative capacity.

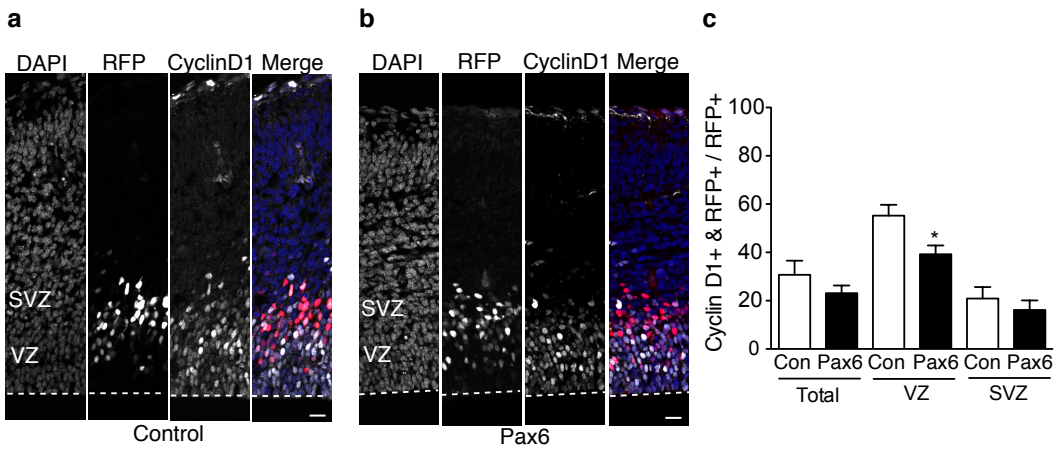

Figure 28: Conditional expression of Pax6 in E14.5 heterozygous *Tis21*–CreER^{T2} embryos at 24 h after IUE reduces percentage of cyclin D1 positive cells. **(a,b)** Immunofluorescence for cyclin D1 (white) in embryos electroporated with **(a)** control or **(b)** Pax6 plasmids. Nuclei were stained with DAPI (blue). Dashed white lines, ventricular surface; scale bar, 20 µm. **(c)** Quantification of the percentage of cyclin D1+ and RFP+ cells in electroporated cells (RFP+) within a 200 µm wide electroporated area in the dorsal telencephalon in control (white bars) and Pax6 (black bars). Mean ± SEM from 3 independent experiments, each experiment = 2-4 embryos. * $p<0.05$.

2.2.6. Conditional expression of Pax6 induces a change in cell fate

As neurogenic aRGs are known to undergo asymmetric proliferation to produce bIPs, we asked whether the progenitors produced by conditional expression of Pax6 were in fact bIPs. To distinguish the various BPs, certain criteria were examined, namely cell marker expression, cell morphology and the type of divisions.

The identity of the progenitor produced was first examined using cell markers. TF markers Tbr2 and Sox2 were used to identify bIP and radial glia cells respectively. In control, we observed around 50% of electroporated cells to be Tbr2 positive, consistent with the fact that neurogenic Tis21 positive aRGs divide asymmetrically to produce one bIP (Tbr2+) and aRG (Tbr2–) (**Fig. 29a,c**). However, in the conditional Pax6 expression, we observed a significant reduction in the number of Tbr2 positive cells, specifically in the

SVZ (**Fig. 29b,c**) suggesting that conditional expression of Pax6 in the neurogenic population may not have produced bIPs as expected.

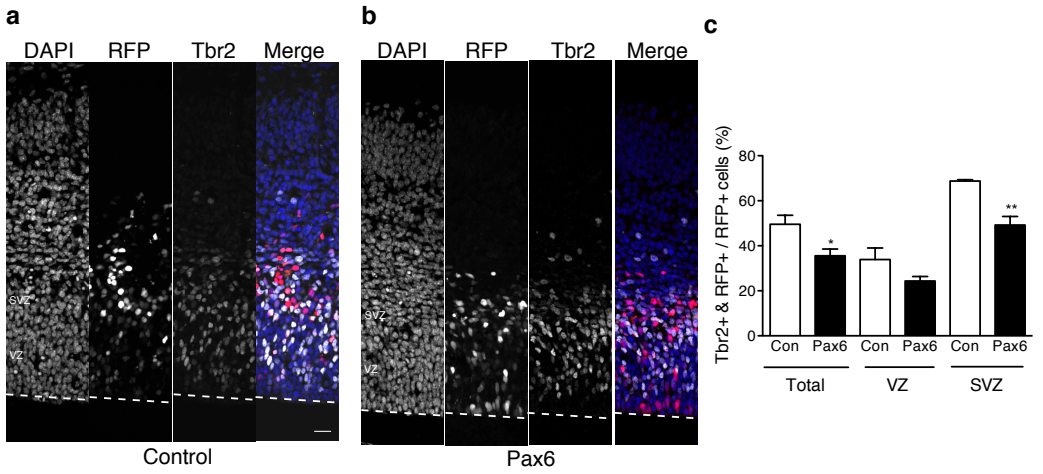

Figure 29: Conditional expression of Pax6 in E14.5 heterozygous *Tis21*–CreER^{T2} embryos at 24 h after IUE reduces percentage of Tbr2 positive cells. **(a,b)** Immunofluorescence for Tbr2 (white) in embryos electroporated with **(a)** control or **(b)** Pax6 plasmids. Nuclei were stained with DAPI (blue). Dashed white lines, ventricular surface; scale bar, 20 µm. **(c)** Quantification of the percentage of Tbr2+ and RFP+ cells in the electroporated cells (RFP+) within a 200 µm wide electroporated area in the dorsal telencephalon in control (white bars) and Pax6 (black bars). Mean ± SEM from 3 independent experiments, each experiment = 2-4 embryos. * p<0.05, ** P<0.01.

We then examined the expression pattern of the radial glia and stem cell marker, Sox2 (**Fig. 30**). A significant increase in the percentage of Sox2 positive cells was observed when Pax6 was conditionally expressed. This increase was again specific to the SVZ and not the VZ (**Fig. 30c**). Together, the data suggest that the conditional expression of Pax6 induces a change in progeny fate. Instead of inducing bIP-genesis, conditional expression of Pax6 downregulates or suppresses Tbr2, while maintains the expression of radial glia marker, Sox2.

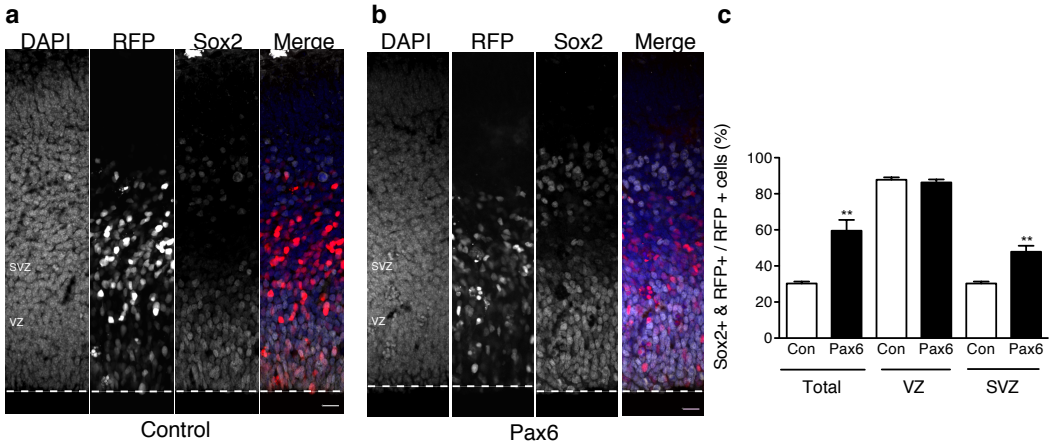

Figure 30: Conditional expression of Pax6 in E14.5 heterozygous *Tis21*–CreER^{T2} embryos at 24 h after IUE increases Sox2 positive cells. **(a,b)** Immunofluorescence for Sox2 (white) in embryos electroporated with **(a)** control or **(b)** Pax6 plasmids. Nuclei were stained with DAPI (blue). Dashed white lines; ventricular surface. Scale bar: 20 µm. **(c)** Quantification of the percentage of Sox2+ and RFP+ cells in electroporated cells (RFP+) within a 200 µm wide electroporated area in the dorsal telencephalon in control (white bars) and Pax6 (black bars). Mean ± SEM from 3 independent experiments, each experiment = 2-4 embryos. ** $p<0.01$.

2.2.7. Conditional expression of Pax6 induces a shift in the fate of sister pairs

As mentioned earlier, neurogenic aRGs are known to undergo asymmetric divisions to produce bIPs. The reduction in the percentage of Tbr2 positive cells with a concurrent increase in the percentage of Sox2 positive cells in the SVZ suggest that these conditionally expressing Pax6 neurogenic aRGs no longer undergo asymmetric division to produce bIPs. To confirm this, the fate of the progeny of the electroporated neurogenic aRG was studied. Videos from live imaging of organotypic slice tissues have shown that sister pairs normally migrate away from the ventricular surface with their cell bodies on top of one another after mitosis (Attardo et al., 2008; Shitamukai et al., 2011; Wang et al., 2011). Using this knowledge, closely located sister pairs in VZ in a sparsely electroporated area were identified (**Fig. 31**). Unsurprisingly, in control, almost half of the sister pairs observed were asymmetric in Tbr2 expression (43%, **Fig. 31b**). Around 30% of sister pairs observed were both negative for Tbr2 (**Fig. 31b**). Most of these sister pairs were located close to

the surface (**Fig. 31c**). As Tbr2 expression begins only at G1 phase and is rarely seen at the ventricular surface (Englund et al., 2005), we hypothesized that for the sister pairs that were both Tbr2 negative, the Tbr2 expression was low and may not be detectable yet via immunofluorescence. Similarly, if there was indeed a reduction in the percentage of Tbr2 positive cells in the SVZ when conditionally expressing Pax6, a corresponding increase in sister pairs that were both Tbr2 negative, located away from the ventricular surface should be observed. Supporting this idea, we observed an increase in the number of sister pairs where both were Tbr2 negative, located away from the ventricular surface (63%, **Fig. 31 b,c**).

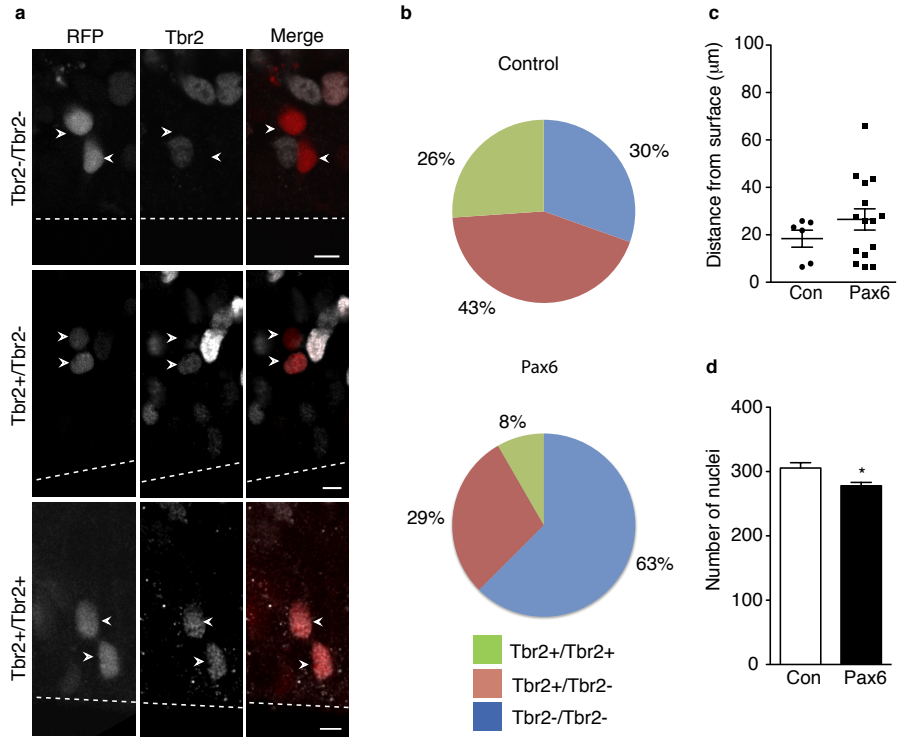

Figure 31: Conditional expression of Pax6 in E14.5 heterozygous *Tis21*–CreER^{T2} embryos at 24 h after IUE alters fate of the progeny. **(a)** Immunofluorescence for Tbr2 (white) in embryos electroporated with Pax6 plasmids (RFP+, red). Dashed white lines, ventricular surface; White arrowheads, sister pairs; scale bar, 10 µm. (**b)** Percentage of sister pairs that are Tbr2+/Tbr2+ (green), Tbr2+/Tbr2– (red) and Tbr2–/Tbr2– (blue) in control (top) and Pax6 (bottom) in electroporated brains. **(c)** Distance of sister pairs that are Tbr2–/Tbr2– from the ventricular surface in embryos electroporated with the control (circle) and Pax6 (square). Control= 23 pairs, Pax6= 24 pairs. (**d**) Number of DAPI positive nuclei in the VZ within a 200 µm wide electroporated area in the dorsal telencephalon in control (white bar) and Pax6 (black bar). Mean ± SEM from more than 3 independent experiments, each experiment = 2-4 embryos. *p<0.05.

As there is a switch in the type of division made, we then wanted to investigate whether both sister pairs would migrate separately to different germinal zones or whether both would migrate together towards the SVZ. The total number of DAPI positive nuclei in the VZ of an electroporated region (with normal construct concentration) was quantified. Intriguingly, a significant reduction in the total number of nuclei in the VZ of a 200 μm width electroporated region was observed when conditionally expressing Pax6 (**Fig. 31d**). This reduction suggests that both sister pairs migrate away from the VZ into the SVZ and may thus account for the increase in cycling cells observed in the SVZ.

2.2.8. Conditional expression of Pax6 produces more basal radial glia

We next sought to determine which BP was produced based on cell morphology. As described previously, bIPs and TAPS are both non-polar (Haubensak et al., 2004) while bRGs are typically basal process-bearing cells during mitosis (Betizeau et al., 2013; Fietz et al., 2010; Hansen et al., 2010; Reillo et al., 2011; Shitamukai et al., 2011; Wang et al., 2011)(**Table 1**). To reveal the morphology, the phospho-vimentin (PVim) staining was used to outline the cell during mitosis. In control, most of these basal mitotic cells were non-polar (89%) in agreement with the high abundance of bIP in the mouse SVZ (**Fig. 32d**). However, a subset of basal mitotic cells was basal process-bearing monopolar cells, reflective of the low abundance of bRG (11%, **Fig. 32d**) (Fietz et al., 2010; Hansen et al., 2010; Reillo et al., 2011; Wang et al., 2011). However, when conditionally expressing Pax6, a doubling in the percentage of basal process-bearing cells was observed (21%, **Fig. 32b-d**). The change in cell morphology together with TF expression suggests that conditional expression of Pax6 increases bRG production at the expense of bIP production.

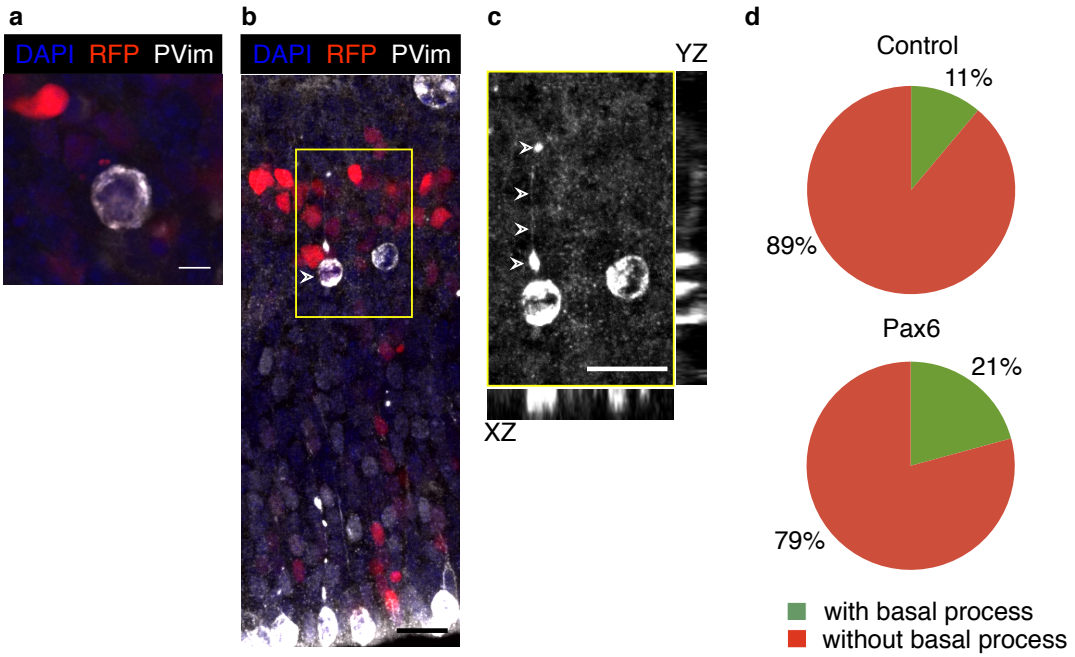

Figure 32: Conditional expression of Pax6 in E14.5 heterozygous *Tis21*–CreER^{T2} embryos at 24 h after IUE increases bRG production. **(a-c)** Immunofluorescence for phosphovimentin (white) in embryos electroporated with Pax6 plasmids. Two different morphologies were observed in basal mitoses; **(a)** nonpolar **(b,c)** basal process bearing cells. Nuclei were stained with DAPI (blue). Yellow box inset in **(b)** is magnified image in **(c)** together with the z-planes. **(b,c)** Maximum projection intensity images from 7 images. Scale bar, 10 µm. **(d)** Quantification of the percentage of cells with (green) and without basal process (red) in basal mitotic cells among RFP positive cells. Data obtained from 4 independent experiments; control = 99 cells, Pax6= 77 cells.

2.2.9. Conditional expression of Pax6 produces BPs that can re-enter the cell cycle

The final criterion in identifying BP, in addition to cell marker expression and cell morphology, is the type of division these cells make. bIPs undergo symmetric self-consuming divisions where after mitosis, both daughter cells become post-mitotic neurons. For bRGs and TAPS, these progenitors are capable of undergoing multiple rounds of cell division, where at least one of the progeny can re-enter the cell cycle. Hence, to further corroborate the data where conditional expression of Pax6 increases bRG production, the capability of the progeny of these electroporated cells to re-enter the cell cycle (**Fig. 33**) and also the identity of these cells (**Fig. 34b,c**) were studied.

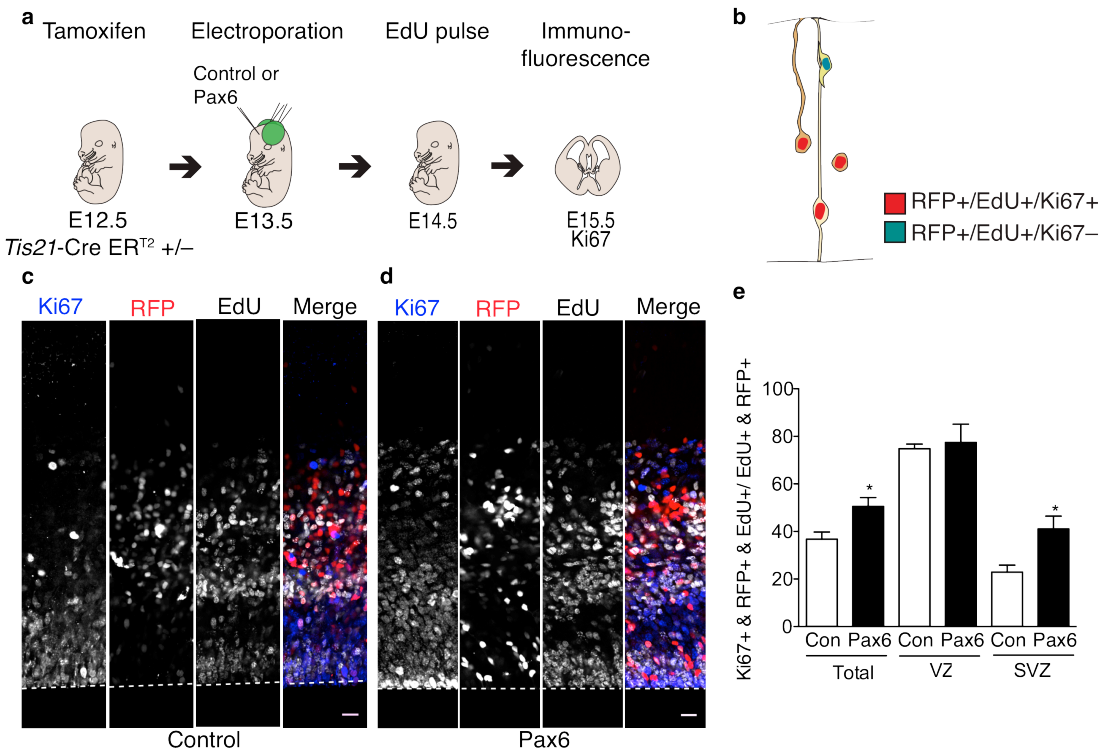

Figure 33: Conditional expression of Pax6 in heterozygous *Tis21*–CreER^{T2} embryos reduces the number of cells exiting the cell cycle. **(a)** Drawings demonstrating how the experiment was conducted **(b)** Drawings of the fate of EdU labelled cells at 48 h after IUE. **(c)** Immunofluorescence for Ki67 (blue) and EdU (white) in embryos electroporated with **(c)** control or **(d)** Pax6 plasmids. Dashed white line, ventricular surface; scale bar, 20 µm. **(e)** Percentage of cells that were positive for Ki67, GFP, RFP and EdU among EdU, GFP and RFP positive cells from embryos electroporated with control (white bars) and Pax6 (black bars) plasmids. Mean ± SEM obtained from three independent experiments, each experiment = 2-4 embryos. * $p<0.05$.

In this experiment, 1 mg ml^{-1} EdU was administered to dams at 24 h and sacrificed at 48 h after electroporation (**Fig. 33a**). The cell cycle length of BPs at this developmental stage is ≈24 h (Arai et al., 2011). At 24 h after IUE, cells undergoing S-phase would incorporate the EdU. These EdU positive cells would either remain or exit the cell cycle after mitosis. A Ki67 positive cell (at 48 h) would hence be a cycling progenitor that had re-entered the cell cycle while a Ki67 negative cell would be a differentiated cell (i.e. neuron, **Fig. 33b**). In control, we observed around 60% of electroporated cells labelled with EdU had exited the cell cycle (i.e. Ki67–, GFP+, RFP+, EdU+) suggesting that these cells had differentiated to become neurons. However when conditionally expressing Pax6, a significant increase in the percentage of cells that

remained in the cell cycle (i.e. Ki67+, GFP+, RFP+, EdU+) (**Fig. 33d**) was observed, suggesting that progeny produced by the electroporated neurogenic aRG had the capability to undergo another round of cell cycle.

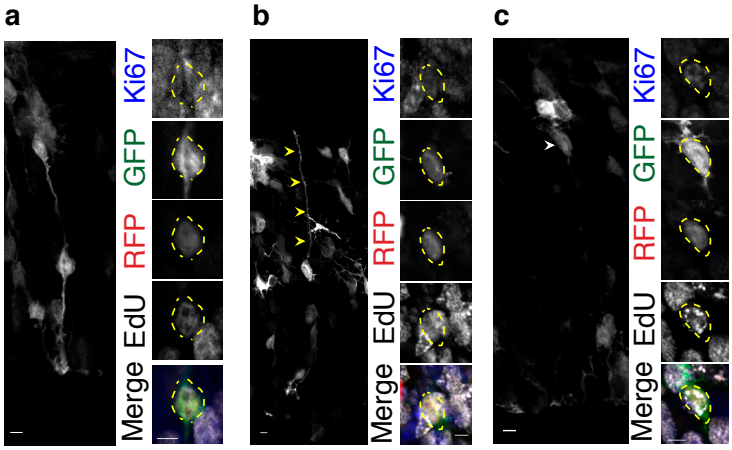

Figure 34: Conditional expression of Pax6 in heterozygous *Tis21*–CreER^{T2} embryos after IUE induces a switch in BP production. **(a-c)** GFP (green) expression revealed that cells that re-entered the cell cycle were **(a)** bipolar (VZ), **(b)** with a basal process (SVZ) and **(c)** multipolar (SVZ) morphology. Images on the left are maximum projection intensity images from **(a)** 7 **(b)** 15 and **(c)** 8 images. Images on the right are magnification of the cells body with the immunofuorescence for Ki67 (blue), RFP (red) and EdU (white) from a single optical section. Yellow arrow heads, basal process; white arrow head, cell body; dashed yellow lines, outline of cell body; scale bar, 5 µm.

We then went a step further to determine the cell identity of progenitors that had this capability to re-enter the cell cycle based on cell morphology via GFP expression. In the VZ, the majority of cells that re-entered the cell cycle (i.e. Ki67+, GFP+, RFP+, EdU+) had a bipolar morphology, characteristic of an aRG (**Fig. 34a**). This is unsurprising as these cells are most abundantly found progenitors in the VZ and are known to undergo multiple rounds of division. In the SVZ, two types of cells that re-entered the cell cycle were observed– basal process-bearing cells (i.e. bRG, **Fig. 34b**) and multi-polar cells (i.e. tbRG or TAPS, **Fig. 34c**). Hence, based on cell morphology, type of cell division and TF expressions, conditional expression of Pax6 is unlikely to produce bIPs. Instead, as these cells have the capacity to re-enter the cell cycle, the data suggest that there is a switch in the fate of BP produced,

where not only the conditional expression produces more bRGs, but at the same time multipolar cells that are most likely to be tbRGs or TAPs.

2.2.10. Conditional expression of Pax6 induces a shift in apical and basal cleavage orientation

It was recently reported in mouse (Shitamukai et al., 2011), ferret (Gertz et al., 2014; Reillo and Borrell, 2012) and human (LaMonica et al., 2013) that aRGs that divide with a non-vertical cleavage with respect to the ventricular surface (i.e. obliquely or horizontally) have a higher propensity to produce bRGs. To understand how this increase in bRGs arose when conditionally expressing Pax6, the cleavage orientation of electroporated mitotic cells was studied both apically and basally. In control, more than 90% of neurogenic aRGs divided vertically (**Fig. 35a,b**), while a subset of these group divided obliquely. This is in line with what was previously published on the neurogenic, Tis21 positive aRG (Kosodo et al., 2004). Upon conditional expression of Pax6, a shift in the cleavage orientation was observed where the percentage of non-vertical cleavages doubled (**Fig. 35b**), hence increasing the propensity of these cells to produce bRG. As the cleavage orientation is dependent on the mitotic spindle, this suggests that Pax6 may affect mitotic spindle dynamics, which ultimately increases the percentage of non-vertical cleavages.

In addition to apical cleavage orientation, the cleavage orientation in basal mitoses was examined. In control, similar to what was reported previously (Farkas et al., 2008; Fietz et al., 2010), these mitoses have a random orientation as usually observed in cells with no intrinsic polarity (**Fig. 36a,b**). When conditionally expressing Pax6, a shift in the cleavage angle was observed where an increase preference for basal mitotic cells to divide with a horizontal cleavage with respect to the ventricular surface was observed (**Fig. 36b**). The increase preference for horizontal cleavages is consistent with the increased presence of cells that has an intrinsic polarity (i.e. bRG) where previous work has demonstrated that bRGs divide preferentially with a horizontal cleavage (Gertz et al., 2014; LaMonica et al., 2013).

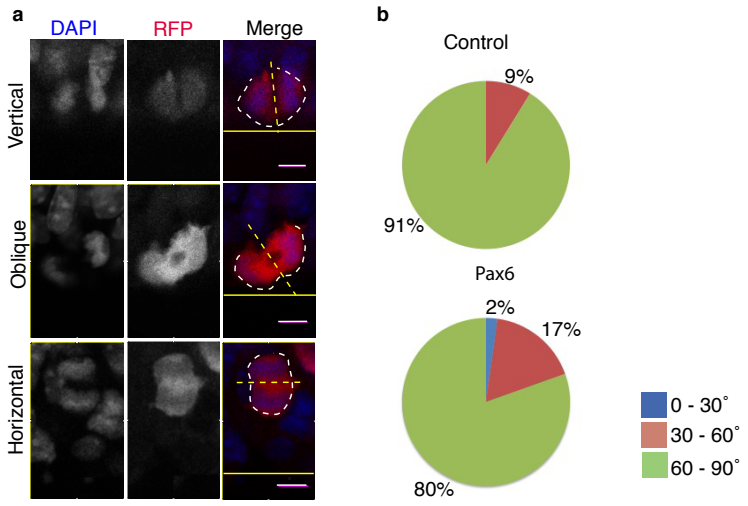

Figure 35: Conditional expression of Pax6 in E14.5 heterozygous *Tis21*–CreER^{T2} embryos at 24 h after IUE alters apical mitoses cleavage angle. **(a)** Immunofluorescence for embryos electroporated with Pax6 plasmid. Nuclei were stained with DAPI (blue). Dashed white line, mitotic cell; dashed yellow line, cleavage orientation; solid yellow line, plane of ventricular surface; scale bar, 10 μm. (**b)** Percentage of cells that have a vertical (green), oblique (red) and horizontal (blue) cleavages in control (top) and Pax6 (bottom) electroporated brains. Data from eight independent experiments, control = 34 cells, Pax6 = 45 cells.

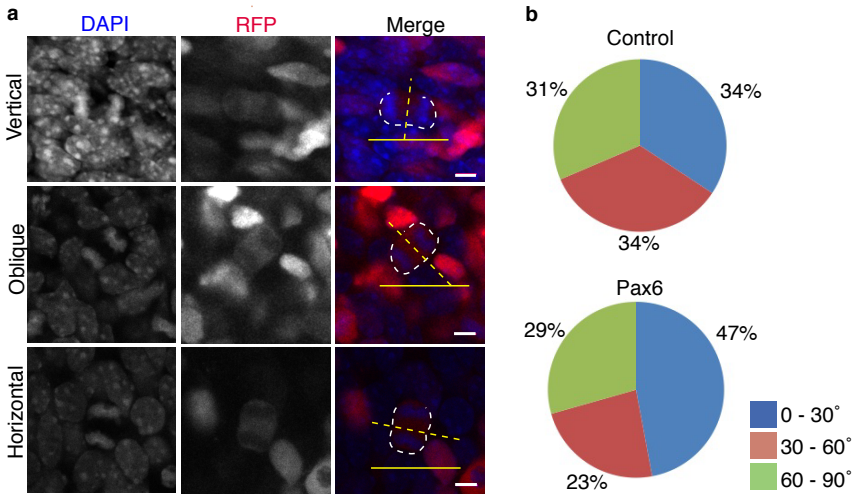

Figure 36: Conditional expression of Pax6 in E14.5 heterozygous *Tis21*–CreER^{T2} embryos at 24 h after IUE alters basal mitoses cleavage angle. **(a)** Immunofluorescence for embryos electroporated with Pax6 plasmid. Nuclei were stained with DAPI (blue). Dashed white line, mitotic cell; dashed yellow line, cleavage orientation; solid yellow line, plane of ventricular surface; scale bar, 10 μm. (**b)** Percentage of cells that have a vertical (green), oblique (red) and horizontal (blue) cleavages in control (top) and Pax6 (bottom) electroporated brains. Data from eight independent experiments, control = 35 cells, Pax6 = 34 cells.

2.2.11. Effect of conditional expression of Pax6 on neuronal migration and production

To determine the effect of Pax6 on neuronal production, the neuronal marker, Tbr1 was used and examined the effect first at 48 h after IUE (**Fig. 37**). No significant difference was observed between groups, suggesting that the conditional expression of Pax6 did not have an immediate effect on neuronal production, although the percentage of Tbr1 and RFP double positive cells tend to be lower when conditionally expressing Pax6.

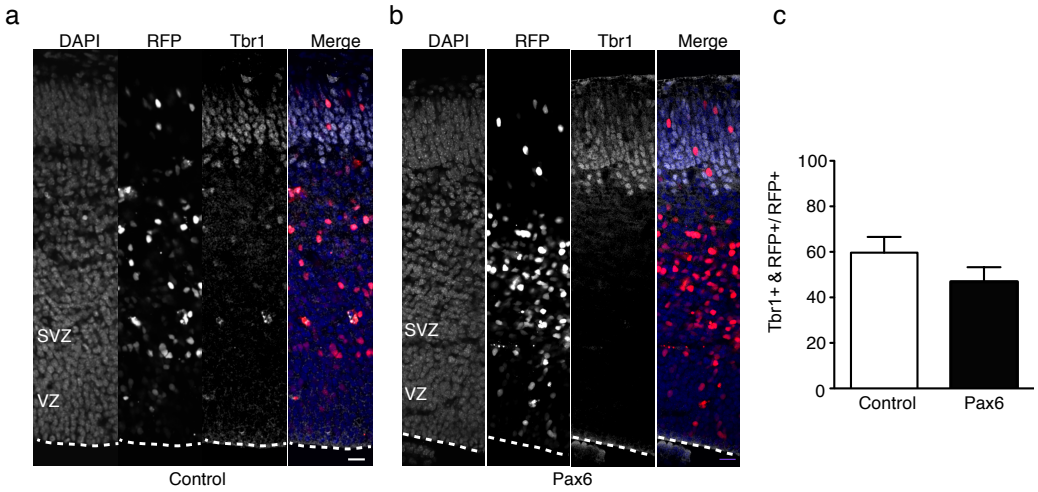

Figure 37: Conditional expression of Pax6 in E15.5 heterozygous *Tis21*-CreER^{T2} embryos at 48 h after IUE has no effect on neuron production. **(a,b)** Immunofluorescence for Tbr1 (white) in embryos electroporated with **(a)** control or **(b)** Pax6 plasmids. Nuclei were stained with DAPI (blue). Dashed white lines, ventricular surface; scale bar, 20 µm. **(c)** Quantification of the percentage of Tbr1+ and RFP+ cells in the electroporated cells (RFP+) within a 200 µm wide electroporated area in the dorsal telencephalon in control (white bars) and Pax6 (black bars). Mean ± SEM from 3 independent experiments, each experiment = 2-4 embryos.

Interestingly, a reduction in the number of conditionally expressed Pax6 electroporated cells that had successfully migrated to the CP at 48 h was noted. To confirm this observation, the distribution of the electroporated cells was quantified by dividing the cortical layer to 10 equally sized bins starting from the ventricular surface (bin 1) up to the CP (bin 10) for samples obtained at 24 and 48 h after IUE (**Fig. 38**). At 24 h, no significant differences was observed in the distribution of the RFP positive cells between both groups. At

48 h, however, a significant reduction was observed in the percentage of electroporated cells at the higher bins (starting from bin 8 up to bin 10), coinciding with the CP. Interestingly, a significant increase in the number of conditionally expressing Pax6 cells in the middle of the tissue (bin 5) was observed, suggesting that these cells may have some defects in terms of cell migration.

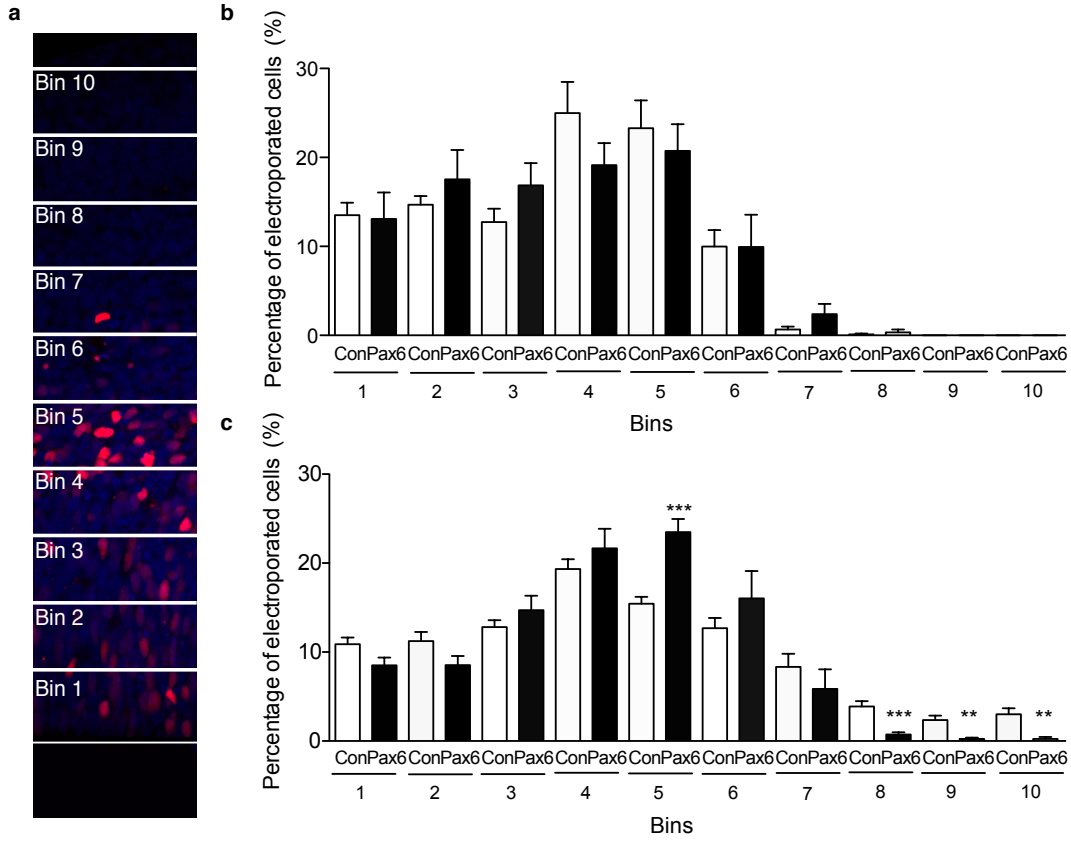

Figure 38: Conditional expression of Pax6 in heterozygous *Tis21*–CreER^{T2} embryos at **(a,b)** 24 and **(c)** 48 h after IUE show altered distribution of electroporated cells throughout the cortical wall at 48 h. **(a)** Immunofluorescence for embryos electroporated with Pax6 plasmids. Nuclei were stained with DAPI (blue). The distribution of electroporated cells (red) were categorized into equally sized bins starting from the ventricular surface right up to the CP (1 being closest to the ventricular surface and 10 at the CP). **(b,c)** Quantification of RFP+ cells according to the equal sized bins within a 200 µm wide electroporated area in the dorsal telencephalon in control (white bars) and Pax6 (black bars). Mean ± SEM from 3 independent experiments, each experiment = 2-4 embryos. ** $p<0.01$, *** $p<0.001$.

We then investigated the effect of conditionally expressing Pax6 at a late stage of development by performing IUE at E13.5 and administered 1 mg ml^{-1}

EdU 10 hours after IUE to coincide with the start of the Pax6 expression in the electroporated cells. Animals were sacrificed at 4 days (E17.5) after IUE and the fate of the progeny was determined. In control, most of the electroporated cells successfully migrated to the CP (**Fig. 39**). For the conditionally expressing Pax6 cells, some of these cells successfully migrated to the CP. Like the Pax6 overexpression and knockout models (Georgala et al., 2011a), some tend to form a heterotopia between the SVZ and IZ. Strikingly, most of the cells that formed the heterotopia were stained strongly positive for Pax6. The immunofluorescence intensity of Pax6 was then measured in cells that had successfully migrated to the CP and those that formed the heterotopia. Heterotopic cells tend to have a much higher fluorescent intensity of Pax6 as compared to those that have successfully migrated to the CP (**Fig. 39d**). This suggests that the differential level of Pax6 expressed may induce differential effect on cell migration.

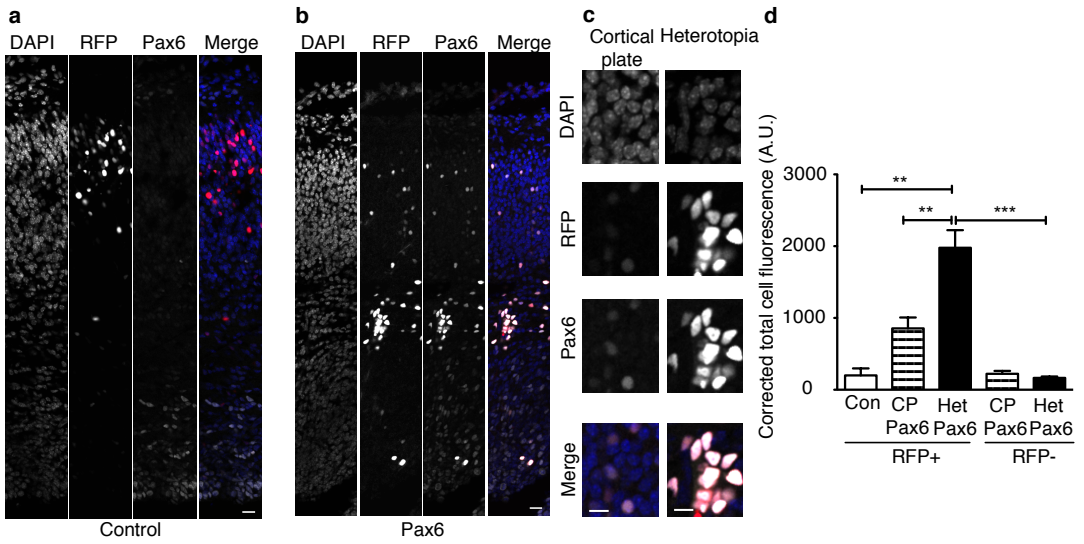

Figure 39: Conditional expression of Pax6 in E17.5 heterozygous *Tis21*–CreER^{T2} embryos at 4 days after IUE. **(a-c)** Immunofluorescence of Pax6 (white) in **(a)** control and **(b,c)** Pax6 electroporated cells. Nuclei were counterstained with DAPI (blue). **(c)** Immunofluorescence of Pax6 in electroporated cells that were in the cortical plate (left) and in heterotopic (right) regions. Scale bar, 20 µm. **(d)** Quantification of the immunofluorescence intensity of Pax6 protein. The fluorescence intensity of the RFP+ and RFP– were measured in control (white bars) and Pax6 plasmid from the cortical plate (CP, stripe bars) and from heterotopia (Het, black bars) region. Values are mean corrected for total cell fluorescence (against background) ± SEM of 4 embryos. ** $p<0.01$, *** $p<0.005$.

The fate of these heterotopic cells was next investigated. As these cells were stained negative for Ki67 (data not shown), these cells were thus differentiated cells. Towards the end of gestation, neurogenesis decreases while gliogenesis increases. Hence, to determine whether these cells were gliogenic or neurogenic in nature, sections were stained for astrocyte, oligodendrocyte, immature and mature neuronal markers respectively. Conditionally expressing Pax6 cells in the heterotopia were stained negative for Olig2 (marker for oligodendrocytes), GFAP (marker for astrocytes) and NeuN (marker for mature neurons). Interestingly, these cells were stained positive for the immature neuron marker, Tuj1 (**Fig. 40**). This suggests that these heterotypic cells from the conditional expression of Pax6 were neuronal in nature. The high level of Pax6 expression may have affected the maturation process and thus further prevented these cells from entering the CP.

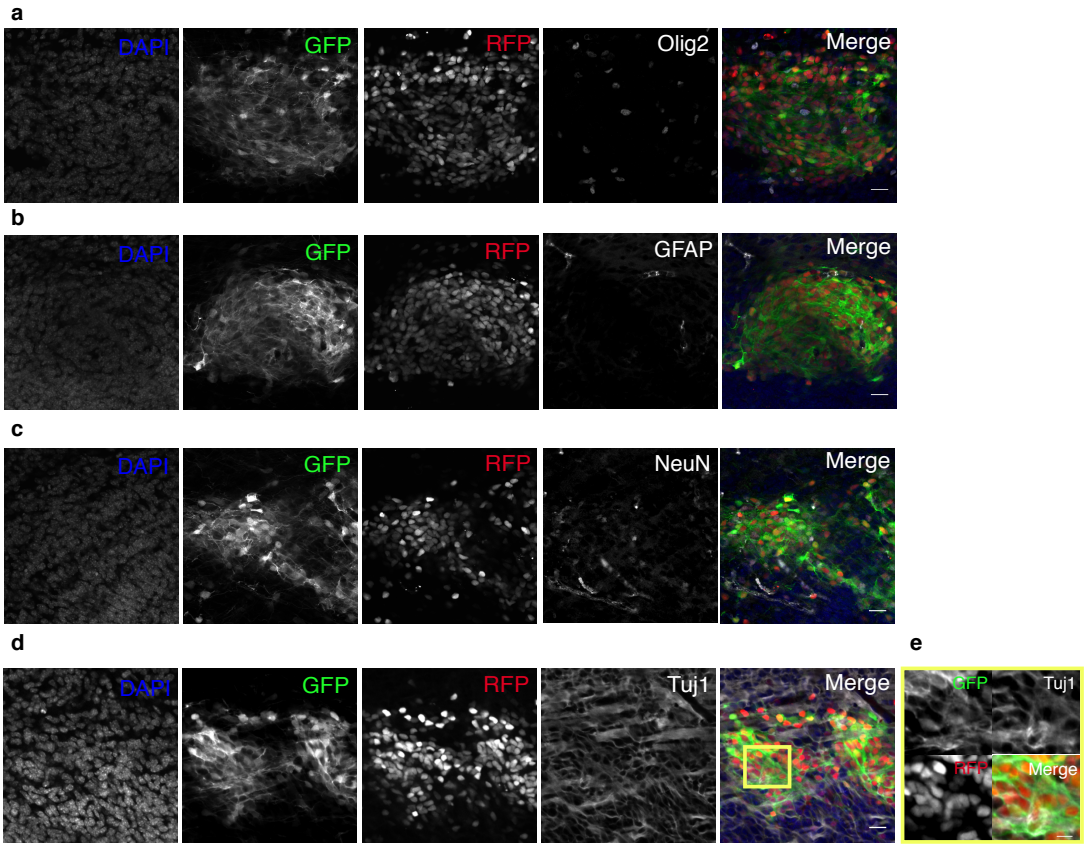

Figure 40: Conditional expression of Pax6 in E17.5 heterozygous *Tis21*–CreER^{T2} embryos at 4 days after IUE. **(a-e)** Immunofluorescence of **(a)** Olig2 (white), **(b)** GFAP (white), **(c)** NeuN (white), **(d,e)** Tuj1 (white) in the heterotopia of Pax6 electroporated cells. Nuclei were counterstained with DAPI (blue). Yellow box in **(d)** is magnified in **(e)**. Scale bar, 20 µm.

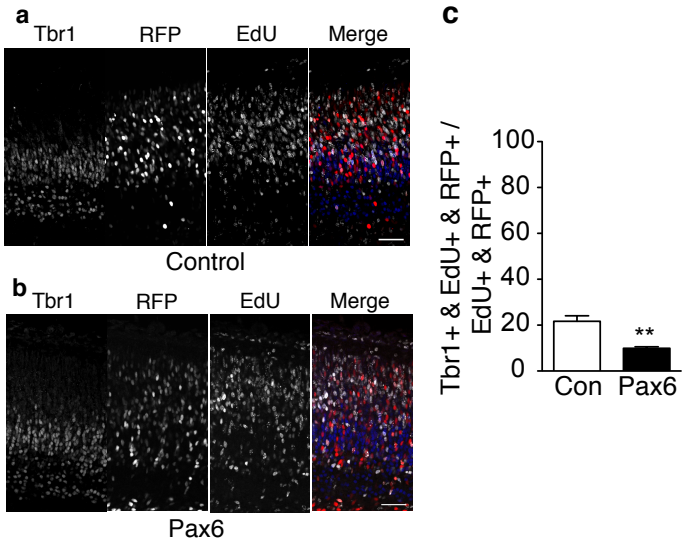

Figure 41: Conditional expression of Pax6 in E17.5 heterozygous *Tis21*–CreER^{T2} embryos at 4 days after IUE reduces Tbr1 positive cells. **(a,b)** Immunofluorescence for Tbr1 (blue) and EdU (white) in embryos electroporated with **(a)** control or **(b)** Pax6 plasmids. Scale bar, 20 µm. **(c)** Quantification of the percentage of Tbr1+, EdU+ and RFP+ (red) cells in the electroporated cells (RFP+) that are EdU positive within a 200 µm wide electroporated area in the dorsal telencephalon in control (white bars) and Pax6 (black bars). Mean ± SEM from 3 independent experiments, each experiment = 2-4 embryos. ** p<0.01.

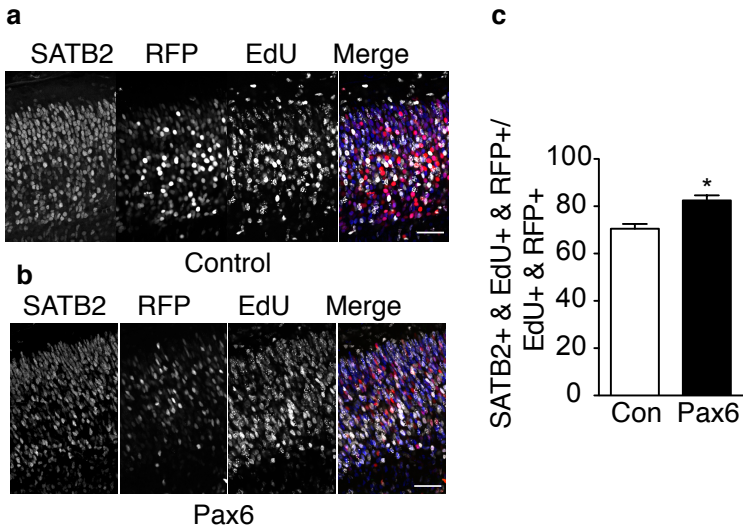

Figure 42: Conditional expression of Pax6 in E17.5 heterozygous *Tis21*–CreER^{T2} embryos at 4 days after IUE increases SATB2 positive cells. **(a,b)** Immunofluorescence for SATB2 (blue) and EdU (white) in embryos electroporated with **(a)** control or **(b)** Pax6 plasmids. Scale bar, 20 µm. **(c)** Quantification of the percentage of SATB2+, EdU+ and RFP+ (red) cells in the electroporated cells (RFP+) that are EdU positive within a 200 µm wide electroporated area in the dorsal telencephalon in control (white bars) and Pax6 (black bars). Mean ± SEM from 3 independent experiments, each experiment = 2-4 embryos. * p<0.05.

Neurons from each cortical layer are generated according to their birth date (Molyneaux et al., 2007). Early born neurons would migrate to the deep layers while late born neurons would migrate pass the deep layer neurons to become the upper layer neurons in an inside-out manner. If the progeny of the conditionally expressing Pax6 were indeed progenitors that had maintained the capability to undergo self-renewal and not differentiated to become neurons, a delay in neuronal production should be observed. To distinguish the deep layer and upper layer neurons, neuronal markers Tbr1 (which labels layer V and VI) and SATB2 (which labels layer II-IV) (Molyneaux et al., 2007) were used. When stained for the deep layer neuron markers, Tbr1, a significant reduction in the number of Tbr1, EdU and RFP triple positive cells was observed (**Fig. 41**). Conversely when stained for the upper layer neuron marker, SATB2, a significant increase in the upper layer neuron marker was observed (**Fig. 42**). This data further strengthen the previous data showing that the progeny obtained by conditionally expressing Pax6 cells maintains their self-renewing capacity and delays neuronal production. This is reflected by the concurrent increase in upper layer neurons and a decrease in deep layer neurons, especially since the production of the specific neurons is birth date dependent. Interestingly, this is also reflective of the difference between the lissencephalic and gyrencephalic brains as the expanded SVZ had allowed for the increased production of the upper layer neurons.

Chapter 3
Discussion

3.1. Generation of bRG in the dorsal-lateral telencephalon in embryonic mouse

In this work, we sought to generate more bRGs in the dorsal-lateral telencephalon of the E14.5 mouse. To achieve this aim, two approaches were undertaken:

1) General approach via microinjection of ferret poly-A^+ RNA
2) Candidate approach via conditional expression of Pax6

Both approaches successfully generated excessive bRGs (or bRG-like cells) in the mouse dorsal-lateral telencephalon. These results, which confer important information underlining developmental differences between lissencephalic and gyrencephalic species, are discussed in light of evolutionary expansion of the neocortex.

3.2. General approach

3.2.1. Establishment of the microinjection technique in the mouse and ferret dorsal telencephalon

In the general approach, the previously described microinjection technique (Taverna et al., 2012) was adapted to the dorsal-lateral telencephalon (Wong et al., 2014). Microinjection is a powerful means of manipulating NPCs as a plethora of compounds not limited by size, charge and permeability can be microinjected into a cell. In this work, we successfully manipulated and tracked the fate of microinjected aRGs and their progeny in an organotypic slice culture. As a proof of principle, the recombinant Rac1 DN protein was microinjected and a change in cell fate was observed at 6 h after microinjection. Not limited to mouse, this technique could be adapted to non-conventional species such as ferret and can subsequently be used to track the fate of these cells. This provides an additional avenue in which one can

manipulate NPCs in non-conventional species in order to study and manipulate the cell biological properties of these cells.

3.2.2. Generation of bRG via microinjection of pool of ferret poly-A$^+$ RNA messages

As the main aim of this work is to generate more bRGs in the mouse dorsal-lateral telencephalon, pools of P1 to P2 ferret poly-A$^+$ RNA, the developmental stage, during which the generation of bRGs is at its peak (Fietz et al., 2010; Reillo and Borrell, 2012; Turrero García, 2013) were isolated. It is not unreasonable to assume that the poly-A$^+$ RNA messages isolated from this developmental stage would have the highest amount of poly-A$^+$ RNA messages to instruct for bRG generation. At 24 h after microinjection all dextran and RFP positive cells (i.e. cells that translated the ferret poly-A$^+$ RNA) observed were aRG-like based on cell morphology. At 48 h after microinjection, all the dextran positive but RFP negative cells (i.e. cells that did not translate the ferret poly-A$^+$ RNA) were neuronal-like. Intriguingly, among the dextran and RFP positive cells, 75% were monopolar cells that had a basal process, suggestive of a bRG-like morphology. This effect was not observed after only 24 h, however, likely due to species differences in cell-cycle length (Arai et al., 2011; Reillo and Borrell, 2012; Turrero García, 2013). We hypothesize that at 24 h the translated ferret poly-A$^+$ RNA messages may not have sufficient time to “instruct” for the generation of bRG (i.e. by delamination of only the apical process of the aRG) or to complete one round of cell cycle to generate bRG after cell division.

The high recovery of bRG-like cells, especially in a species where bRG exist at low abundance (Martinez-Cerdeno et al., 2012; Shitamukai et al., 2011; Wang et al., 2011), suggests that the ferret poly-A$^+$ RNA messages preferentially generate bRG-like cells. That is, the ferret poly-A$^+$ RNA messages were sufficient to override the mouse developmental programme that was geared towards neuronal differentiation (as observed in the dextran positive but RFP negative population).

As the repertoire of known TFs involved in neurogenesis in mouse, ferret and even human are similar in terms of protein albeit the expression level may differ (Englund et al., 2005; Fietz et al., 2010; Hansen et al., 2010; Reillo et al., 2011; Wang et al., 2011), the question therein lies, how does the phenotypic difference in cell lineage occurs during evolution? In a recent set of work that compared the transcriptome of different organisms and their organs, it was demonstrated that while tissues-specific genes were largely conserved between species, alternative splicing was significantly variable between species where there is a significant increase in alternative splicing complexity within the vertebrate lineage, with the highest in the primate lineage (Barbosa-Morais et al., 2012; Merkin et al., 2012). It is tempting at this point to hypothesise that differences in pre-RNA processing together with variation in alternative splicing may provide a possible explanation to the species difference in the cell specific lineages that we observed. The differences in RNA processing and alternative splicing, culminating in the differences in the final microinjected pool of ferret poly-A^+ RNA compared to the inherent mouse poly-A^+ RNA, suggest that RNAs instructive for the generation of bRG have been positively selected, in a manner that confers increased stability and translation efficiency. Thus, it would be interesting to study the transcripts present within this pool of ferret poly-A^+ RNA in order to discern the differences in the poly-A^+ transcript variation between species (i.e. species specific differences in alternative splicing, presence of different non-coding RNAs rather for novel genes) that may be involved in the generation of bRGs in the gyrencephalic brain.

3.2.3. Shortcomings of the general approach

While we had successfully generated bRG-like cells via microinjection, there were several shortcomings by using this approach. One of the main shortcomings was the low translational efficiency of these poly-A^+ RNA messages. Currently, the exact cause attributed to this low translational efficiency is unknown. Nonetheless, the low recovery of these cells made it

challenging to study these bRG-like cells. In addition, these bRG-like cells were only generated after 48 h in culture. This prolongation in the length of the cell cycle thus extended the amount of time required to run these experiments and further limits the number of cell divisions that can be tracked using the organotypic slice cultures. Furthermore, by microinjecting all poly-A+ mRNA, it is impossible to draw conclusions about the specific genomic elements driving the observed phenotype. Hence, to circumvent the limitation provided by this approach, we opted to study the generation of bRG in the dorsal telencephalon using a candidate approach, namely by conditionally expressing Pax6.

3.3. Candidate approach

3.3.1 Geneneration of bRG via conditional expression of Pax6

By using the candidate approach, we demonstrated that conditional expression of Pax6 in neurogenic Tis21 positive progenitors led to a specific increase in Pax6 levels in the mouse SVZ. To our knowledge, this is the first study that examines the ectopic expression of Pax6 in the mouse SVZ, even though Pax6 is a widely studied TF in the brain. As far as we are aware of, all of the studies done so far in the mouse neocortex, regarding the role of Pax6 in progenitor behaviour have been limited to APs where its functional roles on specification, proliferation, neurogenesis and migration have been molecularly dissected (Asami et al., 2011; Berger et al., 2007; Georgala et al., 2011a; Haubst et al., 2004; Holm et al., 2007; Stoykova et al., 1997; Walcher et al., 2013). However, with a significant increase in Pax6 positive cells (i.e. bRGs) observed in the SVZ of gyrencephalic brains such as humans and monkeys (Fietz et al., 2010; Hansen et al., 2010; Kelava et al., 2012; Reillo et al., 2011), we believe that these earlier studies do not necessarily address the evolutionary role Pax6 may play in the expansion and diversification of the neocortex.

In order to determine the role of Pax6 in expansion and diversification of the SVZ, a mouse line that allows for the ectopic expression of Pax6 in the SVZ was required. For that, the *Tis21*–CreER^{T2} mice was used. Tis21 is a pan-neurogenic marker that is expressed when aRGs switch from a proliferative division to a neurogenic division (Haubensak et al., 2004). Hence, conditional expression of Pax6 in these Tis21 positive progenitors allowed for the manipulation of the switch from lateral to radial expansion and at the same time induced the ectopic expression of Pax6 in the SVZ that is typically downregulated in the mouse. This experimental paradigm makes this work different from previously reported studies on the conditional expression of Pax6 (Berger et al., 2007) and, not unsurprisingly, resulted in discoveries both unfounded in and contradictory to those studies.

Previous study on the conditional expression of Pax6 has been conducted using the Emx2-Cre and hGFAP-Cre mouse lines (Berger et al., 2007). Emx2 and hGFAP are expressed by aRGs, albeit at different time during development. In these studies, conditional expression of Pax6 has induced a significant increase in apoptotic cells. However, this is not observed in this study, as no significant difference in caspase-3 positive and pyknotic cells were observed. Interestingly, it was also reported that such apoptosis was not observed when Pax6 was conditionally expressed in E1-Ngn2-Cre mouse line (Berger et al., 2007). In a mechanism that is still unknown, the expression of Ngn2 confer these progenitors resistance against high levels of Pax6 induced by the conditional expression of Pax6 (Berger et al., 2007). Ngn2 is expressed four fold higher in Tis21 positive progenitors compared to Tis21 negative progenitors (Arai et al., 2011). Hence, the expression of Ngn2 in Tis21 positive cells may have protected these cells from undergoing apoptosis when conditionally expressing Pax6.

In this work, upon conditional expression of Pax6, a significant increase in proliferating cells in the SVZ was observed. As neurogenic aRG are known to be the main producer of bIPs in mouse (Götz and Huttner, 2005), it was

initially assumed that these progenitors in the SVZ were bIPs. Based on the change in TF expression, however, the data suggested the contrary: instead of generating bIPs, conditional expression of Pax6 generated more self-renewing bRGs and/or TAPs. While bRGs have traditionally been defined to be monopolar with a basal process, it was recently reported in the macaque that the morphology of bRGs is dynamic and can be divided into several subtypes (Betizeau et al., 2013). One of these subtypes is the tBRG, which alternates between being process-bearing (basally, apically, or both) and non-process-bearing (Betizeau et al., 2013). This discovery blurs the distinction between a TAP and a bRG, as both cell types are multipolar and have the capacity to self-renew. Thus, these non-polar cells that could re-enter the cell cycle could either be TAPs or tbRGs but not bIPs. Nonetheless, based on the cell morphology, TF expression and cell division obtained, we believe that conditional expression of Pax6 increased the production of bRG and/or TAPs at the expense of bIPs in the mouse SVZ.

Pax6 has been shown to be pivotal in the specification of bIP, as it acts upstream of several TFs, such as Ngn2 (Britz et al., 2006; Kikkawa et al., 2013; Miyata et al., 2004; Scardigli et al., 2003), AP2γ (Holm et al., 2007; Pinto et al., 2009) and Tbr2 (Englund et al., 2005; Sansom et al., 2009). The current data seem to be in contradiction with this. Furthermore, conditional expression of Pax6 induced a significant increase in the percentage of Sox2 positive cells which is consistent with previously reported microarray data from Pax6 overexpressing cells using the D6-promoter (Sansom et al., 2009). Sox2 has been known to interact with other TFs to form a heterodimer to regulate distinct set of target genes (Kondoh et al., 2004), one of which is Pax6 (Kamachi et al., 2001). As Sox2 has been implicated in proliferation by regulating the expression of fibroblast growth factor 4 (Fgf4) and Nestin (Osumi et al., 2008; Osumi and Kikkawa, 2013), it is likely that the co-transcription regulation by Pax6 and Sox2 could affect bIP specification by driving target genes favouring proliferation at the expense of neurogenesis.

3.3.2. Conditional expression of Pax6 increases non-vertical cleavages during mitosis

We next sought to determine the potential mechanism leading to this increase in bRGs when conditionally expressing Pax6. It was previously shown in mouse (Shitamukai et al., 2011), ferret (Gertz et al., 2014) and human (LaMonica et al., 2013) that the cleavage orientation of mitotic cells is linked to bRG generation, where an increase in non-vertical cleavages generates more bRGs. In mouse, where bRGs exist in low abundance (Martinez-Cerdeno et al., 2012; Shitamukai et al., 2011; Wang et al., 2011), at the peak of neurogenesis the majority of aRGs divide with a vertical cleavage orientation (Kosodo et al., 2004; Shitamukai et al., 2011). In contrast, in the developing human cortex, between 37.5% and 50% of aRG divisions have a non-vertical cleavage orientation, and not surprisingly this is reflected by a concomitant increase in the proportion of bRGs (≈50%) (Hansen et al., 2010; LaMonica et al., 2013; Lui et al., 2011). Consistently, our data demonstrate that conditional expression of Pax6 in neurogenic aRG increases the percentage of bRG in the SVZ by altering cleavage orientation. Furthermore, the number of nuclei in the VZ is significantly reduced when we conditionally express Pax6. In addition to the generation of bRG, the reduction of nuclei in the VZ suggests that the other daughter cell, instead of remaining in the VZ, migrates up to the SVZ. The reduction in the number of nuclei in the VZ is unlikely to be due to premature delamination of these conditionally expressing Pax6 cells, as the percentage of apical mitoses was significantly increased compared to the control suggesting that the increase in basal mitoses was not at the expense of apical mitoses. Hence, similar to the gyrencephalic brain, the data suggest that the conditional expression of Pax6 may play a role in switching the main proliferative zone from the VZ to the SVZ.

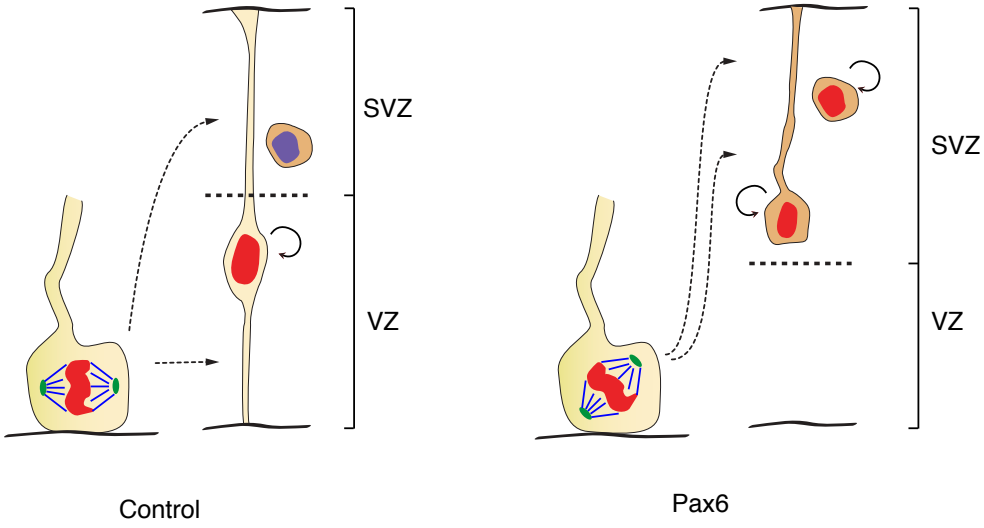

Figure 43: Conditional expression of Pax6 induced an increase in non-vertical cleavages and the fate of the daughter cells.

As cleavage orientation is tightly linked to spindle dynamics during mitosis, it is likely that conditional expression of Pax6 may alter cleavage orientation by tampering with microtubule dynamics. It was previously shown that compared to Tis21 negative cells, Tis21 positive cells have an increase tendency to undergo non-vertical cleavages (Kosodo et al., 2004). However, when we conditionally express Pax6 in these Tis21 positive cells, this tendency is increased even further, suggesting that conditional expression of Pax6 may induce modification of the microtubules dynamics by making these Tis21 positive progenitors even more susceptible to factors inducing non-vertical cleavages. It was previously reported that Pax6 acts upstream of microtubule-associated proteins, such as SPAG5 (Asami et al., 2011; Sansom et al., 2009). Manipulation of Pax6 and SPAG5 levels induced a significant change in cleavage orientation (Asami et al., 2011). Hence, it is likely the increase in the non-vertical cleavages is related to the downstream effect of Pax6 on microtubule-associated proteins (**Fig. 43**).

3.3.3. Role of Pax6 in proliferation and self-renewal of BPs

The role and function of Pax6 in terms of proliferation and neurogenesis has been studied extensively in aRG. However, little has been done to investigate

the role Pax6 may play in BP proliferation, even though the number of Pax6 positive bRGs increases in the SVZ of gyrencephalic animals during the course of neurogenesis. In this work, we demonstrate that upon conditional expression of Pax6 there is a significant increase in proliferating cells in the SVZ that are able to re-enter the cell cycle, supporting the idea that Pax6 is important in maintaining the proliferative and self-renewal capacity of BPs.

It was previously described that the inherent difference in the age of centrosomes plays a role in determining the fate of the progeny. In a nutshell, the self-renewing daughter inherits the mother/older centrosome while the differentiating daughter inherits the daughter/younger centrosome (Wang et al., 2009). As the age of the centrosome is associated with more pericentriolar materials, an older or more mature centrosome will inherit and accumulate more pericentriolar materials as compared to the younger centrosome (Wang et al., 2009). One of the centrosomal proteins that is typically associated to the mother centrosome is ninein (Piel et al., 2000), a protein that localizes to the appendages (Mogensen et al., 2000). Consistently, knockdown of ninein induces premature depletion of progenitors in the VZ, together with a reduction of Pax6 positive cells and an increase in Tuj1 positive cells (Shinohara et al., 2013). Pax6 has been shown to act upstream of ninein where in the Sey mouse, ninein levels are downregulated and follows the premature depletion of progenitors observed in the knockdown studies (Asami et al., 2011; Cheng et al., 2007). While it is currently unknown how the inherent centrosomal difference is distributed in bRG progeny, it will be interesting to understand how the conditional expression of Pax6 affects the asymmetric inheritance of centrosome. It is tempting to speculate that conditional expression of Pax6 may increase the overall ninein levels in both daughter cells, thus producing two daughter cells with the same proliferative and self-renewing capacity.

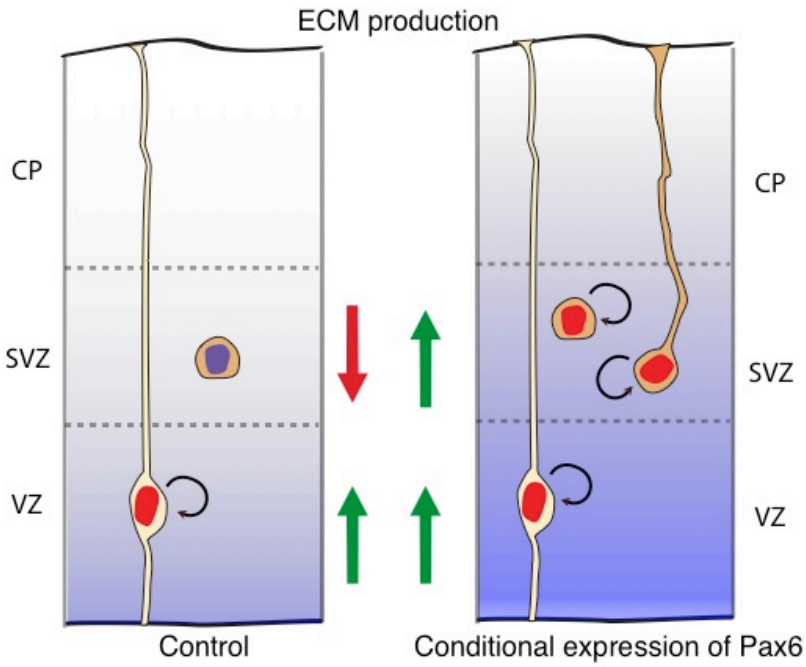

Figure 44: Conditional expression of Pax6 (red nucleus) increases the production of ECM in the SVZ, making it more amenable for self-renewing basal progenitors to reside.

Our lab has previously reported that the production of ECM plays an important role during evolution in maintaining progenitor self-renewal capacity (Arai et al., 2011; Fietz et al., 2012; Stenzel et al., 2014). In mouse, progenitors residing in the SVZ downregulate ECM production, while in human it is maintained. Furthermore, transcriptome analysis of neurogenic Tis21 positive cells *versus* proliferative Tis21 negative cells demonstrate that ECM production is downregulated in Tis21 positive cells (Arai et al., 2011). Consistently, the majority of cells in the mouse SVZ are neurogenic and hence are Tis21 positive, in line with data obtained by comparing ECM expression in the various germinal zones (Fietz et al., 2012). The maintenance of ECM production in the human SVZ thus enables and supports those self-renewing BPs (Fietz et al., 2012). Interestingly, Pax6 acts upstream to several genes relating to ECM such as Tenascin-C (Götz et al., 1998; von Holst et al., 2007) and integrins (Berger et al., 2007). Both factors have been shown to be important in maintaining the self-renewing capacity of progenitors (Berger et al., 2007; Besser et al., 2012; Fietz et al., 2010; Stenzel et al., 2014; von Holst et al., 2007). Although it may not be the only factor involved in

regulating ECM production, the increase expression of Pax6 positive cells in the basal compartment may alter the microenvironment in the human SVZ, making it more amenable for BPs with higher self-renewing capacity to self-renew and proliferate. The conditional expression of Pax6 may thus alter the ECM composition in the mouse SVZ, making it more permissive for more self-renewing BPs to reside (**Fig. 44**).

3.3.4. Pax6 and neuronal migration

Migration of neurons to the correct layer and position in the cortex is vital in forming functional connectivity that allows neurons to encode for a specific behaviour. Any inaccuracy in neuronal migration often leads to neurodevelopmental diseases. There are two major types of migration used by projection neurons to translocate to the proper lamina – somal translocation and glia-mediated migration (Hippenmeyer, 2014; Nadarajah and Parnavelas, 2002; Valiente and Marin, 2010; Wu, 2014). Somal translocation is normally observed in early born neurons where these cells form the preplate. As development progresses, the distance between the ventricular surface and pia increases, rendering it more difficult for neurons to undergo somal translocation. Instead, migratory neurons opt for the glia-mediated migration by using the radial fibres of the bipolar aRG. The glia-mediated migration follows a sequence of steps as listed below (**Fig. 45**).

1. Newly generated neurons in the VZ, delaminates from the ventricular surface and migrates towards the SVZ.
2. In the SVZ, neurons adopt a multipolar morphology, allowing them to survey the area prior to polarisation to the predetermined future axon.
3. Polarisation of neurons to form the bipolar morphology adopted by migratory neurons.
4. Migration of neurons along the radial fibre of aRGs. Migratory neurons undergo a repetition of several steps as shown in **Fig. 45(b-e)**.
5. Entry into the CP via the SP.

6. Establishment of the leading edge to the tip of the MZ.
7. Terminal somal translocation. After formation of a strong attachment to the MZ, neurons downregulate cell adhesion molecules that are used to attach neurons to the radial fibres and translocate to the appropriate and correct lamina via somal translocation, passing through older born neurons in an inside-out fashion.

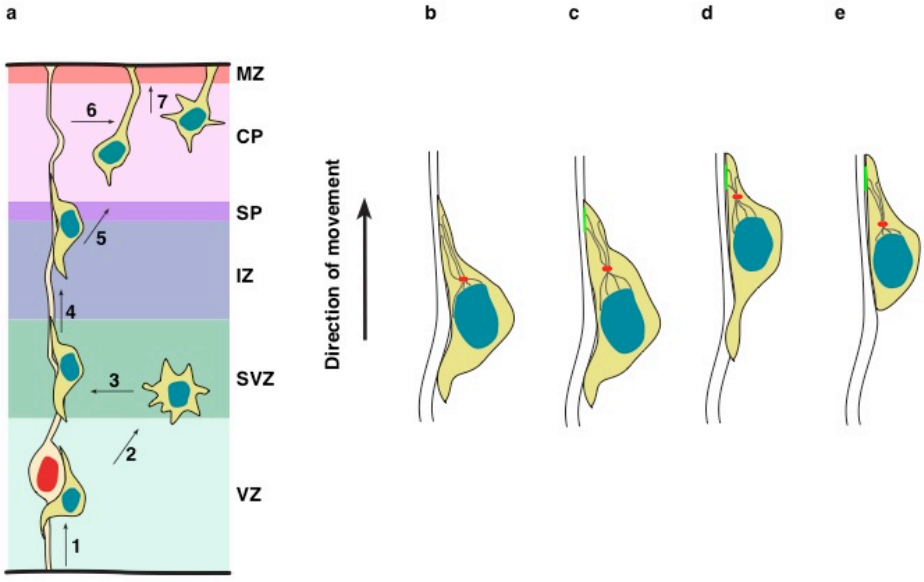

Figure 45: Glia-mediated neuronal migration in the dorsal telencephalon. **(a)** Overview of steps involved in migration of neurons generated in the VZ into the cortical plate. **(b-d)** Sequential changes in neuron from step 4 (from **a**) while moving along the radial glia fibres. **(b)** Formation of the leading edge **(c)** Attachment of the leading edge to the glia fibre (green) and the swelling of the leading edge **(d)** Remodelling of the microtubules and the translocation of the centrosome (red) and nucleus (cyan). **(e)** Retraction of the trailing edge. Adapted from Hippenmeyer (2014) and Wu et al., (2014).

In control, we observed that most electroporated cells have successfully migrated to the CP at 4 days after IUE. Conditional expression of Pax6, however, produced a phenotype that is similar to the previously described overexpression of Pax6 chimeric animals and Sey mice (Georgala et al., 2011a), although the mechanisms leading to this phenotype may not be similar. Conditional expression of Pax6 induced an accumulation of electroporated cells in the SVZ/IZ. Interestingly, this is only specific to the highly expressing Pax6 but not for those lowly expressing Pax6 cells.

This led us to ask how does Pax6 affect neuronal migration? During development, as neurogenesis begins in the telencephalon, Pax6 is normally downregulated as progenitors begin to differentiate into neurons. Hence, continual expression of Pax6 would thus disrupt proper migration of differentiated neurons. As neuronal migration involves the remodelling of cell cytoskeleton, it is not surprising that alteration in protein expression involved in cytoskeletal remodelling may affect neuronal migration. It has been previously reported that Pax6 acts upstream of proteins involved in cytoskeleton remodelling, such as doublecortin (DCX), Cdc42, nuclear distribution element 1 (NDE1), NDE-like 1 (NDEL1) and CDK5rap2 (Sansom et al., 2009). Alteration in any one of these proteins' levels could ultimately affect the organization and stability of the cytoskeleton dynamics, thus ultimately altering the migration along the radial fibres or the dynamic change in morphology (i.e. from the multipolar to bipolar) (Hippenmeyer et al., 2010; Manent et al., 2009; Patrick et al., 1998; Tsai and Gleeson, 2005; Vallee et al., 2009)

Pax6 has also been shown to affect expression of several cell-adhesion molecules, such as N-CAM and R-Cadherin where overexpression of Pax6 elevates the levels of these proteins (Berger et al., 2007; Stoykova et al., 1997). It was recently hypothesised that membrane trafficking pathways involving Rab5 and Rab11 are important in controlling the multipolar transition and final CP positioning by regulating the expression of cell adhesion molecules on the surface of migrating neurons (Kawauchi et al., 2010). Pax6 has been shown to act upstream of Rab5, where overexpression of Pax6 has been linked to the reduction in Rab5 expression (Sansom et al., 2009). It is thus likely that the reduced Rab5-dependent endocytosis may have led to the accumulation of cell adhesion molecules on the surface of migrating neurons, altering the adhesive properties of these cells. Hence, the clustering of electroporated cells (most of the heterotopia consists only of electroporated cells) suggests that the abnormal accumulation of these cells reflects the

increased “stickiness” of the cells due to the elevated expression of cell-adhesion molecules.

Accumulation of these cells in the SVZ/IZ is suggestive of another potential migratory problem that may arise from the inability of these cells to enter the CP via the SP. The microenvironment of the SP is suggested to be different from the IZ. The SP may act as a checkpoint to ensure that only neurons that have met a certain prerequisite could pass through and migrate into the CP (Hippenmeyer, 2014). The exact mechanism of the entry of migratory neurons into the SP is still currently unknown. What is known, however, is that the expression of certain proteins may be key for these cells to enter the CP. Abnormal levels of Ndel (Hippenmeyer et al., 2010), Dab1 (Feng et al., 2007) and APP (Young-Pearse et al., 2007) have been shown to accumulate neurons in the SVZ and/or IZ, similar to the phenotype observed in the conditional expression of Pax6. Because these proteins are downstream of Pax6 (Sansom et al., 2009), they may be responsible for preventing entry into the SP in the Pax6 mouse. Furthermore, the observed immaturity of the neurons accumulated in the SVZ/IZ may also explain the heterotopia, as the SP may act as a maturation checkpoint.

3.3.5. Pax6 and evolutionary changes

Through this work, we have demonstrated that the maintenance of Pax6 in BPs is important in diversifying the type of BPs while maintaining progenitors’ proliferative and self-renewal capacity. How, then is Pax6 expression and its downstream targets maintained in BPs of humans and monkeys but not in mice?

Pax6 is a highly conserved TF. A quick comparison between the human and mouse Pax6 demonstrates that these two species encode identical proteins of 422 amino acids in length (Callaerts et al., 1997). Furthermore, the TF is prevalent in the phylogeny to the extent that even in the eyeless, brainless

sea urchin expresses a homolog of this TF (Osumi and Kikkawa, 2013). What sparked the interest and a torrent of research on this particular TF was work that demonstrated how interchangeable Pax6 is across species. It was shown that the fly *eyeless*, mouse *Pax6*, and human *PAX6* were each sufficient to induce compound eyes in the imaginal discs of the fly (Halder et al., 1995), touting Pax6 as a master regulator of eye development. Hence, we hypothesise that because *Pax6* is so highly conserved, differences in expression levels between species should be due to subtle differences in the regulatory sequences or the expression in the downstream targets.

Pax6 expression is orchestrated by various promoters and enhancers that are distributed over a hundred kilobases (Xie et al., 2013), thus making the study on the regulation of Pax6 expression daunting especially while doing a species comparison. The presence of multiple promoters and regulatory elements provide a possible hypothesis as to how the regulation of Pax6 expression may vary across species. This difference was first illumed by Xu et al. (1999) where the Drosophila elements could reproduce *Pax6* expression in mouse but not the reverse, suggesting that the regulatory elements may not be entirely conserved even though the coding sequence for Pax6 is (Xu et al., 1999). It is thus, tempting to speculate that changes in the regulatory elements during evolution may have favoured the maintenance of Pax6 expression in BPs, and thus altering the BP composition and proliferative capacity in gyrencephalic animals.

In addition to changes in the regulatory elements, variation could also arise in the expression of target genes recognised by the DNA-binding domain of Pax6. Within the *Pax6* gene, there are five highly interactive DNA-binding domains (i.e. PAI, RED, ß-turn, linker and HD, see **Fig. 9**) that has been suggested to recognise over 50 000 genomic loci (Xie et al., 2013). Molecular dissection of these DNA-binding regions has elegantly demonstrated that in different organs lies a preferential binding to certain sets of DNA binding regions. For instance, the HD has been shown to preferentially bind to genes

that are known for the development of the eye. Deletion of the HD has no known effect on the forebrain but has deleterious effect on eye development (Haubst et al., 2004; Walcher et al., 2013), thus elucidating at the gene level how *Pax6* may be differentially regulated in different organs.

Recent studies have shown that the putative Pax6-binding sites on target genes can vary significantly when compared to the more conserved TF-binding sites such as E-box (Osumi and Kikkawa, 2013). Thus, any alteration in the binding sites may affect the affinity of the TF to bind to a particular site and furthermore alter the rate and efficiency of transcription of target genes. Not limited to that, heritable mutations in the genome may allow for new Pax6-binding sites, especially with its varied recognition sequence. The alteration in expression pattern or the acquisition of new downstream target genes may play an important role during evolution in the generation of more bRGs. Thus, it may be interesting to compare the downstream targets of Pax6 in different species in order to discover whether any specific alteration or acquisition of new target genes that may have led to the generation of more bRG and ultimately an expanded neocortex.

3.4. bRG, a prerequisite to an expanded neocortex?

The quest in understanding how the mammalian neocortex expanded has produced various elegant sets of experiments on the contribution of each progenitor type (Chenn and Walsh, 2003; Nonaka-Kinoshita et al., 2013; Stahl et al., 2013). To understand the role of aRG may play in the expansion of the neocortex, expression of a constitutively stabilized form of beta-catenin in aRGs has led to an interesting phenotype in the mouse cortex (Chenn and Walsh, 2003). The expression of the constitutively stabilized form of beta-catenin enhances the proliferative capacity of aRG, leading to the expansion of the founder pool, and ultimately causing the ventricular surface to expand laterally. When the rate of lateral expansion at the ventricular surface exceeds the rate of expansion of the pia surface, it results in aberrant folding at the

ventricular surface. Similar phenotypes have also been observed in models that prevent cell death in the founder pool (Kuida et al., 1998). This suggests that although expansion of aRG may be important in increasing the neurogenic capacity of the overall cortical layer, the phenotype obtained however suggests that the pia surface needs to expand at a much higher rate as compared to the ventricular surface in order for gyrification to occur at the pia.

The intermediate progenitor hypothesis expounded by Kriegstein proposes that expansion of the neocortex is closely related to expansion of the SVZ via TAPs (Kriegstein et al., 2006, Fish et al. 2008). The validity of the intermediate progenitor hypothesis was recently verified by the overexpression of the cdk4/cyclinD1 complex in mouse bIPs (Lange et al., 2009; Nonaka-Kinoshita et al., 2013). These cells have an increased proliferative capacity where they are able to re-enter the cell cycle, unlike their control counterpart where these cells would undergo symmetric differentiative division and exit the cell cycle. While these TAPs converted from bIPs are able to expand the neocortex, they fail to induce gyrification in the mouse neocortex. These results suggest that a proportional increase in TAPs is sufficient to increase neuron number, but not to induce gyrification.

The initial discovery of bRG in ferret and human suggested bRG as a progenitor type specific to gyrencephalic species (Fietz et al., 2010; Hansen et al., 2010; Reillo et al., 2011). However, studies on mouse and later marmoset disproved this hypothesis as bRGs are present in lissencephalic animals as well (Kelava et al., 2012; Shitamukai et al., 2011; Wang et al., 2011). Therefore, what distinguishes a gyrencephalic brain from a lissencephalic brain is not merely the presence of bRG but rather the proportion of bRG present in the SVZ and the type of divisions these bRGs make. In large-brained animals, bRGs exist at a higher proportion as compared to the small-brained animals (Fietz et al., 2010; Gertz et al., 2014; Kelava et al., 2012; LaMonica et al., 2013; Reillo et al., 2011; Shitamukai et

al., 2011; Wang et al., 2011, Fietz and Huttner, 2011). Furthermore, in a recent study conducted by Stahl et al. (2013), it was demonstrated that knockdown of the DNA-associated protein Trnp1 increases the proportion of bRGs in the mouse neocortex significantly (Stahl et al., 2013). Intriguingly, this increase in bRGs was accompanied by gyrification of the mouse cerebral cortex. This was not observed in the other experiments that had led to the expansion of the aRG and bIPs. The crucial role of bRG in the expansion and gyrification of the neocortex was further corroborated by the finding that in the developing ferret brain, regions of the prospective gyral region were shown to have higher number of bRGs as compared to the prospective sulcus region (Nonaka-Kinoshita et al., 2013; Reillo and Borrell, 2012; Reillo et al., 2011). The presence of more bRG in the prospective gyral region plays two roles. Firstly, it increases the proliferative capacity of this particular region. Secondly, the basal process of the bRG allows for additional radial fibre tracks that allows for the migration of the newborn neurons into the CP. Together, this further strengthens the link between the proportion of bRG and the expansion and gyrification of the neocortex.

3.5 Outlook

So, where do we go from here?

For the general approach, we have demonstrated through this work that microinjection of ferret poly-A^+ RNA is able to generate bRG-like cells instead of neurons. As the identity of a progenitor is currently defined by its cell morphology, TF expression, and the type of division these cells make, it would be of importance to determine whether these cells were in fact bRGs. This can be confirmed by characterising these cells further by TF expression and if possible the mode of division of these cells (i.e. via live imaging or clonal analysis). Furthermore as the “instructions” to generate bRGs are present in the ferret poly-A^+ RNA, it would be interesting to determine which genes are required to generate bRGs. In addition, as bRG specific markers are currently

unavailable, it is possible that the marker for bRG may very well lie within this set of “instructions”. It would therefore be interesting to determine whether these sets of “instructions” will be able to reconstitute bRGs in the mouse dorsal telencephalon.

For the candidate gene approach, it would be of interest to develop a system that allows for the transient expression of the Pax6 protein. Ideally, this system would allow for the temporal control of Pax6 expression. One strategy is by combining the current Cre-lox system together with the tet-off system. In this system, the conditional expression of Pax6 is induced by tamoxifen administration and can be switched off via doxycycline treatment. This would limit Pax6 expression and reduce the neuronal migratory issues that are typical in animal models involved in Pax6 manipulation. With normal migration, it would be interesting to see whether conditional and temporal expression of Pax6 would lead to a mouse that has an expanded and folded cortex.

Chapter 4
Materials and methods

4.1. Materials

4.1.1.Equipment

Centrifuges	Beckman Coulter Avanti J-25 Heraeus, Biofuge, Pico Table top centrifuge (Thermo)
Balances	Sartorius, BL3100 Sartorius, BL121S
DNA/RNA electrophoresis	EMBL, DNA gel chamber Amersham Pharmacia Biotech, EPS301, power supply Vilber Lourmat, Bio-Vision, Gel documentation system
Thermocycler	MJ research, PTC-200
Pipettes	Gilson
Histology	Microm, cryostat, HM560 Leica, vibratome, VT1000S
Light microscopes	Olympus, SZX12 (dissection) Zeiss, Axiovert 200
Heating block	Labtech international, Dri block Digi2
Dissecting lamp	Olympus, Highlight 3100
Confocal microscopes	Zeiss, LSM 700
Transjector	Eppendorf, Transjector 5246
Cell and slice culture	SterilGARD III Advance, cell culture hood, The Baker Company HeraCell, cell culture incubator, Heraus Ikemoto scientific technology, RKI-10-0310 (slice tissue incubator)
Needle puller	Sutter instruments, Flaming/Micropipette puller
Anaesthesia system	VetEquip, Pleasanton, California
Electro square porator	BTX genetronics, Inc., ECM 830
Tweezertrodes	BTX genetronics Inc., 45-0488

4.1.2. Antibodies

Primary antibodies

Antigen	Description	Dilution	Source
βIII –tubulin	Mouse, monoclonal, IgG	1:500	Sigma
Caspase 3	Rabbit, polyclonal, IgG	1:500	Abcam
Cyclin D1	Rabbit, monoclonal, IgG	1:200	Thermo
Dextran	Mouse, monoclonal, IgG	1:500	Stemcell
eGFP	Chicken, monoclonal, IgG	1:1000	MPI
GFAP	Mouse,monoclonal, IgG	1:500	Milipore
HSV	Goat, polyclonal, IgG	1:250	Abcam
Ki67	Rabbit, polyclonal, IgG	1:300	Abcam
Olig2	Mouse, monoclonal, IgG	1:200	Thermo
Pax6	Rabbit, polyclonal, IgG	1:200	Covance
Phospho-histone H3	Rat, polyclonal, IgG	1:500	Abcam
Phospho-vimentin	Mouse, polyclonal, IgG	1:500	MBL
RFP	Rabbit, polyclonal IgG	1:1000	Molecular probes
SATB2	Mouse, monoclonal, IgG	1:200	Abcam
Sox2	Goat, polyclonal, IgG	1:500	Santa Cruz
Tbr1	Rabbit, polyclonal, IgG	1:200	Chemicon
Tbr2	Rabbit, polyclonal, IgG	1:200	Abcam

Secondary antibodies

Antigen	Conjugate	Dilution	Source
Goat anti-Mouse	Alexafluor® 405	1:500	Molecular probes
Goat anti-Rabbit	Alexafluor® 405	1:500	Molecular probes
Donkey anti-Rabbit	Alexafluor® 594	1:500	Molecular probes
Donkey anti-Goat	Alexafluor® 647	1:500	Molecular probes
Donkey anti-Mouse	Alexafluor® 647	1:500	Molecular probes
Donkey Anti-Rabbit	Alexafluor® 647	1:500	Molecular probes
Goat anti-Rat	Alexafluor® 647	1:500	Molecular probes
Dextran	FITC	1:1000	Stemcell

4.1.3. Common buffers

Bacteria culture

LB-medium	10 mg ml^{-1} NaCl, pH7.0 10 mg ml^{-1} Bacto-Tryptone 5 mg ml^{-1} Bacto-Yeast extract
LB-Agar	15 mg ml^{-1} Bacto-Agar in LB-medium
Ampicillin (100x)	100 mg ml^{-1} in H_2O
Kanamycin (300x)	50 mg ml^{-1} in H_2O

Immunofluorescence

Permeabilisation buffer	0.3% TritonX-100 in PBS
Quenching solution	0.1 M Glycine in PBS, pH7.4
Tx buffer	0.2% Gelatin 300 mM NaCl 0.3% TritonX-100 in PBS
Mowiol	6.9 g Glycerol 2.4 g Mowiol 120 µl 200 mM Tris/HCl, pH8.5 in 6 ml H_2O
1xPBS	1.37 M NaCl (8g) 2.7 mM KCl (0.2g) 1.4 mM KH_2PO_4 (0.2g) 10 mM Na_2HPO_4 (1.44g) pH to 7.4 in HCl
4% Paraformaldehyde	4 g Paraformaldehyde in 100 ml of 120 mM phosphate buffer

Embryo culture and dissection

Penicillin/Streptomycin (100x)	10.000 U ml^{-1} Penicillin 10.000 U ml^{-1} Streptomycin in PBS
Tyrode	16 g NaCl 0.4 g KCl 0.4 g $CaCl_2$ 0.42 g $MgCl_2.6H_2O$ 0.114 g $NaH_2HPO_4.2H_2O$ 2 g $NaHCO_3$ 2 g Glucose pH 7.4 in H_2O

Mouse slice culture medium	Rat Serum (Charles River, Japan) 1x Penicillin/Streptomycin 1x N2 supplement 1x B27 supplement 0.1 mM HEPES solution in neurobasal medium
Ferret slice culture medium	Ferret Serum (Sera Laboratories international, UK) 1x Penicillin/Streptomycin 1x N2 supplement 1x B27 supplement 0.1 mM HEPES solution in neurobasal medium
Reconstitution buffer	2.2 g Sodium bicarbonate 0.05 M Sodium hydroxide 200 mM HEPES solution

Microinjection

Microinjection medium	DMEM modified (without phenol red) 0.01 M Hepes 1x N2 supplement 1x B27 supplement 1x Penicillin/Streptomycin 20 µM Glutamine in distilled water
Alexa Fluor dextran stock	10 µg μl^{-1} in distilled water

DNA electrophoresis

10x-DNA loading buffer	50 mM Tris/HCl, pH 7.6 2.5 mg ml^{-1} Bromophenol blue 2.5 mg ml^{-1} Xylene Cyanol 60% Glycerol in H_2O
10x TBE	0.89 M Tris 0.89 M Boric acid 20 mM EDTA, pH8.0
50x TAE	2 M Tris 1 M Acetic acid 100 mM EDTA pH 8.5
Ethidium bromide stock	10 mg ml^{-1} in H_2o (1 µl into 50 ml gel)

4.1.4. Plasmids

pCAG–loxP–Gap43–GFP–loxP–nRFP (from Dr Jifeng Fei): This plasmid was used as the control plasmid. It served as the backbone on which the Pax6 and IRES sequence was cloned in between the second loxP site and nRFP. The Gap43 is tagged with a GFP that is flanked by two LoxP sites, which allowed for the Cre recombinase to excise the region in between the plasmid. The RFP has a nuclear localization signal tagged to it.

pCAG-loxP-GAP43-GFP-loxP-Pax6-IRES-RFP: This plasmid was used to conditionally express Pax6.

pCAG-Cre (from Dr Jifeng Fei): This plasmid drives the expression of Cre and was used in plasmid validation.

pMIIXG-Pax6-IRES-GFP (from Dr Magdalena Götz): This plasmid drives the expression of Pax6 and GFP. The Pax6 and IRES sequence was excised and cloned into the control plasmid

pTNT-mRFP (from Dr Elena Taverna): This plasmid was used to obtain *in vitro* transcribed RFP mRNA that was used as a reporter poly-A^+ mRNA for the microinjection.

4.1.5. Primers for cloning

Pax6-sal-F : 5'- CCG TCG ACA TGC AGA ACA GTC ACA GCG GAG TG -3'

IRES-sal-R : 5'- CCG TCG ACT GTG GCC ATA TTA TCA TCG TG-3'

4.1.6. Bacterial strains

Top10 (Invitrogen): F-*, mcr*A Δ(*mrr-hsd*RMS-*mcr*BC),Φ80*lac*ZΔM15, Δ*lac*X74, *rec*A1, *ara*D139, *gal*U, *gal*K, Δ(*ara-leu)*7697, *rps*L(Str^R), *end*A1, *nup*G

4.1.7. Cells

HeLa: Adherent epithelioid cell line derived from cervical cancer cells taken from Heinrietta Lacks (died 1957)

NIH3T3: Mouse adherent fibroblast cell line obtained from Swiss mouse embryo tissue

HEK293T: Human embryonic kidney cells that stably express the SV40 large T antigen

4.1.8. Mice

Tis21–GFP knock-in line: The protein-encoding portion of the exon1 in the Tis21 gene is replaced with a GFP carrying a nuclear localization signal (Haubensak et al., 2004). In this study, this mouse line was used to evaluate the population of the microinjected cells at 0 and 24 h after microinjection and characterisation of the *Tis21–CreER^{T2}* knock-in line. This mouse strain is maintained in C57Bl6OSHD mouse line.

Tis21–CreER^{T2} knock-in line: Like the *Tis21*–GFP mouse, the exon1 of these mice were replaced with a CreER^{T2} cassette (Fei, 2008). In this study, the male homozygous *Tis21*–CreER^{T2} mice were crossed with female wild type C57Bl6OShd mice. The heterozygous embryos were used in the conditional expression of Pax6 experiments.

RCE:loxP line (Jackson)*:* This mouse line harbours a Rosa26 promoter driving the expression of a STOP cassette flanked by two loxP sites followed by GFP.

4.1.9. Ferret

Pregnant ferret were obtained from Marshall BioResources and housed at the Bundesintitut für Risikibewertung or at Biotie Therapies. P1 kits were used for the microinjection of ferret slice culture while P1 and P2 kits were used for RNA extraction. Kits were decapitated and brains were extracted for either microinjection or snap frozen with liquid nitrogen for RNA extraction.

4.2. Methods

4.2.1. Plasmid preparation

4.2.1.1. Preparation and purification of plasmid DNA

DNA was extracted and purified using kits obtained from Qiagen (Miniprep kits for small quantities and Endotoxin Free Maxiprep kits for large quantities), following manufacturer's instruction.

4.2.1.2. Pax6 expression vectors

For the *pCAG–loxP–GAP43–GFP–loxP–Pax6–IRES–nRFP* plasmid, the coding sequence of the Pax6 and IRES sequence were obtained by subcloning from the PMIIXG–Pax6–IRES–GFP plasmid. The Pax6 and IRES region were amplified and a SalI restriction sites were added using the primers Pax6–sal–F and IRES–sal–R. The amplified products were inserted into the control plasmid, *pCAG–loxP–GAP43–GFP–loxP–nRFP* which was linearised using XhoI.

4.2.2. Transient transfection of HEK293T cells

Cells were kept in culture in a humidified incubator at 37°C with 5% CO_2 atmosphere. Transient transfection was conducted using Lipofectamine 2000 reagent (Invitrogen) according to manufacturer's instruction. In summary, cells were plated overnight in cell culture medium (DMEM, Gibco; 10% fetal calf serum, Gibco). In the following morning, cells were transfected with 250 ng of pCAG–Cre and/or 250 ng of control or Pax6 constructs diluted with serum free DMEM in combination with 1 µl of lipofectamine. Cells were incubated for 48 h prior to fixation with 4% paraformaldehyde for 10 mins. The paraformaldehyde was then removed and cells were kept in PBS until further processing.

4.2.3. Mice handling, embryo collection and sectioning

All animal experiments were performed in accordance with German animal welfare. Mice were bred and maintained in strict pathogen-free conditions in the animal facility (MPI-CBG). Mice were housed individually in ventilated cage system (Techniplast). Acidified water (pH 2.8) and autoclaved pellet diet (Harlan Teklad 2018S) were provided *ad libitum*. Animals were kept in a 12 h

light and 12 h dark cycle (6.00 am lights on, 6.00 pm lights off) in a temperature controlled room (22°C) with relative humidity of 55 ± 10%. Matings were done naturally and plug checks were done the following morning. Once the females were plugged positive, that day was designated as E0.5.

Pregnant female dams were sacrificed by cervical dislocation. The abdominal cavity was opened and the uterus was removed. For RNA extraction, the embryos were dissected in 4°C Tyrode's solution. For embryos used for slice culture, embryos were dissected in 37°C Tyrode's solution. To dissect the brains, embryos were decapitated and brains were extracted. The meninges were removed from the ventral part. For RNA extraction, brains were immediately snap frozen with liquid nitrogen and stored at –80°C until use. For organotypic slice culture preparation, brains were embedded in 3% low melting point agarose type XI. Once solidified, brains were sectioned to 250 µm thick sections using the vibratome. For organotypic slice culture preparation using the microknife, hemispheres were separated and sectioned to ≈250 µm thickness without agarose embedding. For fixed tissues, once the brains were harvested, they were fixed in 4% paraformaldehyde overnight at 4°C. For cryosections, on the following day, paraformaldehyde solution was replaced with 30% sucrose solution and left overnight. Tissues were embedded with Tissue-TEK optimal cutting temperature (O.C.T) compound (Sakura Finetek) and stored at -20°C. Tissues were sectioned at a thickness of 10-12 µm. For vibratome sections, after fixation, tissues were washed with PBS before embedded in 3% low melting point agarose at 37°C. Tissues were stored at 4°C and sectioned at a thickness of 50-70 µm. For microinjected slices, the 250 µm slices were fixed in 4% paraformaldehyde overnight at 4°C. On the following day, slices were washed with PBS before embedded in 3% low melting point agarose at 37°C. Tissue was stored at 4°C and were sectioned at 50 µm thickness using vibratome.

4.2.4. Tamoxifen administration

2 mg tamoxifen (Sigma, Cat no: T-5648; 20 mg ml^{-1} in corn oil) was prepared. Pregnant dams were treated with tamoxifen orally. Mice were gripped firmly at the neck while maintaining a straight alignment of the nose, head and spine. The gavage was entered along the roof of the mouth and gently placed all the way through the esophagus without inducing any damage onto the pregnant dams. For characterisation of the *Tis21*–$CreER^{T2}$ mice, tamoxifen was administered at E13.5 and sacrificed at 24 h later. For conditional expression of Pax6, tamoxifen is administered prior to and on the day of IUE.

4.2.5. Isolation of poly-A^+ RNA

Brains from P1 ferret were dissected in ice cold PBS. The telencephala were isolated. Tissues were snap frozen using liquid nitrogen and stored at -80°C until used. The tissue was thawed on ice and the total RNA was isolated using the RNeasy Maxi Kit (Qiagen). In order to obtained sufficient amount of poly-A^+ RNA, a total RNA of 1.5-2 mg of RNA was required as a starting material. To isolate the poly-A RNA, the oligo-dT cellulose column from the Poly(A)Purist kit (Ambion) was used. Following manufacturer's instruction, a yield of 15 µg of poly-A+ RNA can be obtained. The poly-A+ RNA was aliquoted, snap frozen and stored at -80°C until use.

4.2.6. In vitro transcription

To generate the IVT–RFP, the pTNT-mRFP plasmid was linearized using NotI, capped and polyadenylated using the T7 mMESSAGE-mMACHINE kit (Ambion). The IVT–RFP mRNA obtained was dissolved in RNase-free water at 0.3 µg $µl^{-1}$ and snap frozen as 1-2 µl aliquots.

4.2.7. Microinjection in HEK293, HeLa and NIH3T3 cells

Cells were kept in culture until it reached a confluency of 70-80%. The microinjected compound (10 µg $µl^{-1}$ Alexa fluor dye and/or 0.5 µg $µl^{-1}$ IVT–RFP) were centrifuged at 13 000 g at 4°C for 30 mins. The microinjected compounds were kept on ice throughout the microinjection. Cells were

microinjected using glass capillaries with the following parameters: Heat=ramp test temperature; P=100; pull=100; Vel=100; Del=100. Microinjected cells were kept in culture for 24 h. Cells were fixed with 4% paraformaldehyde for 10 mins following which it was removed and kept in PBS until further processing.

4.2.8. Microinjection of mouse and ferret slice tissue

E14.5 mice or P1 ferret sections of 250 µm thickness were used. Organotypic slices were kept in mouse slice culture medium or ferret slice culture medium (depending on species) at 37°C until use. Microinjected compounds were centrifuged at 13 000 g at 4°C for 30 mins. Compounds were kept on ice throughout the microinjection procedure. During microinjection, organotypic slices were kept in CO_2 independent microinjection medium. Slices were oriented and kept in place using the microinjection grid. The grid consists of a 10 mm x 10 mm U-shaped brass frame with 6 nylon wires that are spaced 10 µm apart and 250 µm from the bottom, spanning the two opposite arms of the U. The microinjection was conducted with a transjector (Eppendorf 5246) and a micromanipulator (Eppendorf-InjectMan-5179) coupled to an epifluorescent microscope (Axiovert 200). Microinjection pipettes (with diameter less than 0.5 µm) were pulled from borosilicate glass capillaries (1.2 mm outer diameter x 0.9 mm inner diameter, Harvard Apparatus, GC120TF-10) using a P-97 flaming brown puller. The microinjection compounds were loaded into the glass capillaries and were injected into cells facing the ventricles of the dorsal telencephalon using pressure (100-200 hPA) by gently touching the cell surface. After microinjection, organotypic slices were kept in the slice culture chamber maintained at 37°C in a humidified atmosphere of 40% O_2/ 5% CO_2/ 55% N_2.

4.2.9. Organotypic slice culture

Organotypic slices were embedded at room temperature with ≈75 µl of type Ia collagen (Cellmatrix, Nitta Gelatin) with a concentration of 1.5 mg ml^{-1} together with DMEM and neutralizing buffer according to manufacturer's

protocol on a 35 mm Petri dish with a 14 mm microwell (MatTek Cooperation). Slices were left at 37°C for 40 mins to allow for the solidification of the collagen before adding 1 ml of slice culture medium. Slices were kept in a humidified incubation chamber of POC-Chamber-System (Saur) that is supplied with 40% O_2, 5% CO_2, 55% N_2.

4.2.10. In utero electroporation

The procedure was performed as described by Shimogori and Ogawa (2008) with minor modifications (Shimogori and Ogawa, 2008). Pregnant dams carrying E13.5 embryos were anesthesized using isofluorane. The uterine horns were exposed and plasmid DNA (2-3 µg $µl^{-1}$) together with 0.25% Fast Green FCF was injected into the ventricles of the embryos through the uterine wall using a glass micropipette. A series of pulses (30 V, 6 pulses with 1 ms interval) were delivered across the uterus with the electrode paddles placed on either side of the embryo's head. The uterus were kept moist with pre-warmed PBS to 37°C throughout the experiment. Pregnant dams were kept on the heating block (40°C) throughout the experiments. After IUE, the uterus was placed back into the abdominal cavity and was sutured close. Pregnant dams were sacrificed at specific time points after IUE. The embryos were dissected and fixed in 4% paraformaldehyde for further analysis.

4.2.11. EdU labelling

Edu labelling was performed by injecting 1 mg ml^{-1} EdU intraperitoneally. For the determination of the number of cells that were in S-phase, pregnant mice were injected with EdU 1 h before sacrifice. For the cell cycle exit determination, EdU was injected at 24 h after IUE and were sacrificed 24 h after EdU injection, 48 h after IUE.

For EdU detection, vibratome or cryosections were post-fixed with 4% paraformaldehyde for 20 mins after secondary antibodies incubation. EdU labelling was detected using the Click-iT EdU kit with Alexa Fluor 647 (Invitrogen).

4.2.12. Immunofluorescence of fixed cells

Cells were fixed with 4% paraformaldehyde for 10 mins. Cells were then washed with PBS, permeabilised with 0.3% TritonX-100 in PBS for 30 mins, quenched with 0.1 M glycine in PBS for 30 mins. Cells were sequentially incubated with antibodies first with primary antibodies for 3 h followed by secondary antibodies for 1 h at room temperature. Coverslips were washed with PBS and mounted onto glass slides using Mowiol

4.2.13. Immunofluorescence on tissue

All sections were subjected to antigen retrieval protocol as follow. Cryosections were first rehydrated with PBS before further processing. Sections were heated in 0.01 M citrate buffer pH 6.0 at 70°C for 1 h. Sections were then permeabilized using 0.3% TritonX-100 in PBS for 30 mins and quenched with 0.1 M glycine for 30 mins. Sections were then incubated with primary antibody overnight at 4°C followed by secondary antibody in a solution of 0.2% gelatin, 300 mM NaCl and 0.3% TritonX-100 in PBS for 1 h at room temperature. Floating sections were mounted to Superfrost Plus microscope slides (Thermo Scientific) using Mowiol.

4.2.14. Image acquisition

Images from immunofluorescence were acquired using a Zeiss 700 confocal microscope using 25x and 63x objectives. Images were taken as either 2.1 µm (25x) or 0.9 µm (63x) single optical sections. Images taken as tile scans were stitched together using the ZEN software (Zeiss). Quantifications were performed using Fiji.

4.2.15. Determination of germinal zones and cell counting

The germinal zones were identified based on their different histological characteristics. The VZ was identified by the densely packed, radially aligned cells lining the ventricle. The nuclei of these cells were more elongated than those in the SVZ. The SVZ was identified by the randomly organized, non-

radially orientated cells. These cells were less dense and had a rounded nucleus. The IZ was identified as a cell sparse layer situated above the SVZ. Cells were counted from a 200 μm width parallel to the ventricular surface of the electroporated area in the dorsal telencephalon. For each 200 μm width of electroporated area counted, there are at least more than 100 electroporated (RFP+) cells counted throughout the entire cortical wall unless otherwise specified. The fluorescence was counted without using pseudo-colour. All cells quantified were counted against the electroporated cells that were RFP+. Data was further processed and statistical analysis was conducted using the Prism software (GraphPad software).

Chapter 5
References

Aaku-Saraste, E., Hellwig, A., Huttner, W.B., 1996. Loss of occludin and functional tight junctions, but not ZO-1, during neural tube closure - remodeling of the neuroepithelium prior to neurogenesis. Dev. Biol. 180, 664-679.

Aboitiz, F., Morales, D., Montiel, J., 2001. The inverted neurogenetic gradient of the mammalian isocortex: development and evolution. Brain Res. 38, 129-139.

Alexandre, P., Reugels, A.M., Barker, D., Blanc, E., Clarke, J.D., 2010. Neurons derive from the more apical daughter in asymmetric divisions in the zebrafish neural tube. Nat. Neurosci. 13, 673-679.

Anderson, S.A., Eisenstat, D.D., Shi, L., Rubenstein, J.L., 1997. Interneuron migration from basal forebrain to neocortex: dependence on Dlx genes. Science 278, 474-476.

Arai, Y., Funatsu, N., Numayama-Tsuruta, K., Nomura, T., Nakamura, S., Osumi, N., 2005. Role of Fabp7, a downstream gene of Pax6, in the maintenance of neuroepithelial cells during early embryonic development of the rat cortex. J. Neurosci. 25, 9752-9761.

Arai, Y., Pulvers, J.N., Haffner, C., Schilling, B., Nusslein, I., Calegari, F., Huttner, W.B., 2011. Neural stem and progenitor cells shorten S-phase on commitment to neuron production. Nat. Commun. 2, 154.

Asami, M., Pilz, G.A., Ninkovic, J., Godinho, L., Schroeder, T., Huttner, W.B., Götz, M., 2011. The role of Pax6 in regulating the orientation and mode of cell division of progenitors in the mouse cerebral cortex. Development 138, 5067-5078.

Attardo, A., Calegari, F., Haubensak, W., Wilsch-Bräuninger, M., Huttner, W.B., 2008. Live imaging at the onset of cortical neurogenesis reveals differential appearance of the neuronal phenotype in apical versus basal progenitor progeny. PLoS ONE 3, e2388.

Barakat, I., Wittendorp-Rechenmann, W., Rechenmann, R.V., Sensenbrenner, M., 1981. Influence of meningeal cells on the proliferation of neuroblasts in culture. Dev. Neurosci. 4, 363-372.

Barbosa-Morais, N.L., Irimia, M., Pan, Q., Xiong, H.Y., Gueroussov, S., Lee, L.J., Slobodeniuc, V., Kutter, C., Watt, S., Colak, R., Kim, T., Misquitta-Ali, C.M., Wilson, M.D., Kim, P.M., Odom, D.T., Frey, B.J., Blencowe, B.J., 2012. The evolutionary landscape of alternative splicing in vertebrate species. Science 338, 1587-1593.

Bayer, S.A., Altman, J., 1991. Neocortical development. Raven Press, New York.

Berger, J., Berger, S., Tuoc, T.C., D'Amelio, M., Cecconi, F., Gorski, J.A., Jones, K.R., Gruss, P., Stoykova, A., 2007. Conditional activation of Pax6 in the developing cortex of transgenic mice causes progenitor apoptosis. Development 134, 1311-1322.

Besser, M., Jagatheaswaran, M., Reinhard, J., Schaffelke, P., Faissner, A., 2012. Tenascin C regulates proliferation and differentiation processes during embryonic retinogenesis and modulates the de-differentiation capacity of Muller glia by influencing growth factor responsiveness and the extracellular matrix compartment. Dev. Biol. 369, 163-176.

Betizeau, M., Cortay, V., Patti, D., Sabina Pfister, S., Gautier, E., Bellemin-Ménard, A., Afanassieff, M., Huissoud, C., Douglas, R., Kennedy, H., Dehay, C., 2013. Precursor diversity and complexity of lineage relationships in the outer subventricular zone (OSVZ) of the primate. Neuron 80(20), 442-457.

Bopp, D., Burri, M., Baumgartner, S., Frigerio, G., Noll, M., 1986. Conservation of a large protein domain in the segmentation gene paired and in functionally related genes of Drosophila. Cell 47, 1033-1040.

Borrell, V., Reillo, I., 2012. Emerging roles of neural stem cells in cerebral cortex development and evolution. Dev. Neurobiol. 72, 955-971.

Britz, O., Mattar, P., Nguyen, L., Langevin, L.M., Zimmer, C., Alam, S., Guillemot, F., Schuurmans, C., 2006. A role for proneural genes in the maturation of cortical progenitor cells. Cereb. Cortex 16 Suppl 1, i138-151.

Bulfone, A., Martinez, S., Marigo, V., Campanella, M., Basile, A., Quaderi, N., Gattuso, C., Rubenstein, J.L., Ballabio, A., 1999. Expression pattern of the Tbr2 (Eomesodermin) gene during mouse and chick brain development. Mech. Dev. 84, 133-138.

Bultje, R.S., Castaneda-Castellanos, D.R., Jan, L.Y., Jan, Y.N., Kriegstein, A.R., Shi, S.H., 2009. Mammalian Par3 regulates progenitor cell asymmetric division via notch signaling in the developing neocortex. Neuron 63, 189-202.

Bystron, I., Rakic, P., Molnar, Z., Blakemore, C., 2006. The first neurons of the human cerebral cortex. Nat. Neurosci. 9, 880-886.

Callaerts, P., Halder, G., Gehring, W.J., 1997. PAX-6 in development and evolution. Annu. Rev. Neurosci. 20, 483-532.

Campbell, K., Götz, M., 2002. Radial glia: multi-purpose cells for vertebrate brain development. Trends Neurosci. 25, 235-238.

Campos, L.S., Duarte, A.J., Branco, T., Henrique, D., 2001. mDll1 and mDll3 expression in the developing mouse brain: Role in the establishment of the early cortex. J. Neurosci. Res. 64, 590-598.

Caric, D., Gooday, D., Hill, R.E., McConnell, S.K., Price, D.J., 1997. Determination of the migratory capacity of embryonic cortical cells lacking the transcription factor Pax-6. Development 124, 5087-5096.

Carlo, C.N., Stevens, C.F., 2013. Structural uniformity of neocortex, revisited. Proc. Natl. Acad. Sci. U.S.A. 110, 1488-1493.

Cheng, T.S., Hsiao, Y.L., Lin, C.C., Hsu, C.M., Chang, M.S., Lee, C.I., Yu, R.C., Huang, C.Y., Howng, S.L., Hong, Y.R., 2007. hNinein is required for targeting spindle-associated protein Astrin to the centrosome during the S and G2 phases. Exp. Cell Res. 313, 1710-1721.

Chenn, A., Walsh, C.A., 2003. Increased neuronal production, enlarged forebrains and cytoarchitectural distortions in beta-catenin overexpressing transgenic mice. Cereb. Cortex 13, 599-606.

Dehay, C., Kennedy, H., 2007. Cell-cycle control and cortical development. Nat. Rev. Neurosci. 8, 438-450.

Dong, Z., Yang, N., Yeo, S.Y., Chitnis, A., Guo, S., 2012. Intralineage directional notch signaling regulates self-renewal and differentiation of asymmetrically dividing radial glia. Neuron 74, 65-78.

Douglas, R.J., Martin, K.A., 2004. Neuronal circuits of the neocortex. Annu. Rev. Neurosci. 27, 419-451.

Dziegielewska, K.M., Evans, C.A.N., Lai, P.C.W., Lorscheider, F.L., Malinowska, D.H., Mollgard, K., Saunders, N.R., 1981. Proteins in Cerebrospinal-Fluid and Plasma of Fetal Rats during Development. Dev. Biol. 83, 193-200.

Englund, C., Fink, A., Lau, C., Pham, D., Daza, R.A., Bulfone, A., Kowalczyk, T., Hevner, R.F., 2005. Pax6, Tbr2, and Tbr1 are expressed sequentially by radial glia, intermediate progenitor cells, and postmitotic neurons in developing neocortex. J. Neurosci. 25, 247-251.

Estivill-Torrus, G., Pearson, H., van Heyningen, V., Price, D.J., Rashbass, P., 2002. Pax6 is required to regulate the cell cycle and the rate of progression from symmetrical to asymmetrical division in mammalian cortical progenitors. Development 129, 455-466.

Farkas, L.M., Haffner, C., Giger, T., Khaitovich, P., Nowick, K., Birchmeier, C., Paabo, S., Huttner, W.B., 2008. Insulinoma-associated 1 has a panneurogenic role and promotes the generation and expansion of basal progenitors in the developing mouse neocortex. Neuron 60, 40-55.

Fei, J., 2008. Studies on the progeny of neuronal progenitors in the developing mouse brain using novel transgenic models of the *Tis21* locus. PhD thesis: Technische Universität Dresden.

Feng, L., Allen, N.S., Simo, S., Cooper, J.A., 2007. Cullin 5 regulates Dab1 protein levels and neuron positioning during cortical development. Genes Dev. 21, 2717-2730.

Fietz, S.A., Huttner, W.B., 2011. Cortical progenitor expansion, self-renewal and neurogenesis-a polarized perspective. Curr. Opin. Neurobiol. 21, 23-35.

Fietz, S.A., Kelava, I., Vogt, J., Wilsch-Brauninger, M., Stenzel, D., Fish, J.L., Corbeil, D., Riehn, A., Distler, W., Nitsch, R., Huttner, W.B., 2010. OSVZ progenitors of human and ferret neocortex are epithelial-like and expand by integrin signaling. Nat. Neurosci. 13, 690-699.

Fietz, S.A., Lachmann, R., Brandl, H., Kircher, M., Samusik, N., Schroder, R., Lakshmanaperumal, N., Henry, I., Vogt, J., Riehn, A., Distler, W., Nitsch, R., Enard, W., Paabo, S., Huttner, W.B., 2012. Transcriptomes of germinal zones of human and mouse fetal neocortex suggest a role of extracellular matrix in progenitor self-renewal. Proc. Natl. Acad. Sci. U.S.A. 109, 11836-11841.

Fish, J.L., Dehay, C., Kennedy, H., Huttner, W.B., 2008. Making bigger brains-the evolution of neural-progenitor-cell division. J. Cell Sci. 121, 2783-2793.

Fukuda, T., Kawano, H., Osumi, N., Eto, K., Kawamura, K., 2000. Histogenesis of the cerebral cortex in rat fetuses with a mutation in the Pax-6 gene. Brain Res. Dev. Brain Res. 120, 65-75.

Gaiano, N., Nye, J.S., Fishell, G., 2000. Radial glial identity is promoted by Notch1 signaling in the murine forebrain. Neuron 26, 395-404.

Gal, J.S., Morozov, Y.M., Ayoub, A.E., Chatterjee, M., Rakic, P., Haydar, T.F., 2006. Molecular and morphological heterogeneity of neural precursors in the mouse neocortical proliferative zones. J. Neurosci. 26, 1045-1056.

Gan, Q., Lee, A., Suzuki, R., Yamagami, T., Stokes, A., Nguyen, B.C., Pleasure, D., Wang, J., Chen, H.W., Zhou, C.J., 2014. Pax6 mediates ss-catenin signaling for self-renewal and neurogenesis by neocortical radial glial stem cells. Stem Cells 32, 45-58.

Georgala, P.A., Carr, C.B., Price, D.J., 2011a. The role of Pax6 in forebrain development. Dev. Neurobiol. 71, 690-709.

Georgala, P.A., Manuel, M., Price, D.J., 2011b. The generation of superficial cortical layers is regulated by levels of the transcription factor Pax6. Cereb. Cortex 21, 81-94.

Gertz, C.C, Lui, J.H., LaMonica, B.E., Wang, X., Kriegstein, A.R., 2014. Diverse behaviors of outer radial glia in developing ferret and human cortex. J. Neurosci. 34, 2559-2570.

Glickstein, S.B., Alexander, S., Ross, M.E., 2007. Differences in cyclin D2 and D1 protein expression distinguish forebrain progenitor subsets. Cereb. Cortex 17, 632-642.

Götz, M., Huttner, W.B., 2005. The cell biology of neurogenesis. Nat. Rev. Mol. Cell Biol. 6, 777-788.

Götz, M., Stoykova, A., Gruss, P., 1998. Pax6 controls radial glia differentiation in the cerebral cortex. Neuron 21, 1031-1044.

Halder, G., Callaerts, P., Gehring, W.J., 1995. Induction of ectopic eyes by targeted expression of the eyeless gene in Drosophila. Science 267, 1788-1792.

Hansen, D.V., Lui, J.H., Flandin, P., Yoshikawa, K., Rubenstein, J.L., Alvarez-Buylla, A., Kriegstein, A.R., 2013. Non-epithelial stem cells and cortical interneuron production in the human ganglionic eminences. Nat. Neurosci. 16, 1576-1587.

Hansen, D.V., Lui, J.H., Parker, P.R., Kriegstein, A.R., 2010. Neurogenic radial glia in the outer subventricular zone of human neocortex. Nature 464, 554-561.

Haubensak, W., Attardo, A., Denk, W., Huttner, W.B., 2004. Neurons arise in the basal neuroepithelium of the early mammalian telencephalon: A major site of neurogenesis. Proc. Natl. Acad. Sci. U.S.A. 101, 3196-3201.

Haubst, N., Berger, J., Radjendirane, V., Graw, J., Favor, J., Saunders, G.F., Stoykova, A., Götz, M., 2004. Molecular dissection of Pax6 function: the specific roles of the paired domain and homeodomain in brain development. Development 131, 6131-6140.

Herculano-Houzel, S., Collins, C.E., Wong, P., Kaas, J.H., Lent, R., 2008. The basic nonuniformity of the cerebral cortex. Proc. Natl. Acad. Sci. U.S A. 105, 12593-12598.

Hippenmeyer, S., 2014. Molecular pathways controlling the sequential steps of cortical projection neuron migration. Cellular and molecular control of neuronal migration, 1-24.

Hippenmeyer, S., Youn, Y.H., Moon, H.M., Miyamichi, K., Zong, H., Wynshaw-Boris, A., Luo, L., 2010. Genetic mosaic dissection of Lis1 and Ndel1 in neuronal migration. Neuron 68, 695-709.

Holm, P.C., Mader, M.T., Haubst, N., Wizenmann, A., Sigvardsson, M., Götz, M., 2007. Loss- and gain-of-function analyses reveal targets of Pax6 in the developing mouse telencephalon. Mol. Cell Neurosci. 34, 99-119.

Huang, X., Liu, J., Ketova, T., Fleming, J.T., Grover, V.K., Cooper, M.K., Litingtung, Y., Chiang, C., 2010. Transventricular delivery of Sonic hedgehog

is essential to cerebellar ventricular zone development. Proc. Natl. Acad. Sci. U.S.A. 107, 8422-8427.

Huttner, W.B., Kosodo, Y., 2005. Symmetric versus asymmetric cell division during neurogenesis in the developing vertebrate central nervous system. Curr. Opin. Cell Biol. 17, 648-657.

Kamachi, Y., Uchikawa, M., Tanouchi, A., Sekido, R., Kondoh, H., 2001. Pax6 and SOX2 form a co-DNA-binding partner complex that regulates initiation of lens development. Genes Dev. 15, 1272-1286.

Kawauchi, T., Sekine, K., Shikanai, M., Chihama, K., Tomita, K., Kubo, K., Nakajima, K., Nabeshima, Y., Hoshino, M., 2010. Rab GTPases-dependent endocytic pathways regulate neuronal migration and maturation through N-cadherin trafficking. Neuron 67, 588-602.

Kelava, I., 2012. Basal radial glia in mammalian neocortical development - insights into brain evolution. PhD thesis: Technische Universität Dresden.

Kelava, I., Huttner, W.B., 2013. Neural progenitors and evolution of mammalian neocortex, in: Calegari, F., Waskow, C. (Eds.), Stem Cells. Science Publishers, Edenbridge Ltd., CRC Press/Taylor & Francis Group, Enfield, USA.

Kelava, I., Reillo, I., Murayama, A.Y., Kalinka, A.T., Stenzel, D., Tomancak, P., Matsuzaki, F., Lebrand, C., Sasaki, E., Schwamborn, J.C., Okano, H., Huttner, W.B., Borrell, V., 2012. Abundant occurrence of basal radial glia in the subventricular zone of embryonic neocortex of a lissencephalic primate, the common marmoset Callithrix jacchus. Cereb. Cortex 22, 469-481.

Kiecker, C., Niehrs, C., 2001. A morphogen gradient of Wnt/beta-catenin signalling regulates anteroposterior neural patterning in Xenopus. Development 128, 4189-4201.

Kikkawa, T., Obayashi, T., Takahashi, M., Fukuzaki-Dohi, U., Numayama-Tsuruta, K., Osumi, N., 2013. Dmrta1 regulates proneural gene expression downstream of Pax6 in the mammalian telencephalon. Genes Cells 18, 636-649.

Kondoh, H., Uchikawa, M., Kamachi, Y., 2004. Interplay of Pax6 and SOX2 in lens development as a paradigm of genetic switch mechanisms for cell differentiation. Int. J. Dev. Biol. 48, 819-827.

Konno, D., Shioi, G., Shitamukai, A., Mori, A., Kiyonari, H., Miyata, T., Matsuzaki, F., 2008. Neuroepithelial progenitors undergo LGN-dependent planar divisions to maintain self-renewability during mammalian neurogenesis. Nat. Cell Biol. 10, 93-101.

Kosodo, Y., Röper, K., Haubensak, W., Marzesco, A.-M., Corbeil, D., Huttner, W.B., 2004. Asymmetric distribution of the apical plasma membrane during

neurogenic divisions of mammalian neuroepithelial cells. EMBO J. 23, 2314-2324.

Kosodo, Y., Toida, K., Dubreuil, V., Alexandre, P., Schenk, J., Kiyokage, E., Attardo, A., Mora-Bermudez, F., Arii, T., Clarke, J.D., Huttner, W.B., 2008. Cytokinesis of neuroepithelial cells can divide their basal process before anaphase. EMBO J. 27, 3151-3163.

Kriegstein, A., Noctor, S., Martinez-Cerdeno, V., 2006. Patterns of neural stem and progenitor cell division may underlie evolutionary cortical expansion. Nat. Rev. Neurosci. 7, 883-890.

Kuida, K., Haydar, T.F., Kuan, C.Y., Gu, Y., Taya, C., Karasuyama, H., Su, M.S., Rakic, P., Flavell, R.A., 1998. Reduced apoptosis and cytochrome c-mediated caspase activation in mice lacking caspase 9. Cell 94, 325-337.

LaMonica, B.E., Lui, J.H., Hansen, D.V., Kriegstein, A.R., 2013. Mitotic spindle orientation predicts outer radial glial cell generation in human neocortex. Nat. Commun. 4, 1665.

Lange, C., Huttner, W.B., Calegari, F., 2009. Cdk4/cyclinD1 overexpression in neural stem cells shortens G1, delays neurogenesis, and promotes the generation and expansion of basal progenitors. Cell Stem Cell 5, 320-331.

Lee, M.K., Tuttle, J.B., Rebhun, L.I., Cleveland, D.W., Frankfurter, A., 1990. The expression and posttranslational modification of a neuron-specific beta-tubulin isotype during chick embryogenesis. Cell Motil. Cytoskeleton 17, 118-132.

Lehtinen, M.K., Walsh, C.A., 2011. Neurogenesis at the Brain-Cerebrospinal Fluid Interface. Annu. Rev. Cell Dev. Biol. 27, 653-679.

Lehtinen, M.K., Zappaterra, M.W., Chen, X., Yang, Y.J., Hill, A.D., Lun, M.L., Maynard, T., Gonzalez, D., Kim, S., Ye, P., D'Ercole, A.J., Wong, E.T., LaMantia, A.S., Walsh, C.A., 2011. The Cerebrospinal Fluid Provides a Proliferative Niche for Neural Progenitor Cells. Neuron 69, 893-905.

Leone, D.P., Srinivasan, K., Brakebusch, C., McConnell, S.K., 2010. The rho GTPase Rac1 is required for proliferation and survival of progenitors in the developing forebrain. Dev. Neurobiol. 70, 659-678.

Levitt, P., Rakic, P., 1980. Immunoperoxidase localization of glial fibrillary acidic protein in radial glial cells and astrocytes of the developing rhesus monkey brain. J. Comp. Neurol. 193, 815-840.

Lewitus, E., Kelava, I., Huttner, W.B., 2013a. Conical expansion of the outer subventricular zone and the role of neocortical folding in evolution and development. Front. Hum. Neurosci. 7, 424.

Lewitus, E., Kelava, I., Kalinka, A.T., Tomancak, P., Huttner, W.B., 2013b. An adaptive threshold in mammalian neocortical evolution. bioRxiv doi: 10.1101/001289.

LoTurco, J., Owens, D., Heat, M., Davis, M., Kriegstein, A., 1995. GABA and glutamate depolarize cortical progenitor cells and inhibit DNA synthesis. Neuron 15, 1287-1298.

Louvi, A., Grove, E.A., 2011. Cilia in the CNS: The Quiet Organelle Claims Center Stage. Neuron 69, 1046-1060.

Lui, J.H., Hansen, D.V., Kriegstein, A.R., 2011. Development and evolution of the human neocortex. Cell 146, 18-36.

Lukaszewicz, A., Savatier, P., Cortay, V., Giroud, P., Huissoud, C., Berland, M., Kennedy, H., Dehay, C., 2005. G1 phase regulation, area-specific cell cycle control, and cytoarchitectonics in the primate cortex. Neuron 47, 353-364.

Ma, T., Wang, C., Wang, L., Zhou, X., Tian, M., Zhang, Q., Zhang, Y., Li, J., Liu, Z., Cai, Y., Liu, F., You, Y., Chen, C., Campbell, K., Song, H., Ma, L., Rubenstein, J.L., Yang, Z., 2013. Subcortical origins of human and monkey neocortical interneurons. Nat. Neurosci. 16, 1588-1597.

Maden, M., 1999. Heads or tails? Retinoic acid will decide. Bioessays 21, 809-812.

Malatesta, P., Hartfuss, E., Götz, M., 2000. Isolation of radial glial cells by fluorescent-activated cell sorting reveals a neuronal lineage. Development 127, 5253-5263.

Manent, J.B., Wang, Y., Chang, Y., Paramasivam, M., LoTurco, J.J., 2009. Dcx reexpression reduces subcortical band heterotopia and seizure threshold in an animal model of neuronal migration disorder. Nat. Med. 15, 84-90.

Martinez-Cerdeno, V., Cunningham, C.L., Camacho, J., Antczak, J.L., Prakash, A.N., Cziep, M.E., Walker, A.I., Noctor, S.C., 2012. Comparative analysis of the subventricular zone in rat, ferret and macaque: evidence for an outer subventricular zone in rodents. PLoS ONE 7, e30178.

Martinez-Cerdeno, V., Noctor, S.C., Kriegstein, A.R., 2006. The role of intermediate progenitor cells in the evolutionary expansion of the cerebral cortex. Cereb. Cortex 16 Suppl 1, i152-161.

Marzesco, A.M., Janich, P., Wilsch-Brauninger, M., Dubreuil, V., Langenfeld, K., Corbeil, D., Huttner, W.B., 2005. Release of extracellular membrane particles carrying the stem cell marker prominin-1 (CD133) from neural progenitors and other epithelial cells. J. Cell Sci. 118, 2849-2858.

Merkin, J., Russell, C., Chen, P., Burge, C.B., 2012. Evolutionary dynamics of gene and isoform regulation in Mammalian tissues. Science 338, 1593-1599.

Mi, D., Carr, C.B., Georgala, P.A., Huang, Y.T., Manuel, M.N., Jeanes, E., Niisato, E., Sansom, S.N., Livesey, F.J., Theil, T., Hasenpusch-Theil, K., Simpson, T.I., Mason, J.O., Price, D.J., 2013. Pax6 exerts regional control of cortical progenitor proliferation via direct repression of Cdk6 and hypophosphorylation of pRb. Neuron 78, 269-284.

Minobe, S., Sakakibara, A., Ohdachi, T., Kanda, R., Kimura, M., Nakatani, S., Tadokoro, R., Ochiai, W., Nishizawa, Y., Mizoguchi, A., Kawauchi, T., Miyata, T., 2009. Rac is involved in the interkinetic nuclear migration of cortical progenitor cells. Neurosci. Res. 63, 294-301.

Miyata, T., Kawaguchi, A., Saito, K., Kawano, M., Muto, T., Ogawa, M., 2004. Asymmetric production of surface-dividing and non-surface-dividing cortical progenitor cells. Development 131, 3133-3145.

Mogensen, M.M., Malik, A., Piel, M., Bouckson-Castaing, V., Bornens, M., 2000. Microtubule minus-end anchorage at centrosomal and non-centrosomal sites: the role of ninein. J. Cell Sci. 113 (Pt 17), 3013-3023.

Molnar, Z., Metin, C., Stoykova, A., Tarabykin, V., Price, D.J., Francis, F., Meyer, G., Dehay, C., Kennedy, H., 2006. Comparative aspects of cerebral cortical development. Eur. J. Neurosci. 23, 921-934.

Molyneaux, B.J., Arlotta, P., Menezes, J.R., Macklis, J.D., 2007. Neuronal subtype specification in the cerebral cortex. Nat. Rev. Neurosci. 8, 427-437.

Nadarajah, B., Parnavelas, J.G., 2002. Modes of neuronal migration in the developing cerebral cortex. Nat. Rev. Neurosci. 3, 423-432.

Ninkovic, J., Pinto, L., Petricca, S., Lepier, A., Sun, J., Rieger, M.A., Schroeder, T., Cvekl, A., Favor, J., Götz, M., 2010. The transcription factor Pax6 regulates survival of dopaminergic olfactory bulb neurons via crystallin alphaA. Neuron 68, 682-694.

Noctor, S.C., Martinez-Cerdeno, V., Ivic, L., Kriegstein, A.R., 2004. Cortical neurons arise in symmetric and asymmetric division zones and migrate through specific phases. Nat. Neurosci. 7, 136-144.

Nomura, T., Gotoh, H., Ono, K., 2013. Changes in the regulation of cortical neurogenesis contribute to encephalization during amniote brain evolution. Nat. Commun. 4, 2206.

Nonaka-Kinoshita, M., Reillo, I., Artegiani, B., Martinez-Martinez, M.A., Nelson, M., Borrell, V., Calegari, F., 2013. Regulation of cerebral cortex size and folding by expansion of basal progenitors. EMBO J. 32, 1817-1828.

Nordstrom, U., Jessell, T.M., Edlund, T., 2002. Progressive induction of caudal neural character by graded Wnt signaling. Nat. Neurosci. 5, 525-532.

Numayama-Tsuruta, K., Arai, Y., Takahashi, M., Sasaki-Hoshino, M., Funatsu, N., Nakamura, S., Osumi, N., 2010. Downstream genes of Pax6 revealed by comprehensive transcriptome profiling in the developing rat hindbrain. B.M.C. Dev. Biol. 10, 6.

Osumi, N., Shinohara, H., Numayama-Tsuruta, K., Maekawa, M., 2008. Concise review: Pax6 transcription factor contributes to both embryonic and adult neurogenesis as a multifunctional regulator. Stem Cells 26, 1663-1672.

Osumi, N., Kikkawa, T., 2013. The role of the transcription factor Pax6 in brain development and evolution: evidence and hypothesis. Cortical Development, 43-61.

Owens, D.F., Kriegstein, A.R., 1998. Patterns of intracellular calcium fluctuation in precursor cells of the neocortical ventricular zone. J. Neurosci. 18, 5374-5388.

Owens, R., 1857. On the characters, principles of division and primary groups of the class Mammalia. Journal of the Proceedings of the Linnean Society of London Zoology 2, 1-37.

Parada, C., Gato, A., Bueno, D., 2005. Mammalian embryonic cerebrospinal fluid proteome has greater apolipoprotein and enzyme pattern complexity than the avian proteome. J. Proteome Res. 4, 2420-2428.

Paridaen, J.T., Wilsch-Brauninger, M., Huttner, W.B., 2013. Asymmetric inheritance of centrosome-associated primary cilium membrane directs ciliogenesis after cell division. Cell 155, 333-344.

Patrick, G.N., Zhou, P., Kwon, Y.T., Howley, P.M., Tsai, L.H., 1998. p35, the neuronal-specific activator of cyclin-dependent kinase 5 (Cdk5) is degraded by the ubiquitin-proteasome pathway. J. Biol. Chem. 273, 24057-24064.

Piel, M., Meyer, P., Khodjakov, A., Rieder, C.L., Bornens, M., 2000. The respective contributions of the mother and daughter centrioles to centrosome activity and behavior in vertebrate cells. J. Cell Biol. 149, 317-330.

Pilz, G.A., Shitamukai, A., Reillo, I., Pacary, E., Schwausch, J., Stahl, R., Ninkovic, J., Snippert, H.J., Clevers, H., Godinho, L., Guillemot, F., Borrell, V., Matsuzaki, F., Götz, M., 2013. Amplification of progenitors in the mammalian telencephalon includes a new radial glial cell type. Nat. Commun. 4, 2125.

Pinto, L., Drechsel, D., Schmid, M.T., Ninkovic, J., Irmler, M., Brill, M.S., Restani, L., Gianfranceschi, L., Cerri, C., Weber, S.N., Tarabykin, V., Baer, K., Guillemot, F., Beckers, J., Zecevic, N., Dehay, C., Caleo, M., Schorle, H., Götz, M., 2009. AP2gamma regulates basal progenitor fate in a region- and layer-specific manner in the developing cortex. Nat. Neurosci. 12, 1229-1237.

Quinn, J.C., Molinek, M., Martynoga, B.S., Zaki, P.A., Faedo, A., Bulfone, A., Hevner, R.F., West, J.D., Price, D.J., 2007. Pax6 controls cerebral cortical cell number by regulating exit from the cell cycle and specifies cortical cell identity by a cell autonomous mechanism. Dev. Biol. 302, 50-65.

Rakic, P., 1988. Specification of cerebral cortical areas. Science 241, 170-176.

Rakic, P., 1995. Radial versus tangential migration of neuronal clones in the developing cerebral cortex. Proc. Natl. Acad. Sci. U.S.A. 92, 11323-11327.

Rakic, P., 2009. Evolution of the neocortex: a perspective from developmental biology. Nat. Rev. Neurosci. 10, 724-735.

Rallu, M., Machold, R., Gaiano, N., Corbin, J.G., McMahon, A.P., Fishell, G., 2002. Dorsoventral patterning is established in the telencephalon of mutants lacking both Gli3 and Hedgehog signaling. Development 129, 4963-4974.

Reillo, I., Borrell, V., 2012. Germinal zones in the developing cerebral cortex of ferret: ontogeny, cell cycle kinetics, and diversity of progenitors. Cereb. Cortex 22, 2039-2054.

Reillo, I., de Juan Romero, C., Garcia-Cabezas, M.A., Borrell, V., 2011. A role for intermediate radial glia in the tangential expansion of the mammalian cerebral cortex. Cereb. Cortex 21, 1674-1694.

Rockel, A.J., Hiorns, R.W., Powell, T.P., 1980. The basic uniformity in structure of the neocortex. Brain 103, 221-244.

Sansom, S.N., Griffiths, D.S., Faedo, A., Kleinjan, D.J., Ruan, Y., Smith, J., van Heyningen, V., Rubenstein, J.L., Livesey, F.J., 2009. The level of the transcription factor Pax6 is essential for controlling the balance between neural stem cell self-renewal and neurogenesis. PLoS Genet 5, e1000511.

Sauer, F.C., 1935. Mitosis in the neural tube. J. Comp. Neurol. 62, 377-405.

Scardigli, R., Baumer, N., Gruss, P., Guillemot, F., Le Roux, I., 2003. Direct and concentration-dependent regulation of the proneural gene Neurogenin2 by Pax6. Development 130, 3269-3281.

Schmahl, W., Knoedlseder, M., Favor, J., Davidson, D., 1993. Defects of neuronal migration and the pathogenesis of cortical malformations are associated with Small eye (Sey) in the mouse, a point mutation at the Pax-6-locus. Acta Neuropathol. 86, 126-135.

Shibata, T., Yamada, K., Watanabe, M., Ikenaka, K., Wada, K., Tanaka, K., Inoue, Y., 1997. Glutamate transporter GLAST is expressed in the radial glia-astrocyte lineage of developing mouse spinal cord. J. Neurosci. 17, 9212-9219.

Shimogori, T., Ogawa, M., 2008. Gene application with in utero electroporation in mouse embryonic brain. Dev. Growth Differ. 50, 499-506.

Shinohara, H., Sakayori, N., Takahashi, M., Osumi, N., 2013. Ninein is essential for the maintenance of the cortical progenitor character by anchoring the centrosome to microtubules. Biol. Open 2, 739-749.

Shitamukai, A., Konno, D., Matsuzaki, F., 2011. Oblique radial glial divisions in the developing mouse neocortex induce self-renewing progenitors outside the germinal zone that resemble primate outer subventricular zone progenitors. J. Neurosci. 31, 3683-3695.

Shitamukai, A., Matsuzaki, F., 2012. Control of asymmetric cell division of mammalian neural progenitors. Dev. Growth Differ. 54, 277-286.

Siegenthaler, J.A., Ashique, A.M., Zarbalis, K., Patterson, K.P., Hecht, J.H., Kane, M.A., Folias, A.E., Choe, Y., May, S.R., Kume, T., Napoli, J.L., Peterson, A.S., Pleasure, S.J., 2009. Retinoic acid from the meninges regulates cortical neuron generation. Cell 139, 597-609.

Smart, I.H., Dehay, C., Giroud, P., Berland, M., Kennedy, H., 2002. Unique morphological features of the proliferative zones and postmitotic compartments of the neural epithelium giving rise to striate and extrastriate cortex in the monkey. Cereb. Cortex 12, 37-53.

Stahl, R., Walcher, T., De Juan Romero, C., Pilz, G.A., Cappello, S., Irmler, M., Sanz-Aquela, J.M., Beckers, J., Blum, R., Borrell, V., Götz, M., 2013. Trnp1 regulates expansion and folding of the Mammalian cerebral cortex by control of radial glial fate. Cell 153, 535-549.

Stancik, E.K., Navarro-Quiroga, I., Sellke, R., Haydar, T.F., 2010. Heterogeneity in ventricular zone neural precursors contributes to neuronal fate diversity in the postnatal neocortex. J. Neurosci. 30, 7028-7036.

Stenzel, D., Wilsch-Bräuninger, M. , Wong, F.K., Heuer, H., Huttner, W.B., 2014. Integrin αvβ3 and thyroid hormones promote expansion of progenitors in embryonic neocortex. Development 141, 795-806.

Storey, K.G., Goriely, A., Sargent, C.M., Brown, J.M., Burns, H.D., Abud, H.M., Heath, J.K., 1998. Early posterior neural tissue is induced by FGF in the chick embryo. Development 125, 473-484.

Stoykova, A., Fritsch, R., Walther, C., Gruss, P., 1996. Forebrain patterning defects in Small eye mutant mice. Development 122, 3453-3465.

Stoykova, A., Götz, M., Gruss, P., Price, J., 1997. Pax6-dependent regulation of adhesive patterning, R-cadherin expression and boundary formation in developing forebrain. Development 124, 3765-3777.

Takahashi, T., Nowakowski, R.S., Caviness, V.S., Jr., 1996. The leaving or Q fraction of the murine cerebral proliferative epithelium: a general model of neocortical neuronogenesis. J. Neurosci. 16, 6183-6196.

Taverna, E., Haffner, C., Pepperkok, R., Huttner, W.B., 2012. A new approach to manipulate the fate of single neural stem cells in tissue. Nat. Neurosci. 15, 329-337.

Taverna, E., Huttner, W.B., 2010. Neural progenitor nuclei IN Motion. Neuron 67, 906-914.

Ton, C.C., Hirvonen, H., Miwa, H., Weil, M.M., Monaghan, P., Jordan, T., van Heyningen, V., Hastie, N.D., Meijers-Heijboer, H., Drechsler, M., et al., 1991. Positional cloning and characterization of a paired box- and homeobox-containing gene from the aniridia region. Cell 67, 1059-1074.

Tsai, L.H., Gleeson, J.G., 2005. Nucleokinesis in neuronal migration. Neuron 46, 383-388.

Tsunekawa, Y., Britto, J.M., Takahashi, M., Polleux, F., Tan, S.S., Osumi, N., 2012. Cyclin D2 in the basal process of neural progenitors is linked to non-equivalent cell fates. EMBO J. 31, 1879-1892.

Turrero García, M., 2013. Analysis of the cell cycle of neural progenitors in the developing ferret neocortex. PhD thesis: Technische Universität Dresden.

Tyler, W.A., Haydar, T.F., 2013. Multiplex genetic fate mapping reveals a novel route of neocortical neurogenesis, which is altered in the Ts65Dn mouse model of Down syndrome. J. Neurosci. 33, 5106-5019.

Valiente, M., Marin, O., 2010. Neuronal migration mechanisms in development and disease. Curr. Opin. Neurobiol. 20, 68-78.

Vallee, R.B., Seale, G.E., Tsai, J.W., 2009. Emerging roles for myosin II and cytoplasmic dynein in migrating neurons and growth cones. Trends Cell Biol. 19, 347-355.

von Holst, A., Egbers, U., Prochiantz, A., Faissner, A., 2007. Neural stem/progenitor cells express 20 tenascin C isoforms that are differentially regulated by Pax6. J. Biol. Chem. 282, 9172-9181.

Walcher, T., Xie, Q., Sun, J., Irmler, M., Beckers, J., Ozturk, T., Niessing, D., Stoykova, A., Cvekl, A., Ninkovic, J., Götz, M., 2013. Functional dissection of the paired domain of Pax6 reveals molecular mechanisms of coordinating neurogenesis and proliferation. Development 140, 1123-1136.

Wang, D.D., Kriegstein, A.R., 2009. Defining the role of GABA in cortical development. J. Physiol-London 587, 1873-1879.

Wang, X., Tsai, J.W., Imai, J.H., Lian, W.N., Vallee, R.B., Shi, S.H., 2009. Asymmetric centrosome inheritance maintains neural progenitors in the neocortex. Nature 461, 947-955.

Wang, X., Tsai, J.W., LaMonica, B., Kriegstein, A.R., 2011. A new subtype of progenitor cell in the mouse embryonic neocortex. Nat. Neurosci. 14, 555-561.

Watt, F.M., Huck, W.T., 2013. Role of the extracellular matrix in regulating stem cell fate. Nat. Rev. Mol. Cell Biol. 14, 467-473.

Wilsch-Bräuninger, M., Peters, J., Paridaen, J.T.M.L., Huttner, W.B., 2012. Basolateral rather than apical primary cilia on neuroepithelial cells committed to delamination. Development 139, 95-105.

Wojcik-Stanaszek, L., Gregor, A., Zalewska, T., 2011. Regulation of neurogenesis by extracellular matrix and integrins. Acta Neurobiol. Exp 71, 103-112.

Wong, F.K., Haffner., C., Huttner, W.B., Taverna, E., 2014. Microinjection of membrane-impermeable molecules into single neural stem cells in brain tissue. Nat. Prot., In press.

Wu, Q.L., J.; Fang, A.; Li, R.; Bai, Y.; Kriegstein, A.R.; Wang, X., 2014. The dynamics of neuronal migration. Cellular and molecular control of neuronal migration, 25-36.

Xie, Q., Yang, Y., Huang, J., Ninkovic, J., Walcher, T., Wolf, L., Vitenzon, A., Zheng, D., Götz, M., Beebe, D.C., Zavadil, J., Cvekl, A., 2013. Pax6 interactions with chromatin and identification of its novel direct target genes in lens and forebrain. PLoS ONE 8, e54507.

Xu, P.X., Zhang, X., Heaney, S., Yoon, A., Michelson, A.M., Maas, R.L., 1999. Regulation of Pax6 expression is conserved between mice and flies. Development 126, 383-395.

Yoon, K.J., Koo, B.K., Im, S.K., Jeong, H.W., Ghim, J., Kwon, M.C., Moon, J.S., Miyata, T., Kong, Y.Y., 2008. Mind bomb 1-expressing intermediate progenitors generate notch signaling to maintain radial glial cells. Neuron 58, 519-531.

Young-Pearse, T.L., Bai, J., Chang, R., Zheng, J.B., LoTurco, J.J., Selkoe, D.J., 2007. A critical function for beta-amyloid precursor protein in neuronal migration revealed by in utero RNA interference. J. Neurosci. 27, 14459-14469.

Zappaterra, M.D., Lisgo, S.N., Lindsay, S., Gygi, S.P., Walsh, C.A., Ballif, B.A., 2007. A comparative proteomic analysis of human and rat embryonic cerebrospinal fluid. J. Proteome Res. 6, 3537-3548.

Chapter 6
Appendix

6.1.List of publications

Stenzel, D., Wilsch-Bräuninger, M., **Wong, F.K.**, Heuer, H., Huttner, W.B. (2014*) Integrin αvβ3 and thyroid hormones promote expansion of progenitors in embryonic neocortex*. Development. 141(4):795-806.

Wong, F.K., Haffner, C., Huttner, W.B., Taverna, E. (2014) *Microinjection of membrane-impermeable molecules into single neural stem cells in brain tissue.* Nature protocol. In press.

6.2. Manuscript in preparation

Wong, F.K*., Fei, J*., Taverna, E., Haffner, C., Huttner, W.B., *Conditional expression of Pax6 generates basal radial glia in the mouse dorsal telencephalon.*

Fei, J.*, **Wong, F.K.***, Haffner, C., Huttner, W.B. *Clonal analysis of the neurogenic progenitor in the mouse dorsal telencephalon.*

* equal contribution.

6.3. Conference participation

Presentation
3rd German-Japanese Bilateral Event on Neural Stem Cells and Mammalian Neurogenesis
Sendai, Japan, 13-16 October 2013

Abstract / Poster
Society of Neuroscience (SFN)
San Diego, USA, 9-13 November 2013

Attendance
International Congress on Stem Cells and Tissue Formation
Dresden, 18-20 July 2012

Cortical development
Crete, 19-22 May 2011

Acknowledgments

A certain philosopher – I knew that even then – had called the architecture of Dresden, its cathedrals and palaces, "frozen music".

~Erich Kästner~

Dresden will always have a special place in my heart. With it's magnificent spires and landscapes, its old world charm but more importantly, the people that intersected with my life during my period here that had enriched my life, infusing it not only with scientific wisdom and inspiration but also with kindness and joy.

In particular, I would like to thank the following people…

Professor Wieland B. Huttner
For that certain amount of "blind" faith in taking in a student that has no background in molecular and cell biology or even neurodevelopment. I have learned a lot from your attention to details, that I believe I will carry with me for the rest of my life.

Elena Taverna
For being that wonderful, kind and responsible supervisor that every PhD student should be lucky to have. Thank you for your patience, guidance, logical mind and encouragement.

My TAC members, *Elizabeth Knust and Frank Buchholz*
For your insightful comments and contribution that expanded my view on how to look at my project with different eyes.

MPI-CBG facilities
All this work would not be possible without the amazing facilities provided by MPI-CBG such as the BMS, LMF, DNA, microarray and transgenic facility. Thank you from the bottom of my heart.

JiFeng Fei
This work would not be possible without your wonderful Tis21–CreERT2 and for all the advices you have given me through the years.

Elena Taverna, Denise Stenzel and Eric Lewitus
For reading through this thesis, pointing out the imperfections and for the suggestions to make it better.

Alex Sykes, Judith Paridaen and JiFeng Fei
For your patience as you taught me on the various things from molecular cloning, electroporation, to the different sounds animals make in various countries. For listening to my woes and offering invaluable advises and of course food to fatten me up through the cold winter months.

Kanako Saito and Miguel Turrero García
For your patience and great advises on slice culture. My slices have never looked this great. And not forgetting Miguel for your advices, handling the orders and taking care of the ferrets.

Christiane Haffner and Jula Peters
For again being ever so patient with me with my endless questions and requests. Thank you also for your invaluable advice both scientific and on life, especially one on a particular house with closed doors that came at the most opportune of time.

Yoko Arai
For your advice and discussion at the start of my PhD that started off the Pax6 project. Without you, this project would not exist.

Iva Kelava
For your beautiful cakes, discussions on books and everything else.

Denise Stenzel and Marta Florio
For being there. I don't think there are enough words to describe how much I value our friendships.

Carine Stapel
Dank u zeer, heel veel. Voor dat u, omdat hij een vriend. Voor het voeden van mij de hele tijd en voor alle lieve, mooie tijden die we hebben. (Thank you google translate!)

Christian Rochford
I believe it was your words, your advice that had led me to this magical place. Thank you for making me take this experience of a lifetime. I suppose this thesis would not have existed without you.

The rest of the people in the Huttner lab
For their intelligence, experience and their generosity in dispensing their wisdom and advice. Also for all the kind words that kept me going during dark times and of course my numerous panic attacks. It was a wonderful experience to work in this lab. I wouldn't be the same without each and every one of your presence.

Family and friends
We've been through a lot. And I am eternally grateful and in constant wonderment on the strength of your love, support, believe and trust. To know that regardless of time and distance that you are always there when I needed you.

To everyone else
Thank you from the deepest recess of my heart.

Erklärung entsprechend §5.5 der Promotionsordnung

Hiermit versichere ich, dass ich die vorliegende Arbeit ohne unzulässige Hilfe Dritter und ohne Benutzung anderer als der angegebenen Hilfsmittel angefertigt habe; die aus fremden Quellen direkt oder indirekt übernommenen Gedanken sind als solche kenntlich gemacht. Die Arbeit wurde bisher weder im Inland noch im Ausland in gleicher oder ähnlicher Form einer anderen Prüfungsbehörde vorgelegt.

Die Dissertation wurde im Zeitraum vom 1-September-2010 bis 31-March-2014 verfasst und von Prof. Dr.Wieland B. Huttner , Max Planck Institute of Molecular Cell Biology and Genetics, Dresden Germany, Huttner group/Biology betreut.

Meine Person betreffend erkläre ich hiermit, dass keine früheren erfolglosen Promotionsverfahren stattgefunden haben.

Ich erkenne die Promotionsordnung der Fakultät für Mathematik und Naturwissenschaften, Technische Universität Dresden an.

_____

Date, Signature